Trinity College Dublin
Coláiste na Tríonóide, Baile Átha Cliath
The University of Dublin

SCHOOL OF PHYSICS

HEAT TRANSFER IN OPEN QUANTUM SYSTEMS

MARIA POPOVIC

2023

SUBMITTED IN FULFILMENT OF THE REQUIREMENTS FOR THE DEGREE OF
DOCTOR OF PHILOSOPHY

Declaration

I declare that this thesis has not been submitted as an exercise for a degree at this or any other university and it is entirely my own work.

I agree to deposit this thesis in the University's open access institutional repository or allow the library to do so on my behalf, subject to Irish Copyright Legislation and Trinity College Library conditions of use and acknowledgement.

I consent to the examiner retaining a copy of the thesis beyond the examining period, should they so wish (EU GDPR May 2018).

Signed: _____ Date: _____

Summary

In most situations of practical interest, quantum systems are not isolated from their surroundings but are interacting with an environment. The importance of such situations has been highlighted, for example, in the fields of quantum optics, interacting many-body systems, quantum computation and, as will be the focus of this thesis, thermodynamics of quantum systems. Scientific interest in the fabrication and control of small devices has fuelled attention to nonequilibrium thermodynamics of open quantum systems, and in particular, to detailed understanding of heat transfer in order to minimize wasteful dissipation.

In Part I of this thesis the theory of open quantum systems is introduced. Coupling with an environment leads to the buildup of correlations and as consequence the dynamics of the open quantum system can no longer be described with a unitary time evolution operator. In many cases of interest the presence of strong coupling between system and environment and the presence of memory effects make the dynamics of the system non-Markovian. A numerically exact method based on the path integral formulation, the time-evolving matrix product operator (TEMPO) algorithm, has recently been developed for retrieving the system reduced density matrix in such cases.

In Part II we use the theory presented in Part I to develop a numerically exact method to compute the full counting statistics of heat transfer in non-Markovian open quantum systems, based on the TEMPO algorithm. This approach is applied to the paradigmatic spin-boson model in order to calculate the mean and fluctuations of the heat transferred to the environment during thermal equilibration. We

show that system-reservoir correlations make a significant contribution to the heat statistics at low temperature and present a variational theory that quantitatively explains our numerical results. We also demonstrate a fluctuation-dissipation relation connecting the mean and variance of the heat distribution at high temperature.

Next, we investigate the nonequilibrium thermodynamics of pure decoherence. In a pure decoherence process, the system Hamiltonian is in a constant of motion and there is no direct energy exchange between the system and its surroundings. Nevertheless, we find the presence of nontrivial heat dissipation as a result of decoherence alone. We show that the heat distribution for a pure decoherence process corresponds to a mixture of work distributions of cyclical processes, each conditioned on a state of the open system. Inspired by recent experiments on impurities in ultra-cold gases, we demonstrate our general results by studying the heat generated by the decoherence of a qubit immersed within a degenerate Fermi gas in the lowest band of a species-selective optical lattice. Finally, we discuss the heat dissipation generated by a single projective measurement performed on the open system during a pure decoherence process.

Acknowledgements

I dedicate this thesis to my grandparents, Dara and Mile.

First of all, I thank my supervisors Paul Eastham and John Goold for their guidance and patience.

I would also like to thank Brendon Lovett, Aidan Strathearn and the research group at the University of St Andrews for the enlightening discussions and for helping me navigate the details of the TEMPO algorithm.

I'm grateful to Mark Mitchison for his help throughout all of my projects, and to my friends the QuSys group, especially Cecilia, Artur, Laetitia, Marlon, Alessandro, Oisín and Nathan for the good (and bad) times spent together.

Lastly, I would like to thank all the friends I've met in Dublin, without whom these last four years would not have been the same.

List of publications

The results discussed in this thesis appeared in the following publications:

1. M. Popovic, M. T. Mitchison, A. Strathearn, B. W. Lovett, J. Goold, and P. R. Eastham, *Quantum Heat Statistics with Time-Evolving Matrix Product Operators*, PRX Quantum **2**, 020338 (2021).

2. M. Popovic, M. T. Mitchison, and J. Goold, *Thermodynamics of Decoherence*, Proc. R. Soc. A **479**, 20230040 (2023).

The following work, although unrelated to the main topics of this thesis, was completed and published during the course of the PhD:

1. S. Campbell, M. Popovic, D. Tamascelli, B. Vacchini, *Precursors of non-Markovianity*, New Journal of Physics **21**, 053036 (2019).

Contents

List of Figures

Part I

Introduction & motivation

1 Introduction

The dynamics of a system interacting with its environment is studied through the theory of open quantum systems [1]. Examples of open quantum systems include atoms in a solid [2], spins coupled to thermal baths [3, 4], and excitons involved in biological processes [5]. More broadly, the relevance of this theory reaches the fields of quantum biology, quantum Darwinism, quantum computation, construction of quantum thermal machines and a variety of other diverse topics [6–8]. What makes the theory of open quantum systems widely applicable is the fact that in realistic, experimentally relevant settings, no system can truly be isolated from its surroundings. The total system composed by the quantum system and its environment is a closed one, as schematically represented in Fig. 1.1, and therefore its evolution can be defined by means of an unitary time evolution operator. Due to the coupling with its surroundings, however, the time evolution of the reduced density matrix of the open system alone can no longer be described with an unitary time evolution operator. If such an interaction satisfies the conditions of the weak coupling limit and the Markov approximation, then the dynamics of the system is referred to as memoryless and can be described with a Markovian theory. Specifically, the weak coupling approximation states that the environment is not influenced by its coupling to the system and therefore its density matrix is time independent. The Markov approximation states that the changes in the environmental state are cancelled before influencing the time evolution of the system [1]. In many cases of interest, however, such conditions are not satisfied and the presence of memory effects makes the dynamics of the system non-Markovian. There exist in the literature many different

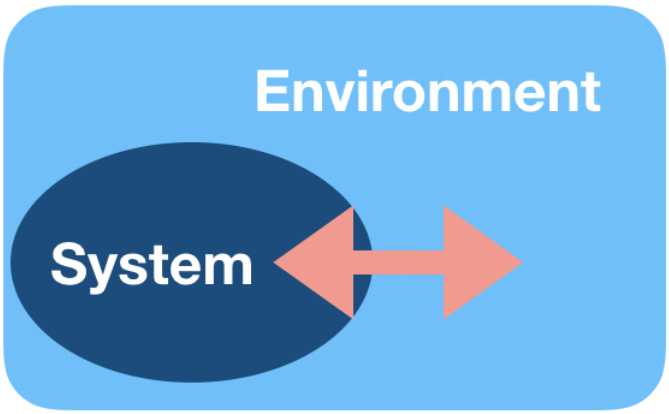

Figure 1.1: Representation of a system interacting with its surrounding environment. The total system composed by open system and environment is a closed one.

definitions of a non-Markovian process [9]. A common case is where the degrees of freedom of the environment are infinite compared with those of the system, and the environment can be described as a thermal bath of some constant temperature T. This allows for the study of thermodynamic properties of open quantum systems. Non-Markovian behaviour is an important and so far little explored topic in modern thermodynamics. Its characteristic feature, information back-flow from the environment to the system, or memory effects, has been studied in the context of different thermodynamic quantities such as work [10, 11] and entropy production rate [4]. It is therefore of great interest to study the thermodynamic properties of a quantum system in regimes that can't be described by the Markovian theory, or even in the presence of strong system-environment coupling, where few studies have been so far conducted.

There exist several techniques for studying the dynamics of an open quantum system weakly coupled to an environment. The spin-boson model can be solved, for example, through perturbative calculations in the coupling constant, the Heisenberg approach, or the expansion method [12]. Some of these techniques in principle already allow for a study of the dynamics beyond the Markovian regime. However, strong coupling between the system and the environment precludes the application

of perturbative methods and there exists no general method for solving the dynamics. In this case, the system's reduced density matrix can be retrieved, among other techniques, with the path integral method [13, 14]. The path integral formulation has been the basis for a recently developed exact numerical method for modelling strongly interacting environments [15, 16].

In the following chapters the formalism with which to compute the non-Markovian dynamics of an open quantum system is introduced, focusing on the path integral formulation and introducing the TEMPO algorithm, on which we will base our method for calculating the full counting statistics of heat transfer. Quantum thermodynamic quantities will be outlined starting from a discussion of classical thermodynamics [17–19].

2 | Master equations for open systems

The dynamics of an open quantum system coupled to an environment is generally derived from the dynamics of the overall closed system that is comprised of both the open system and its surroundings [1]. The Hilbert space of such a composite system is a tensor product of the two components' Hilbert spaces, $\mathcal{H} = \mathcal{H}_S \otimes \mathcal{H}_B$, where with S and B we denote the degrees of freedom of the open system and environment respectively. Setting $\hat{\rho}$ to be the density matrix of the composite system, the reduced density matrix of the open system $\hat{\rho}_S$ is obtained by tracing out the environmental degrees of freedom,

$$\hat{\rho}_S = \mathrm{Tr}_B[\hat{\rho}], \tag{2.1}$$

and similarly for the reduced density matrix of the environment, $\hat{\rho}_B = \mathrm{Tr}_S[\hat{\rho}]$. The total Hamiltonian that governs the overall closed system is

$$\hat{H} = \hat{H}_S + \hat{H}_B + \hat{H}_I, \tag{2.2}$$

where $\hat{H}_S$ is the free Hamiltonian of the open quantum system, $\hat{H}_B$ is the free Hamiltonian of the environment, and $\hat{H}_I$ is the Hamiltonian that describes the interaction between these two components. In general, $\hat{H}$ is time dependent. The dynamics of the overall closed system is governed by a von Neumann equation whose solution defines a unitary time evolution operator. From this solution, under a specific set of assumptions and approximations, a Markovian master equation for the density ma-

trix Eq. (2.1) can be obtained, as discussed in the literature [1, 20]. In the following, this derivation will be reviewed.

2.1 Dynamics of a closed quantum system

Let $\hat{U}(t, t_0)$ be the unitary operator that governs the time evolution of the overall closed system's states, defined as $|\psi\rangle$. Then for any time $t > t_0$, the system's state is given by $|\psi(t)\rangle = \hat{U}(t, t_0)|\psi(t_0)\rangle$. Inserting the expression for $|\psi(t)\rangle$ into the Schrödinger equation, $d|\psi(t)\rangle/dt = -i\hat{H}|\psi(t)\rangle$, gives the equation for the unitary time evolution operator

$$i\frac{d\hat{U}(t, t_0)}{dt} = \hat{H}\hat{U}(t, t_0). \tag{2.3}$$

Units where $\hbar = 1$ are used throughout. The solution to Eq. (2.3) is given by

$$\hat{U}(t, t_0) = \overleftarrow{T}\ \exp\left[-i\int_{t_0}^{t} d\tau \hat{H}(\tau)\right], \tag{2.4}$$

where $\overleftarrow{T}$ is the chronological time-ordering operator, so that the products of time dependent operators are ordered in a way such that the operator's arguments are increasing from right to left. In the case of a time independent Hamiltonian, such as the one that will be the focus of this work, Eq. (2.4) becomes

$$\hat{U}(t, t_0) = \exp[-i\hat{H}(t - t_0)]. \tag{2.5}$$

The dynamics of the composite closed system density matrix is then

$$\hat{\rho}(t) = \hat{U}(t, t_0)\hat{\rho}(t_0)\hat{U}^{\dagger}(t, t_0). \tag{2.6}$$

The von Neumann equation of motion is then obtained by differentiating with respect to time,

$$\frac{d\hat{\rho}(t)}{dt} = -i[\hat{H}, \hat{\rho}(t)]. \tag{2.7}$$

In classical mechanics, the equivalent of the von Neumann equation is the classical Liouville equation,

$$\frac{d\rho\left(t\right)}{dt}=\mathcal{L}\left(t\right)\rho\left(t\right), \tag{2.8}$$

where $\mathcal{L}$ is the Liouville operator. Defining the dynamics of the system in terms of a Liouville operator will prove particularly useful when laying out the theory for our numerically exact computational method for calculating quantum statistics of heat transfer. In a quantum mechanical context, the Liouville operator corresponds to the commutator between the density matrix $\hat{\rho}$ and the total Hamiltonian $\hat{H}$, $\mathcal{L}\rho\rightarrow-i[\hat{H},\hat{\rho}]$. The solution to the classical master equation Eq. (2.8) is given by

$$\rho\left(t\right)=\overleftarrow{T}\ \exp\left[\int_{t_0}^{t}d\tau\mathcal{L}\left(\tau\right)\right]\rho\left(t_0\right), \tag{2.9}$$

which in the case of a time-independent Hamiltonian yields

$$\rho\left(t\right)=\exp\left[\left(t-t_0\right)\mathcal{L}\right]\rho\left(t_0\right). \tag{2.10}$$

The solution to the overall closed system's dynamics is obtained from the initial state of the density matrix and the form of the total Hamiltonian, and it is the starting point for deriving the dynamics of the open quantum system [1].

2.2 CPT dynamical maps

The building up of correlations, both classical and quantum, between the open quantum system and its environment, leads in general to a non-unitary time evolution of $\hat{\rho}_S$. The properties of the dynamical map describing the time evolution distinguish between different possible types of quantum dynamics, namely Markovian or non-Markovian [1, 20]. A completely positive (CP), trace preserving, and divisible dynamical map defines a Markovian time evolution for the open system [1, 21]. In this section such a dynamical map will be defined and described. The assumption maintained throughout this work is the absence of correlations between open

system and surroundings at initial time,

$$\hat{\rho}(t_0) = \hat{\rho}_S(t_0) \otimes \hat{\rho}_B(t_0). \tag{2.11}$$

If the state of the environment $\hat{\rho}_B$ at a given time t is fixed, there exists a correspondence between the time evolution of the open quantum system and a map Λ_t acting from the Banach space of trace class operators $T(\mathcal{H}_S)$ onto itself, $\Lambda_t : T(\mathcal{H}_S) \to T(\mathcal{H}_S)$, such that

$$\hat{\rho}_S(t) = \Lambda_t \hat{\rho}_S(t_0) \equiv \mathrm{Tr}_B \left[\hat{U}(t, t_0) \left[\hat{\rho}_S(t_0) \otimes \hat{\rho}_B(t_0) \right] \hat{U}^\dagger(t, t_0) \right]. \tag{2.12}$$

Eqs. (2.1) and (2.6) were used in Eq. (2.12). In order to be a CP-divisible dynamical map describing the Markovian physical time evolution of a system, Λ_t must satisfy the following properties [1, 21]:

- Be a linear map, that is, $\Lambda_t(\alpha\hat{\rho}_1 + \beta\hat{\rho}_2) = \alpha\Lambda_t\hat{\rho}_1 + \beta\Lambda_t\hat{\rho}_2$ for any two operators $\hat{\rho}_1$ and $\hat{\rho}_2$, where α and β are real numbers.
- Be trace preserving, that is, $\mathrm{Tr}_S[\hat{\rho}_S(t_0)] = \mathrm{Tr}_S[\Lambda_t \hat{\rho}_S(t_0)] = 1$.
- Be completely positive.
- Fulfill the composition law $\Lambda_{t,v} = \Lambda_{t,s}\Lambda_{s,v}$, for $t \geq s \geq v$.

A linear map that is trace preserving and completely positive is a CPT map. Complete positivity can be described as follows. The map in Eq. (2.12) is completely positive if $\forall n \in \mathbb{N}$, the extended map $(\Lambda_t \otimes \mathbb{I}_n) : T(\mathcal{H}_S \otimes \mathbb{C}^n) \mapsto T(\mathcal{H}_S \otimes \mathbb{C}^n)$ sends positive operators into positive operators, where an operator $\hat{\rho}$ is defined as positive if $\langle\psi|\hat{\rho}|\psi\rangle > 0$ for all vectors $|\psi\rangle$ in the domain of $\hat{\rho}$. In other words, complete positivity requires that the map Λ_t extends to a space of generic dimension, through a tensor product with the identity, and remains positive. In the context of quantum systems, the property of positivity is replaced by the stronger requirement of complete positivity, in order to guarantee the positivity of the density matrix for

systems entangled with other systems [21]. By varying the time parameter t of the map Λ_t, one obtains a family of dynamical maps $\{\Lambda_t\}_{t\geq 0}$ describing the time evolution of the open quantum system S. If the one-parameter family of dynamical maps $\{\Lambda_t\}_{t\geq 0}$ has, in addition to being a family of CPT maps, the semigroup property $\Lambda_{t_1}\Lambda_{t_2} = \Lambda_{t_1+t_2}$ for any $t_1, t_2 \geq 0$, as well as $\Lambda_{t=0} = \mathbb{I}$, then it is a quantum dynamical one-parameter semigroup. If there exist an inverse map Λ_t^{-1} for any t, then the dynamical map can be extended to a two-parameter family of dynamical maps defined as $\Lambda_{t,s} = \Lambda_t\Lambda_s^{-1}$, with the condition $\Lambda_{t,0} = \Lambda_t$. If the family $\{\Lambda_{t,s}\}_{t,s}$ is a family of linear, CPT maps that satisfy the composition law $\Lambda_{t,s}\Lambda_{s,v} = \Lambda_{t,v}\ \forall t \geq s \geq v$, then the dynamics is defined as a CP-divisible process and it is Markovian [21].

The Born approximation, the Markov approximation, and the secular approximation, defined in the next sub-section, are the physical conditions sufficient for the CPT maps describing the dynamics of the reduced system to form a quantum dynamical semigroup [1].

2.3 Approximations and Markovian master equation

The assumption of a weak coupling between an open system and its environment is referred to as the Born approximation [1]. It implies that the environment reduced density matrix $\hat{\rho}_B$ is weakly influenced by its coupling to the open system $\hat{\rho}_S(t)$, and can be approximated to be constant in time, so that the initial condition Eq. (2.11) is satisfied $\forall t$. The density matrix of the overall composite system is then always approximated to a tensor product $\hat{\rho}\,(t) \approx \hat{\rho}_S\,(t) \otimes \hat{\rho}_B$.

In general, the state of the open system S depends upon its past evolution. A second relevant approximation can be made in weak coupling regime, referred to as the Markovian approximation [1]. It assumes that the correlation functions of the environment decay quickly with respect to the time scale over which the open system evolves, therefore not retaining memory of the system's previous states. In other words, the changes in the environment that are notwithstanding the constant density matrix $\hat{\rho}_B$ are cancelled before influencing the time evolution of the open system.

The open system S loses memory of its previous states and the time evolution is referred to as a memoryless process. Applying both the Born and the Markov approximation (jointly referred to as Born-Markov approximation) leads to the Markovian quantum master equation for the system's density matrix [1]. The Markovian master equation does not yet, however, imply that the dynamics of system S is described by a quantum dynamical semigroup. In order to guarantee this, a third approximation is necessary.

This last approximation is referred to as the secular approximation. It assumes that in weak coupling regime, the frequencies in the interaction picture that are much larger than the frequency scale defined by the coupling strength, give rise to fast oscillating terms that decay quickly with respect to the time evolution scale, and can be discarded [1]. These three approximations, together, define a Markovian process described by a quantum dynamical semigroup of CPT maps. Moreover, the Markovian master equation can be expressed in the well known Lindblad form.

2.3.1 Lindblad form of the Markovian master equation

With the Born, Markov and secular approximations, the one-parameter family of dynamical maps $\{\Lambda_t\}_{t\geq 0}$ is a quantum dynamical semigroup for which a semigroup generator $\mathcal{K}$ can be found [20]. Then, by definition of a generator of a semigroup,

$$\Lambda_t = \exp\left[(t - t_0)\mathcal{K}\right]. \tag{2.13}$$

Note that $\mathcal{K}$ must be time-independent by definition. The Markovian master equation for the reduced system density matrix is obtained by differentiating Eq. (2.12) and Eq. (2.13) with respect to the parameter t,

$$\frac{d\hat{\rho}_S(t)}{dt} = \mathcal{K}\hat{\rho}_S(t). \tag{2.14}$$

By comparison with the Liouville master equation (2.8) for the composite closed system, it can be seen that the superoperator $\mathcal{K}$ is a generalization of the Liouville

operator $\mathcal{L}$. By taking the spectral decomposition of the initial environment density matrix $\hat{\rho}_B(t_0) = \sum_\alpha \lambda_\alpha |\phi_\alpha\rangle_{BB}\langle\phi_\alpha|$, the dynamical map can be written in terms of its orthonormal eigenvectors $\{|\phi_\alpha\rangle_B\}$ and non-negative real eigenvalues $\{\lambda_\alpha\}$, as

$$\hat{\rho}_S(t) = \Lambda_t \hat{\rho}_S(t_0) = \sum_{\alpha,\beta} \hat{W}_{\alpha\beta}(t,t_0)\,\hat{\rho}_S(t_0)\hat{W}^\dagger_{\alpha\beta}(t,t_0)\,, \tag{2.15}$$

where we define the operators $\hat{W}_{\alpha\beta}(t,t_0) = \sqrt{\lambda_\beta}\,\langle\phi_\alpha|\,\hat{U}(t,t_0)\,|\phi_\beta\rangle_B$ that satisfy $\sum_{\alpha,\beta}\hat{W}^\dagger_{\alpha\beta}(t,t_0)\,\hat{W}_{\alpha\beta}(t,t_0) = \mathbb{I}_S$. Setting a complete basis of orthonormal operators of the Liouville space $\{\hat{F}_i\}$, $i = 1,2,...N^2$, where $N = \dim(\mathcal{H}_S)$, such that the scalar product between two elements of the basis is defined as $\langle\hat{F}_i,\hat{F}_j\rangle = \mathrm{Tr}_S[\hat{F}_i\hat{F}_j^\dagger] = \delta_{ij}$, the operators $\hat{W}_{\alpha\beta}(t,t_0)$ can be expanded as $\hat{W}_{\alpha\beta}(t,t_0) = \sum_{i=1}^{N^2}\hat{F}_i\left\langle\hat{F}_i,\hat{W}^\dagger_{\alpha\beta}(t,t_0)\right\rangle$. It follows that the action of the dynamical map Eq. (2.15) is

$$\hat{\rho}_S(t) = \Lambda_t\hat{\rho}_S(t_0) = \sum_{i,j=1}^{N^2} c_{ij}(t,t_0)\,\hat{F}_i\,\hat{\rho}_S(t_0)\hat{F}_j^\dagger, \tag{2.16}$$

where the coefficients c_{ij} are defined as $c_{ij}(t,t_0) = \sum_{\alpha,\beta}\left\langle\hat{F}_i,\hat{W}^\dagger_{\alpha\beta}(t,t_0)\right\rangle$ $\left\langle\hat{F}_j,\hat{W}^\dagger_{\alpha\beta}(t,t_0)\right\rangle^*$, and form the elements of a positive Hermitian matrix. As an infinitesimal generator of a semigroup, $\mathcal{K}$ is by definition [1]

$$\mathcal{K}\hat{\rho}_S = \lim_{\epsilon\to 0}\frac{1}{\epsilon}\left[\Lambda_\epsilon\,\hat{\rho}_S - \hat{\rho}_S\right]. \tag{2.17}$$

By means of Eq. (2.16), the action of the generator $\mathcal{K}$ is then

$$\mathcal{K}\hat{\rho}_S = -i[\hat{H}_S,\hat{\rho}_S] + \sum_{i,j=1}^{N^2-1} a_{ij}(t_0)\left(\hat{F}_i\hat{\rho}_S\hat{F}_j^\dagger - \frac{1}{2}\left\{\hat{F}_j^\dagger\hat{F}_i,\hat{\rho}_S\right\}\right). \tag{2.18}$$

Here we have defined the coefficients

$$a_{ij}(t_0) = \lim_{\epsilon \to 0} \frac{c_{ij}(\epsilon, t_0)}{\epsilon}, \tag{2.19}$$

$$a_{iN^2}(t_0) = \lim_{\epsilon \to 0} \frac{c_{iN^2}(\epsilon, t_0)}{\epsilon}, \tag{2.20}$$

$$a_{N^2N^2}(t_0) = \lim_{\epsilon \to 0} \frac{(c_{N^2N^2}(\epsilon, t_0) - N)}{\epsilon}, \tag{2.21}$$

for $i, j = 1...N^2 - 1$, and introduced the Hermitian operator $\hat{H}_S = (\hat{F}^\dagger - \hat{F})/2i$, where $\hat{F} = \left(1/\sqrt{N}\right) \sum_{i=1}^{N^2-1} a_{iN^2}(t_0) \hat{F}_i$. The coefficients $a_{ij}(t_0)$ are the elements of a positive matrix that can be diagonalized by means of an appropriate unitary transformation u. We define $\gamma_k(t_0)$ to be the non-negative diagonal elements, $k = 1, ..., N^2 - 1$. Then Eq. (2.18) leads to the most general form for a generator of a quantum dynamical semigroup, known as the Lindblad equation,

$$\frac{d\hat{\rho}_S}{dt} = -i[\hat{H}_S, \hat{\rho}_S] + \sum_{k=1}^{N^2-1} \gamma_k(t_0) \left(\hat{A}_k \hat{\rho}_S \hat{A}_k^\dagger - \frac{1}{2} \left\{ \hat{A}_k^\dagger \hat{A}_k, \hat{\rho}_S \right\} \right). \tag{2.22}$$

The operators $\hat{A}_k$ are defined by the unitary transformation $\hat{F}_j = \sum_{k=1}^{N^2-1} u_{kj} \hat{A}_k$, and are referred to as the Lindblad operators. The second term in Eq. (2.22) is the dissipator operator $\mathcal{D}(\hat{\rho}_S)$. The terms $\gamma_k(t_0)$ are relaxation rates for the decay modes of the open system.

2.4 Definition and relevance of non-Markovianity

It has been discussed how the time evolution of a quantum system defined by a quantum dynamical semigroup of CPT, divisible maps is a Markovian process [21]. The Gorini-Kossakowski-Sudarshan-Lindblad theorem states that a process is Markovian if and only if its master equation can be written in the form of Eq. (2.22) [22]. For time-dependent equations, the terms $\hat{H}_S(t)$, $\hat{A}_k(t)$ and $\gamma_k(t, t_0)$ are generally time dependent as well. One must then add the condition that, in the Lindblad master equation, $\gamma_k(t, t_0) \geq 0$ for any time t and every k in order to have a Marko-

vian dynamics [21, 22]. It follows that a non-Markovian dynamics arises every time the relaxation rates become negative at any point during the process. If the Born-Markov approximation is not satisfied, for example because the environmental correlation times are not small in comparison with the open system's relaxation and decoherence times, or because the coupling between the open system and the environment is strong, the system cannot be described by a dynamical semigroup.

The presence of non-Markovianity in a system can be detected through quantities called witnesses of non-Markovianity [21]. A witness is a quantity that always vanishes for a Markovian dynamics, but might or might not vanish for a non-Markovian one. An example of a witness of non-Markovianity is the trace distance, which measures how much two states are distinguishable from one another. Non-Markovianity can be interpreted as a growth of distinguishability [23]. Since the loss of distinguishability is caused by a flow of information from the open system to the environment, its growth can be interpreted as a flow of information from the environment back to the open system. Quantum relative entropy can also be used as a witness of non-Markovianity [21].

While the Lindblad theory introduced here has many applications in the field of open quantum systems, it presents several limitations when applied to quantum thermodynamics. In some of the more promising experimental realisations of quantum heat engines, heat transfer is accomplished in strong coupling between systems of spins and reservoirs. An example is provided by the recent experiment consisting of a single spin heat engine coupled to a harmonic oscillator flywheel, where the spin polarisation is controlled via optical pumping, implying strong incoherent coupling between spin and reservoirs [24]. Moreover, research has shown that non-Markovian effects can be used to extract work from a single bath via quantum measurements [25, 26]. Quantum correlations, whose build up can lead to non-unitarity and to non-Markovian system dynamics, are linked to the enhancement of work extraction and the efficiency of quantum heat engines, as has been studied, for example, in Otto cycles [27]. Non-Markovian information back-flow has

been linked to quantum thermodynamic quantities, for example, it has been shown that memory effects lead to revivals of extractable work [10]. Due to its experimental importance in the development of quantum heat engines, the thermodynamics of non-Markovian processes will be the main topic of discussion in the following chapters.

3 | Numerical methods for quantum dynamical calculations of open systems

There exist several techniques for calculating the non-Markovian dynamics of an open system. However, many of these techniques rely on some form of approximation. These include the expansion method, the projection-operator method, and embedding methods, among others [12]. One of the main limitations of these methods is that they cease to be valid for strong coupling between open system and environment, or require a truncation in the expansion of a perturbative parameter to a certain order. Path integral methods, on the other hand, allow for a framework which does not require any particular assumptions on the coupling. The only necessary assumptions are that of a factorized initial state, and that of an initial thermal equilibrium state for the environment. Path integral methods are the basis of numerical simulations of non-Markovian quantum dynamics. Here we will focus on one particular exact numerical method, the TEMPO algorithm.

3.1 Feynman's path integral formulation

The path integral formalism [28, 29] was first used by Feynman and Vernon to calculate the dynamics of a system coupled to a second external system, such as a measuring apparatus [30]. It is based on the consideration that given two space-

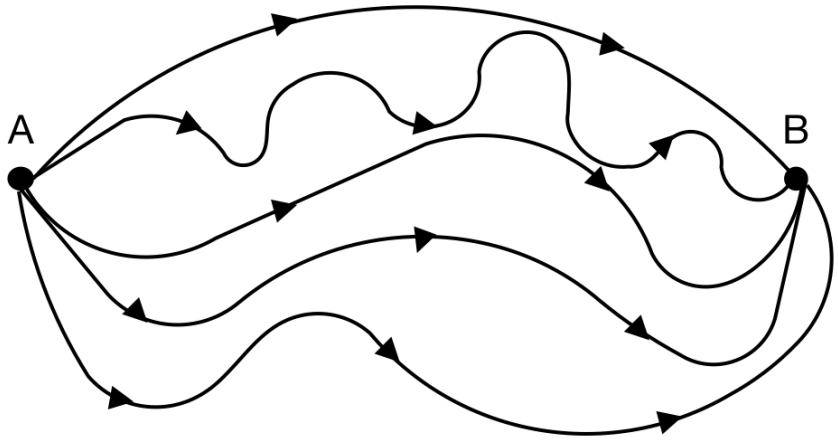

Figure 3.1: Representation of some possible path-integral trajectories between a point A and a point B.

time points $A = (x_0, t_0)$ and $B = (x_f, t_f)$, the total transition probability amplitude between a single system's states $|\psi(A)\rangle$ and $|\psi(B)\rangle$ is given by the sum of the amplitudes arising from all the possible trajectories the system can take from point A to point B. This concept is schematically illustrated in Fig. 3.1. For example, a final state $|\psi(B)\rangle$, assumed to be an eigenstate of the position operator $\hat{x}$, is then

$$|\psi(x_f, t_f)\rangle = \int_{-\infty}^{\infty} |\psi(x', t_f)\rangle\langle\psi(x', t_f)|\psi(x_0, t_0)\rangle dx'. \tag{3.1}$$

The term $\langle\psi(x', t_f)|\psi(x_0, t_0)\rangle$ is defined to be the propagator of the quantum system [28]. Finding the form of this propagator is the crux of the path integral method. In order to do so, it is useful to start from classical mechanics.

In classical mechanics, the specific path $x(t)$ followed by a system is determined through the principle of least action, that is, $x(t)$ is the path for which the action is minimized. In Lagrangian formalism, the action is defined as

$$S(x) = \int_{t_0}^{t_f} L(\dot{x}, x, t)\, dt, \tag{3.2}$$

where $L(\dot{x}, x, t)$ is the Lagrangian of the system. The coordinate x can be generic and does not necessarily represent a space coordinate. Suppose such a coordinate deviates from the path $x(t)$ by an amount $\delta x(t)$, with the condition that at initial and final times the coordinate remains equal to a fixed value and thus $\delta x(t_0) = \delta x(t_f) = 0$. The assumption that $x(t)$ is an extremum of function (3.2) implies that $\delta S = 0$, from which the classical Lagrangian equation of motion is derived,

$$\frac{d}{dt}\frac{\partial L}{\partial \dot{x}} - \frac{\partial L}{\partial x} = 0. \tag{3.3}$$

The followed path $x(t)$ is determined by the solution to Eq. (3.3) [28]. In quantum mechanics, however, all possible paths contribute to the trajectory at different phases. Such phases are $\phi(x) = C\exp[iS(x)]$, with C a constant, and thus dependent to the action Eq. (3.2). The amplitude for the system to go from coordinate $x(t_0)$ to coordinate $x(t_f)$ is defined as the sum over all the possible paths $x(t)$ in coordinate space that start in $x(t_0)$ and end in $x(t_f)$, $K(x_f, t_f; x_0, t_0) = \sum_{x(t)} \phi(x)$. The probability amplitude for the system to transition from the state $\psi(x_0, t_0)$ to the state $\psi(x_f, t_f)$ is then given by $P(x_f, t_f; x_0, t_0) = \mid K(x_f, t_f; x_0, t_0) \mid^2$ [28].

It is possible to approximate the sum $K(x_f, t_f; x_0, t_0)$ to multiple integrals with the introduction of a normalizing factor, as argued in reference [28]. The sum over all paths can then be rewritten as

$$K(x_f, t_f; x_0, t_0) = \int \exp[iS(x)]\mathcal{D}x\,(t), \tag{3.4}$$

where $\mathcal{D}x\,(t)$ is a measure of the space of all paths. Eq. (3.4) is called a path integral, also referred to as a kernel.

The basic concept of Eq. (3.1) can be extended to the theory of open quantum systems coupled to an external environment. Of course, this adds the complication of a dynamics where the degrees of freedom of the environment need to be included.

3.2 Influence functional in quantum mechanics

For an open system coupled to a second system, for example to an environment, the effects of the interaction are described in the path integral by a functional known as the influence functional [30]. Let us assume a density matrix $\hat{\rho}(t)$ describing the composite system, and define s and u the generic coordinates of the open system and environment respectively. Assuming a total Hamiltonian of the form of Eq. (2.2), the composite density matrix evolves in time according to Eq. (2.6). The density matrix element between the coordinate eigenstate $|s_f, u_f\rangle$ and the coordinate eigenstate $\left|s'_f, u'_f\right\rangle$ at a time t_f is [1]

$$\left\langle s_f, u_f\right|\hat{\rho}(t_f)\left|s'_f, u'_f\right\rangle = \int ds_0 \int du_0 \int ds'_0 \int du'_0 \left\langle s_f, u_f\right| e^{-i\hat{H}\left(t_f - t_0\right)} \left|s_0, u_0\right\rangle \times \\ \left\langle s_0, u_0\right| \hat{\rho}\left(t_0\right) \left|s'_0, u'_0\right\rangle \left\langle s'_0, u'_0\right| e^{i\hat{H}\left(t_f - t_0\right)} \left|s'_f, u'_f\right\rangle, \tag{3.5}$$

where resolutions of the identity operator have been inserted into the time evolution of $\hat{\rho}$. The kernel is by definition $K(s_f, u_f, t_f; s_0, u_0, t_0) = \left\langle s_f, u_f\right| e^{-i\hat{H}\left(t_f - t_0\right)} \left|s_0, u_0\right\rangle$. In order to retrieve the time evolution of the reduced density matrix elements from Eq. (2.6), the environmental coordinate u is traced over,

$$\left\langle s_f\right|\hat{\rho}_S(t_f)\left|s'_f\right\rangle = \int du_f \int ds_0 \int du_0 \int ds'_0 \int du'_0 K(s_f, u_f, t_f; s_0, u_0, t_0) \times \\ \left\langle s_0, u_0\right| \hat{\rho}\left(t_0\right) \left|s'_0, u'_0\right\rangle K^*(s'_f, u_f, t_f; s'_0, u'_0, t_0). \tag{3.6}$$

The Lagrangian can be separated into an open system, an environment and an interaction contribution. By virtue of Eq. (3.2), the action can also be separated as $S(s,u) = S_S(s) + S_B(u) + S_I(s,u)$. Consequently, the kernel can be written as

$$K(s_f, u_f, t_f; s_0, u_0, t_0) = \int \exp\left[iS_S\left(s\right) + iS_B\left(u\right) + iS_I(s,u)\right] \mathcal{D}s\left(t\right) \tag{3.7}$$

from Eq. (3.4). With the assumption of a factorized initial state as in Eq. (2.6), the environmental coordinates can be separated from the system ones,

$$\left\langle s_f \middle| \hat{\rho}_S(t_f) \middle| s'_f \right\rangle = \int \mathcal{D}s\,(t) \int \mathcal{D}s'\,(t) \int ds_0 \int ds'_0 \\ I(s,s') \exp[iS_S(s) - iS_S(s')] \left\langle s_0 \right| \hat{\rho}_S\,(t_0) \left| s'_0 \right\rangle, \tag{3.8}$$

where the influence functional is defined to be [30]

$$I(s,s') = \int \mathcal{D}u\,(t) \int \mathcal{D}u'\,(t) \int du_0 \int du'_0 \int du_f \int du'_f \delta(u_f - u'_f) \times \\ \exp[iS_B(u) + iS_I(s,u) - iS_B(u') - iS_I(s',u')] \left\langle u_0 \right| \hat{\rho}_B\,(t_0) \left| u'_0 \right\rangle. \tag{3.9}$$

The coordinates of the environment are enclosed into $I(s,s')$, therefore the influence functional describes the environmental effects on the open system. It can in general be written as $I(s,s') = \exp[i\Phi(s,s')]$, where $\Phi(s,s')$ is an influence phase [30]. This Feynman-Vernon influence functional is well suited to numerically discretized approaches such as QuAPI [13, 14], upon which the TEMPO algorithm is built [16].

3.3 Quasiadiabatic propagator path integral (QuAPI) discretization

The QuAPI approach allows for the time evolution of the reduced density matrix to be calculated through iterative tensor propagation [13, 14]. The construction of a reduced density tensor starts with the discretization of the path integral. The total time $t_f - t_0$ of the quantum dynamics is divided into a number N of time-steps of equal length Δ, such that $t_f - t_0 = N\Delta$. The unitary time evolution operator in Eq. (2.5) is expressed in terms of the time-step Δ as $\hat{U}(N\Delta) = \exp[-i\hat{H}\Delta]^N$. In order to obtain the QuAPI scheme, the degrees of freedom of the open system need to be separated from those of its surroundings and the coupled degrees of freedom, by defining a Hamiltonian $\hat{H}_{env} = \hat{H} - \hat{H}_S$ that includes all of the environmental degrees of free-

dom. The operator $\exp[-i\hat{H}\Delta]$ can be expanded in terms of the Hamiltonians $\hat{H}_S$ and $\hat{H}_{env}$ according to the Baker-Campbell-Hausdorff formula [31]. Taking the Taylor expansion of the terms up to an order of Δ^2, it is easy to see that the resulting terms are expansions of exponential functions truncated at order Δ^2. This leads to a symmetrized Trotter splitting, where the error caused by the approximation is of the order $\mathcal{O}\left(\Delta^3\right)$,

$$e^{-i\hat{H}\Delta} = e^{-i\hat{H}_{env}\Delta/2}e^{-i\hat{H}_S\Delta}e^{-i\hat{H}_{env}\Delta/2} + \mathcal{O}\left(\Delta^3\right). \tag{3.10}$$

The Trotter splitting described in Eq. (3.10) is the first of the approximations made in the QuAPI method. A few assumptions on the initial state of the system are often added. The first is that of a factorized initial condition. Secondly, as the QuAPI method is primarily used to describe the dynamics of finite-level systems coupled to bosonic reservoirs [15], the environment is assumed to be a bosonic bath of harmonic oscillators of some inverse temperature β. Thus the initial state of the bath is taken to be the thermal equilibrium state $\hat{\rho}_B(0) = e^{-\beta\hat{H}_B}/Z_B$, with $Z_B = \mathrm{Tr}_B[e^{-\beta\hat{H}_B}]$.

3.3.1 Discretization of the propagators

The discretization of the propagators previously defined as $K(s_f, u_f, t_f; s_0, u_0, t_0) = \langle s_f, u_f | \, e^{-i\hat{H}\left(t_f - t_0\right)} \, |s_0, u_0\rangle$ follows from the time discretization and the symmetrized Trotter splitting described in Eq. (3.10). Let us define $|s_k\rangle$ the open system coordinate eigenstate at time $t_k - t_0 = k\Delta$, such that $|s_k\rangle = |s\left(t_k\right)\rangle$, with $k = 0, 1...N$. Similarly we can define the eigenstates of the environment $|u_k\rangle$ for any time $t_k - t_0$. It follows that the quasiadiabatic propagator in the time interval $t_k - t_{k-1}$ is

$$\begin{aligned}\langle s_k, u_k|e^{-i\hat{H}\Delta}|s_{k-1}, u_{k-1}\rangle = \\ \langle s_k|e^{-i\hat{H}_S\Delta}|s_{k-1}\rangle\langle u_k|e^{-i\hat{H}_{env}(s_k)\Delta/2}e^{-i\hat{H}_{env}(s_{k-1})\Delta/2}|u_{k-1}\rangle.\end{aligned} \tag{3.11}$$

Here we have defined $\hat{H}_{env}|s, u\rangle = \hat{H}_{env}(s)|u\rangle$. The coordinates of the open system can then be separated from the coordinates of the environment in the expression for

the total propagator over the time interval $t_f - t_0$,

$$K(s_f, u_f, t_f; s_0, u_0, t_0) = \int ds_1 \int ds_2 ... \int ds_{N-1} \int du_1 \int du_2 ... \int du_{N-1} \prod_{k=1}^{N} \langle s_k | e^{-i\hat{H}_S \Delta} | s_{k-1} \rangle \langle u_k | e^{-i\hat{H}_{env}(s_k)\Delta/2} e^{-i\hat{H}_{env}(s_{k-1})\Delta/2} | u_{k-1} \rangle. \tag{3.12}$$

A similar expression can be found for the complex conjugate propagator $K^*(s'_f, u_f, t_f; s'_0, u'_0, t_0)$ in Eq. (3.6). We will adopt the convention, used in the literature, to label s^+ the coordinates appearing in the forward-in-time propagator $K(s^+_f, u_f, t_f; s^+_0, u'_0, t_0)$ and s^- the coordinates appearing in its complex conjugate [13, 14].

3.3.2 Discretized influence functional

Following Eq. (3.9), the environmental coordinates from the propagators in the QuAPI formalism are enclosed into an influence functional. From Eq. (3.6) and the discretization obtained in Eq. (3.12), it follows that such Feynman influence functional is [13]

$$\begin{aligned} I(s^+_0 ... s^+_N; s^-_0 ... s^-_N) = &\mathrm{Tr}_B [e^{-i\hat{H}_{env}(s^+_N)\Delta/2} e^{-i\hat{H}_{env}(s^+_{N-1})\Delta} ... e^{-i\hat{H}_{env}(s^+_0)\Delta/2} \\ &\hat{\rho}_B(0) e^{i\hat{H}_{env}(s^-_0)\Delta/2} ... e^{i\hat{H}_{env}(s^-_{N-1})\Delta} e^{i\hat{H}_{env}(s^-_N)\Delta/2}]. \end{aligned} \tag{3.13}$$

The discretized form of Eq. (3.13) can be equivalently written as the exponential of an influence phase [13, 15], under the assumption of $\hat{\rho}_B(0)$ being a thermal equilibrium state,

$$I(s^+_0 ... s^+_N; s^-_0 ... s^-_N) = \exp\left[- \sum_{k=0}^{N} \sum_{k'=0}^{k} (s^+_k - s^-_k)(\eta_{k-k'} s^+_{k'} - \eta^*_{k-k'} s^-_{k'}) \right], \tag{3.14}$$

where the coefficients $\eta_{k-k'}$ depend on the bath autocorrelation function and describe the non-Markovian effects in the open system between time-steps k and k'.

These coefficients are defined as

$$\eta_{k-k'} = \begin{cases} \int_{t_{k-1}}^{t_k} \int_{t_{k'-1}}^{t_{k'}} C\left(t' - t''\right) dt'' dt' & k \neq k' \\ \\ \int_{t_{k-1}}^{t_k} \int_{t_{k-1}}^{t'} C\left(t' - t''\right) dt'' dt' & k = k', \end{cases} \tag{3.15}$$

where $C\left(t\right)$ is the bath autocorrelation function

$$C\left(t\right) = \int_0^\infty d\omega J\left(\omega\right) \left(\coth\left(\frac{\omega}{2T}\right) \cos\left(\omega t\right) - i \sin\left(\omega t\right)\right). \tag{3.16}$$

Here $J\left(\omega\right)$ is the spectral density function characterizing the bath [13], defined as

$$J\left(\omega\right) = \sum_j g_j^2 \delta\left(\omega - \omega_j\right), \tag{3.17}$$

where g_j is a constant associated with the coupling between the system and the j-th bath mode, and ω_j the mode's angular frequency.

3.3.3 Augmented reduced density tensor (ADT) iterative propagation

For a bosonic bath of harmonic oscillators, non-local interactions contained in the influence functional Eq. (3.14) have a finite temporal range for any temperature [13]. Indeed, even in the presence of a non-Markovian dynamics, dissipative effects tend to erase quantum coherence and correlations decay in finite time. It follows that memory effects are erased over a long enough time period. This means that long time-distant interactions can be neglected, and in the discretized form of Eq. (3.14) one can introduce a maximum number of steps $|k - k'|$ beyond which the coefficients $\eta_{k-k'}$ defined in Eq. (3.15) decrease rapidly, rendering $I(s_0^+ ... s_N^+; s_0^- ... s_N^-)$ effectively equal to an identity operator [13, 14]. Such maximum number of steps, which is defined as the memory cutoff K, is roughly equivalent to τ_C/Δ, where τ_C is the bath correlation time cutoff. Therefore $\eta_{k-k'}$ can be neglected for any $|k - k'| > K$.

It follows that the QuAPI method introduces, along with a Trotter splitting error of the order of $\mathcal{O}\left(\Delta^3\right)$, a finite memory approximation. Such an approximation allows for a description of the quantum system by means of an augmented density tensor (ADT), and for a description of its dynamics as an iterative tensor contraction with a propagator tensor derived from the non-local influence functional in Eq. (3.14) [13, 14]. The use of a propagator tensor resolves the issue of simulating a non-Markovian and non-unitary dynamics. Furthermore, scaling the ADT with a finite memory cutoff K allows for high numerical efficiency in the tensor multiplication scheme [15, 16].

The discretized influence functional subjected to the memory cutoff can be written as $I\left(s_0^+,...s_N^+;s_0^-,...s_N^-\right)=\prod_{\Delta k=0}^{K}\prod_{k=0}^{N-\Delta k}I_{\Delta k}\left(s_k^{\pm},s_{k+\Delta k}^{\pm}\right)$, with $\Delta k=k-k'$ and

$$I_{\Delta k}\left(s_k^{\pm},s_{k+\Delta k}^{\pm}\right)=\exp\left[-\left(s_{k+\Delta k}^{+}-s_{k+\Delta k}^{-}\right)\left(\eta_{\Delta k}s_k^{+}-\eta_{\Delta k}^{*}s_k^{-}\right)\right]. \tag{3.18}$$

The ADT at time t_k is constructed by building a rank-K tensor whose elements are the vectorized reduced density matrices $\hat{\rho}_S$ at time t_k and at the previous $K-1$ times. We will refer to such an ADT as $A^{(K)}$, with initial condition $A^{(K)}\left(s_0^{\pm},s_1^{\pm}...s_{K-1}^{\pm};0\right)=\left\langle s_0^{+}\right|\hat{\rho}_S\left(0\right)\left|s_0^{-}\right\rangle$ at $t_0=0$. A rank-2K propagator tensor $B^{(2K)}$ is then constructed as [13, 14, 16]

$$B^{(2K)}\left(s_k^{\pm},s_{k+1}^{\pm}...s_{k+2K-1}^{\pm}\right)=\prod_{n=k}^{k+K-1}\left(G\left(s_n^{\pm},s_{n+1}^{\pm}\right)\prod_{\Delta k=0}^{K}I_{\Delta k}\left(s_n^{\pm},s_{n+\Delta k}^{\pm}\right)\right), \tag{3.19}$$

where the free propagators for the open system are

$$G\left(s_n^{\pm},s_{n+1}^{\pm}\right)=\left\langle s_{n+1}^{+}\right|e^{-i\hat{H}_S\Delta}\left|s_n^{+}\right\rangle\left\langle s_n^{-}\right|e^{i\hat{H}_S\Delta}\left|s_{n+1}^{-}\right\rangle. \tag{3.20}$$

The time evolution of the reduced tensor $A^{(K)}$ up to a time $t_k = k\Delta$, constructed through time increments of $K\Delta$, is

$$A^{(K)}(s^{\pm}_{k+K}, s^{\pm}_{k+K+1}...s^{\pm}_{k+2K-1}; (k+K)\,\Delta) = \sum_{s^{\pm}_k, s^{\pm}_{k+1}...s^{\pm}_{k+K-1}} B^{(2K)}\left(s^{\pm}_k, ..s^{\pm}_{k+2K-1}\right) A^{(K)}\left(s^{\pm}_k, ...s^{\pm}_{k+K-1}, k\Delta\right). \tag{3.21}$$

The reduced density matrix element at a final time $t_f = N\Delta$ is retrieved from the propagated ADT, by tracing out the $s^{\pm}_k$ system coordinates for $k > N$,

$$\left\langle s^{+}_N\right| \hat{\rho}_S\left(t\right) \left|s^{-}_N\right\rangle = I_0\left(s^{\pm}_N, s^{\pm}_N\right) \sum_{s^{\pm}_{N+1},...,s^{\pm}_{N+K-1}} A^{(K)}\left(s^{\pm}_N, s^{\pm}_{N+1}, ..., s^{\pm}_{N+K-1}; t_f\right). \tag{3.22}$$

If the dimension of the system Hilbert space is d, the dimension of the ADT is d^{2K} and that of the propagator tensor is d^{4K}.

3.4 Time-evolving matrix product operator (TEMPO) algorithm

Starting from the ADT iterative propagation scheme of the QuAPI method, Strathearn *et al.* developed a numerically exact technique to model non-Markovian dynamics of open quantum systems coupled to harmonic baths, and demonstrated the efficiency of the approach with an application to the spin-boson model [16]. The algorithm, called TEMPO, represents a significant improvement to the ADT propagation scheme. The limiting factor for QuAPI is the computational resources needed to store and perform contractions on K-index tensors. TEMPO circumvents this limitation by representing the ADT and the propagators as tensor networks, which can be stored and contracted with drastically reduced resources, enabling very large values of K to be reached. The tensor-network representation is efficient due to the finite range of temporal correlations contained in the ADT. This is analogous to the well-known ability of tensor networks to represent many-body quantum

states exhibiting short-ranged spatial correlations [32]. In the present case, the bond dimension, i.e. the number of singular values retained during the construction of the tensor network, quantifies correlations between different time points induced by the non-Markovian environment. The bond dimension is controlled by retaining only those singular values λ greater than a cutoff λ_C. The cutoff is defined as $\lambda_C = \lambda_{\max} 10^{-p/10}$, with $\lambda_{\max}$ the highest singular value. The accuracy of the TEMPO algorithm is therefore controlled by the exponent p as well as the memory depth K and the numerical time step Δ. In the following, we explain more in detail the construction of the ADT propagation scheme in TEMPO and its parameters. This approach will be the basis for our modified quantum heat statistics calculations.

3.4.1 Superoperator algebra

The correlation functions in the influence functional Eq. (3.14) are easily calculated with superoperator algebra formalism. Let $\hat{K}$ be a superoperator acting on the space of bounded operators $\mathcal{B}(\mathcal{H})$ on a Hilbert space $\mathcal{H}$. Then two superoperators labelled left, $\hat{K}^L$, and right, $\hat{K}^R$, can be defined by their actions on a density matrix operator $\rho \in \mathcal{B}(\mathcal{H})$:

$$\hat{K}^L \rho = \hat{K} \rho, \tag{3.23}$$

$$\hat{K}^R \rho = \rho \hat{K}. \tag{3.24}$$

Similarly, the superoperators $\hat{K}^+$ and $\hat{K}^-$ can be defined as

$$\hat{K}^+ \rho = \hat{K}^L \rho + \hat{K}^R \rho = \left\{ \hat{K}, \rho \right\}, \tag{3.25}$$

$$\hat{K}^- \rho = \hat{K}^L \rho - \hat{K}^R \rho = \left[\hat{K}, \rho \right], \tag{3.26}$$

with inverse transformations

$$\hat{K}^L\rho = \frac{1}{2}\left(\hat{K}^+ + \hat{K}^-\right)\rho = \frac{1}{2}\left[\hat{K},\rho\right] + \frac{1}{2}\left\{\hat{K},\rho\right\}, \tag{3.27}$$

$$\hat{K}^R\rho = \frac{1}{2}\left(\hat{K}^+ - \hat{K}^-\right)\rho = \frac{1}{2}\left\{\hat{K},\rho\right\} - \frac{1}{2}\left[\hat{K},\rho\right]. \tag{3.28}$$

3.4.2 Time evolution of the reduced density matrix in superoperator formalism

With the superoperator formalism, it is possible to express the solution to the Liovillian equation Eq. (2.8) in terms of bath autocorrelation functions that can in turn easily be applied into the influence functional and discretized [15]. From Eq. (2.9), the time evolution of the total density matrix in the interaction picture $\tilde{\hat{\rho}}(t) = e^{i(\hat{H}_S+\hat{H}_B)t}\hat{\rho}(t)e^{-i(\hat{H}_S+\hat{H}_B)t}$ is

$$\tilde{\hat{\rho}}(t) = \overleftarrow{T}\exp\left[\int_{t_0}^{t} dt'\mathcal{L}_I\left(t'\right)\right]\tilde{\hat{\rho}}\left(t_0\right), \tag{3.29}$$

where $\mathcal{L}_I$ is the interaction part of the Liouvillian operator. With the assumption of a factorized initial condition Eq. (2.11), the time evolution of the reduced density matrix can be written in the convenient notation $\tilde{\hat{\rho}}_S\left(t\right) = \overleftarrow{T}_S\left\langle\exp\left[\int_{t_0}^{t} dt'\mathcal{L}_I\left(t'\right)\right]\right\rangle_B \tilde{\hat{\rho}}_S\left(t_0\right)$, where the trace over the bath degrees of freedom is in the average defined as $\left\langle\hat{O}\right\rangle_B = \mathrm{Tr}_B\left[\overleftarrow{T}_B\hat{O}\tilde{\hat{\rho}}_B\left(t_0\right)\right]$ for a generic operator $\hat{O}$. In this notation we have chosen the time ordering $\overleftarrow{T} = \overleftarrow{T}_S\overleftarrow{T}_B$. For a bath of harmonic modes, the environmental coordinates are Gaussian variables [13, 14], that is, variables with normal probability distribution. The average value of the exponential function $\exp X = \exp\left[\int_{t_0}^{t} dt'\mathcal{L}_I\left(t'\right)\right]$ can be written as an exponential of the cumulants of X, $\langle\exp X\rangle = \exp\left[\sum_j \frac{1}{j!}\langle X^j\rangle\right]$ [33]. In particular, for Gaussian variables with normal distribution, cumulants with order higher than second ($j > 2$) are zero. It follows the identity $\langle\exp X\rangle = \exp[\langle X\rangle + \frac{1}{2}\langle X^2\rangle]$ [33]. Since it is possible to shift the Gaussian variable function mean value to centre $\langle X\rangle = 0$, it follows that

$$\tilde{\hat{\rho}}_S\left(t\right) = \overleftarrow{T}_S\exp\left[\int_{t_0}^{t} dt'\int_{t_0}^{t} dt''\left\langle\mathcal{L}_I\left(t'\right)\mathcal{L}_I\left(t''\right)\right\rangle_B\right]\tilde{\hat{\rho}}_S\left(t_0\right). \tag{3.30}$$

The exponential function term in Eq. (3.30) is the continuous equivalent of the influence functional described in Eq. (3.14). The terms $\langle \mathcal{L}_I(t')\,\mathcal{L}_I(t'')\rangle_B$ are the bath autocorrelation functions, which in the case of a bosonic bath are given by Eq. (3.16). Indeed $C(t)$ can be calculated by noticing that $\mathcal{L}_I = \hat{H}_I^L - \hat{H}_I^R$ and applying the superoperator algebra to the operators of the interaction Hamiltonian.

3.4.3 ADT propagation scheme in the TEMPO algorithm

The memory depth of the environmental effects that can be stored during the calculation is improved by representing Eq. (3.21) through matrix product states (MPS) [15, 16]. Matrix product states are states whose probability amplitude is defined in terms of the trace of a product of N square matrices, where N is the number of particles in the system [34]. In reference [16], the procedure through which the ADT is then decomposed through singular value decomposition (SVD) and truncated is discussed. The ADT propagation scheme applied in the TEMPO algorithm is described in references [15] and [16], and is here summarized. Consider $A^{\sigma_n\sigma_{n-1}\cdots\sigma_0}$ the ADT written in the MPS representation and to which the SVD cutoff λ_C has been applied. Here the "superindex" $\sigma_k = \{s_k^+, s_k^-\}$ takes d^2 possible values, where d is the dimension of the system. The time evolution is given by successive contractions with a propagation tensor, followed by an SVD and the application of the cutoff λ_C at each step. The propagator tensor is represented as a matrix product operator (MPO) and is constructed from the QuAPI theory tensor Eq. (3.19) as

$$B^{\sigma_n\cdots\sigma_0}_{\mu_{n-1}\cdots\mu_0} = \left(\prod_{k=1}^{n}\delta^{\sigma_{n-k}}_{\mu_{n-k}}\right) G(s_n^{\pm}, s_{n-1}^{\pm}) \prod_{\Delta k=0}^{n} I_{\Delta k}(s_n^{\pm}, s_{n-\Delta k}^{\pm}), \tag{3.31}$$

with δ^{σ}_{μ} the Kronecker delta symbol. The ADT at the nth time step is given by the contraction $A^{\sigma_n\cdots\sigma_0} = B^{\sigma_n\cdots\sigma_0}_{\mu_{n-1}\cdots\mu_0} A^{\mu_{n-1}\cdots\mu_0}$, with the Einstein summation convention assumed, and is built iteratively starting from the initial condition $A^{\sigma_0} = I_0(s_0^{\pm}, s_0^{\pm})\,\langle s_0^+|\hat{\rho}_S(0)|s_0^-\rangle$. The reduced density matrix is found by summing over all but the final index, i.e., $\langle s_N^+|\hat{\rho}_S(t)|s_N^-\rangle = \sum_{\sigma_0,\cdots,\sigma_{N-1}} A^{\sigma_N\cdots\sigma_0}$. Due to the finite memory depth

K, the propagator (3.31) acts non-trivially on at most K indices of the ADT, since $I_{\Delta k}(s_n^{\pm}, s_{n-\Delta k}^{\pm}) \approx 1$ for $\Delta k > K$. At the n-th time step, therefore, when $n > K$ one needs only to store the object $A^{\sigma_n \cdots \sigma_{n-K}}$, with the remaining indices summed over. (For the first K time steps one stores the full ADT).

4 | Classical and quantum thermodynamics

The main topic of research in this thesis is the thermodynamics of open systems, with a particular focus on the statistics of thermodynamic quantities. Classical thermodynamics describes the average properties of a macroscopic system derived from the statistical mechanics of its microscopic components. A macroscopic system is a system with a large enough number of particles, in general defined by a finite number of parameters, or state variables. Some examples of state variables are the system's particle number, its pressure, its volume and its temperature. Equations of state relate these quantities to one another. A macroscopic system's state is defined by a set $\{X_j\}$ of extensive state variables, each being a function of the points of the system's phase space (for example, momentum and position coordinates). These state variables completely define the region of phase space in which the time evolution takes place. For a fixed macroscopic state, we can define Ω as the number of microscopic configurations accessible to the system, each characterized by a probability p. The volume of the relevant region in phase space then corresponds to the measure of the ensemble of Ω microscopic states.

Thermodynamic definitions can only be applied to systems in equilibrium, that is, systems in which the state variables are constant in time. In this case the system transforms infinitesimally close to its thermal equilibrium state. These transformations are reversible, as the system can always be reversed to its previous state without changing the thermodynamic state of the rest of the universe. Nonequilibrium

thermodynamics, on the other hand, is characterized by irreversible transformations. The system changes from one equilibrium state to another, and cannot be brought back to the previous state without causing a change to the thermodynamic state of the universe. Fluctuations theorems give an insight into the behaviour of nonequilibrium thermodynamic quantities [35].

4.1 Entropy, work and heat and the laws of thermodynamics

Thermodynamic state functions are defined through the laws of thermodynamics and connected to thermodynamic variables. The *zero-th law of thermodynamics* states that equilibrium is a transitive property. The *first law of thermodynamics* is the conservation of energy law, and defines the change of the state function of internal energy ΔU. It states that the change in the system's internal energy is given by the work W performed on the system minus the heat energy Q absorbed by the environment during the process. W and Q are thermodynamic variables. In differential form,

$$dU = \delta W - \delta Q, \tag{4.1}$$

where δW and δQ are infinitesimal changes.

In classical thermodynamics, entropy is an extensive state function conjugate to the temperature T that defines the spontaneous evolution of a system. For an open system interacting with an environment, its variation is given by two contributions, $\Delta S = \Delta S_e + \Delta S_i$. ΔS_e is the external entropy variation cause by entropy flow due to the interaction with the system's surroundings. ΔS_i is the internal entropy variation, caused by changes inside the system [36]. To define these two quantities and the second law of thermodynamics, consider a system in contact with a bath at inverse temperature $\beta = 1/T$ undergoing a closed reversible cyclic process. By approximating the process as a series of adjacent isoentropic and isothermal transformations, each characterized by an infinitesimal exchange in heat $-\delta Q$ taken in by

the system from the bath at temperature T, the total heat exchanged in the process must be null. For every transformation corresponds, due to reversibility, a transformation with opposite sign. This is true whatever the reversible transformation that occurs, that is, the value of the cyclic integral of the exchanged heat over bath temperature $\oint_{rev} \beta\delta Q = 0$ is path independent [37]. The inverse temperature β is the integrating factor which transforms the inexact differential δQ into an exact differential [38]. It follows that the integrand function $\beta\delta Q$ is an exact differential, which can be defined as the infinitesimal entropy variation of the system. Because such entropy depends only on the interaction of the system with its external environment, it can be identified with the external entropy infinitesimal variation, $dS_e = -\beta\delta Q$. It follows that

$$\Delta S_e = -\int_{rev} \beta\delta Q. \tag{4.2}$$

For an isolated system, $\Delta S_e = 0$. The external entropy variation is clearly associated with reversible entropy production. On the other hand, ΔS_i is associated with irreversible entropy production [39], which we define as

$$\delta\Sigma \equiv \delta S_i = dS + \beta\delta Q. \tag{4.3}$$

The *second law of thermodynamics* states that the irreversible entropy production of a system, or equivalently the entropy production in an isolated system, is always non-negative,

$$\Delta S_i \geq 0, \tag{4.4}$$

where equality holds for reversible processes. Lastly, the *third law of thermodynamics* states that it is impossible to reach absolute zero temperature via a finite number of reversible processes.

4.1.1 Classical ensemble averages

In the continuous limit, rather than a discrete set of probabilities associated with the system's microscopic states, the relevant volume in phase space that the system can

occupy is weighted by a probability density $\rho(q, p, t)$, where (q, p) are the position and momentum coordinates. For a system of N particles, the probability of finding the microscopic state of the system in a volume $d^{3N}q\, d^{3N}p$ around the point (q, p) at time t is $\rho\,(q, p, t)\, d^{3N}q\, d^{3N}p$. The average of any quantity $f\,(q, p, t)$ is given by the ensemble average

$$\langle f \rangle\,(t) = \frac{\int f\,(q, p)\ \rho\,(q, p, t)\, d^{3N}q\, d^{3N}p}{\int \rho\,(q, p, t)\, d^{3N}q\, d^{3N}p}, \tag{4.5}$$

where the integration is taken over all the phase space. In nonequilibrium processes, thermodynamic variables like exchanged heat and work are in fact averages over an ensemble of measurements of stochastic variables Q and W, expressed by Eq. (4.5). In Eq. (4.1) we have given the differential form of the first law of thermodynamics. In terms of average quantities over the total process, the first law is

$$\Delta U = \langle W \rangle - \langle Q \rangle. \tag{4.6}$$

Similarly, the average irreversible entropy production is, from Eq. (4.3),

$$\langle \Sigma \rangle = \Delta S + \beta \langle Q \rangle. \tag{4.7}$$

Given the inequality in (4.4), the second law can be written as $\langle \Sigma \rangle \geq 0$, where $\Delta S_i = \langle \Sigma \rangle$ and $\Delta S_e = -\beta \langle Q \rangle$. The probability density $\rho(q, p, t)$ depends on the nature of the ensemble of microscopic states Ω. In the study of open systems coupled to thermal baths, the relevant one is most often the canonical ensemble. The canonical ensemble is an ensemble at thermal equilibrium with bath of temperature T, whose number of particles N and volume V are constant. The energy probability distribution of its microscopic states is given by the Boltzmann distribution.

4.2 Thermodynamic equilibrium

Canonical ensembles describe by definition systems in thermal equilibrium (at constant temperature). On the other hand, definitions of thermodynamic variables are only applicable to systems in equilibrium, where conserved quantities define the macr-oscopic state of the system. The equilibrium state of an isolated system is defined as the state of maximum entropy [35]. If the Ω microscopic states of the system have a discrete set of probabilities $\{p_k\}_{k=1}^{\Omega}$, the associated entropy is the Gibbs entropy

$$S = -k_B \sum_{i=1}^{\Omega} p_i \ln p_i, \tag{4.8}$$

which quantifies the amount of information needed to define the microscopic state of the system. Here $k_B = 1.3807 \cdot 10^{-23} J/K$ is Boltzmann's constant. Starting from the fixed average energy of the system, $\langle E \rangle = \sum_{n=1}^{\Omega} p_n E_n$, where E_n is the energy of the n-th microscopic state, and the normalization $\sum_{n=1}^{\Omega} p_n = 1$, the equilibrium probability distribution of the energy microscopic states is calculated by maximizing Eq. (4.8) using Lagrange multipliers. The result is Boltzmann's probability distribution for every microscopic state,

$$p_n^{eq} = \frac{\exp\left(-\beta E_n\right)}{Z}, \tag{4.9}$$

where $Z = \sum_{n=1}^{\Omega} \exp(-\beta E_n)$ is the partition function.

4.3 Nonequilibrium thermodynamics

Nonequilibrium thermodynamics is defined by irreversible transformations. For open systems coupled to a thermal bath, such transformations are characterized by heat dissipation into the environment. The main feature of nonequilibrium dissipation is the production of positive irreversible entropy, as defined by Eq. (4.7). This entropy production is associated with irreversible work, $\langle \Sigma \rangle = \beta \langle W_{irr} \rangle$ [39, 40], de-

fined as the difference between the total work $\langle W \rangle$ performed on the system during the process and the change in free energy ΔF,

$$\langle W_{irr} \rangle = \langle W \rangle - \Delta F. \tag{4.10}$$

From Eq. (4.10) and the second law of thermodynamics Eq. (4.4), it follows that $\langle W \rangle \geq \Delta F$. The time evolution of the nonequilibrium total entropy production is governed by a local entropy balance equation, which relates the total entropy rate to an "internal" entropy production rate and the divergence of an "external" entropy flow vector [36],

$$\frac{dS}{dt} = \sigma - \nabla \cdot \overrightarrow{J_S}. \tag{4.11}$$

Here $\sigma = dS_i/dt$ is the internal entropy production per unit time, and $\nabla \cdot \overrightarrow{J_S} = -dS_e/dt$ is the divergence of entropy flow vector field.

4.3.1 Fluctuation-dissipation relations

Nonequilibrium processes at the nanoscale feature significant and measurable fluctuations. Therefore, thermodynamic process variables such as work, W, and heat, Q, must be promoted to stochastic quantities described by the corresponding probability distributions, $P(W)$ and $P(Q)$. In thermodynamic equilibrium, the fluctuation-dissipation theorem (FDT) relates fluctuations of thermodynamic observables to the system's response to external perturbations, for example dissipative effects [41]. This theorem is derived from linear response theory. However, extensive work is being done to extend the FDT to nonequilibrium thermodynamics and beyond linear response regime, through fluctuation-dissipation relations (FDRs) [42, 43]. FDRs are generically derived in statistical mechanics, but have validity for quantum systems and quantum thermodynamics. At equilibrium, given a linear perturbation of the system's Hamiltonian $h(\tau)$ at time τ, and an observable O, the FDT states that

$$\frac{dC(s)}{ds} = -TR(s), \tag{4.12}$$

where $C(t,\tau) = \langle O(t)O(\tau)\rangle$ is the autocorrelation function of the observable, $s = t - \tau$, and $R(t,\tau) = \partial\langle O(t)\rangle/\partial h(\tau)|_{h=0}$ is the linear response function. In the work of this thesis the nonequilibrium FDR

$$\langle W\rangle - \Delta F = \frac{\beta\langle\langle W^2\rangle\rangle}{2} \tag{4.13}$$

will be of interest, where $\langle\langle W^2\rangle\rangle = \langle W^2\rangle - \langle W\rangle^2$ is the variance of the work variable W. Eq. (4.13) is derived from the Jarzynski equality $\langle\exp(-\beta W)\rangle = \exp(-\beta\Delta F)$ for Gaussian distributions of work [44].

4.4 Thermodynamics of open quantum systems

The importance of heat management at the nanoscale has grown in tandem with advances in the fabrication and control of small devices, motivating increasing interest in the nonequilibrium thermodynamics of open quantum systems [35, 45–47]. For example, quantum thermal machines have been studied in such diverse experimental platforms as single-electron transistors [48–50], trapped ions [8, 24, 51], superconducting circuits [52], and spin ensembles [53, 54]. Numerous technologically or biologically important systems are also naturally described as quantum heat engines, including lasers [55], light-emitting diodes [56], and light-harvesting complexes [57–60]. These minuscule machines all operate far from equilibrium and are significantly affected by quantum and thermal noise. Strong coupling may blur the boundary between system and environment [61, 62], potentially leading to non-Markovian effects [20, 21] with interesting thermodynamic consequences [4, 10, 11, 63, 64]. In addition, the importance of fluctuations at small scales means that the statistical character of thermodynamic quantities such as work and heat cannot be ignored [65, 66]. These features together give rise to a rich and varied phenomenology with important ramifications for emerging quantum technologies.

The concepts introduced at the beginning of this chapter for classical systems can be translated in the framework of quantum physics. In analogy to classical nonequi-

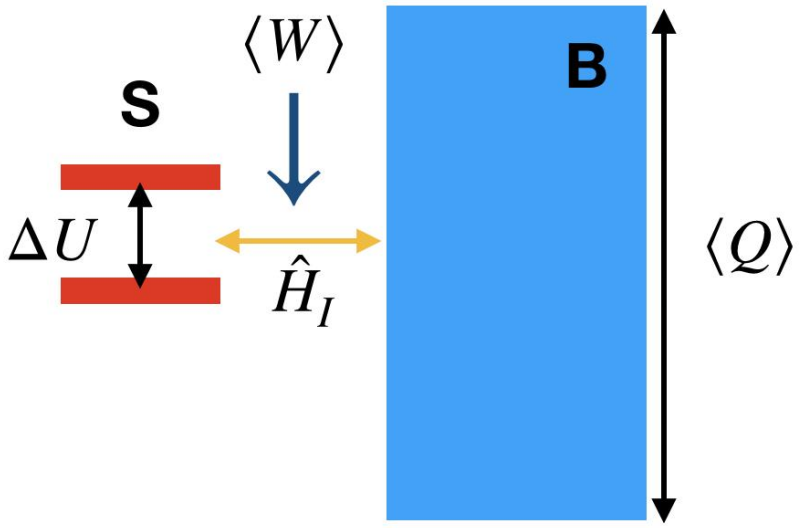

Figure 4.1: Schematic representation of a two-level open quantum system S interacting with a bath B through an interaction Hamiltonian $\hat{H}_I$.

librium thermodynamics, when quantum fluctuations dominate and quantum correlations build up, thermodynamic variables are promoted to stochastic variables described by corresponding probability distributions. Instead of being defined by an ensemble average Eq. (4.5), the mean value at time t is defined as $\langle \bullet \rangle_t \equiv \mathrm{Tr}[\bullet \hat{\rho}(t)]$. The system density matrix $\hat{\rho}$ replaces the classical probability density of the microscopic states. For an open quantum system interacting with a thermal bath at temperature T, thermodynamic quantities like work and exchanged heat are defined in terms of the total system Hamiltonian Eq. (2.2) [17],

$$\langle W \rangle (t) = \int_0^t \mathrm{Tr}_S \left[\hat{\rho}_S(\tau) \frac{d\hat{H}(\tau)}{d\tau} \right] d\tau, \tag{4.14}$$

$$\langle Q \rangle (t) = \int_0^t \mathrm{Tr}_S \left[\frac{d\hat{\rho}_S(\tau)}{d\tau} \hat{H}(\tau) \right] d\tau. \tag{4.15}$$

Eqs. (4.14)-(4.15) are defined for a generic dynamical process. Fig. 4.1 illustrates a set-up in which work and exchanged heat are measured at equilibrium. Here thermodynamic work is associated with changes in the external conditions defining the Hamiltonian, while heat is defined to be the change in energy of the bath. Oper-

ationally, each of these quantities can be extracted from a two-point measurement of $\hat{H}$ (work) or $\hat{H}_B$ (heat) at the beginning and end of the evolution, either with direct projective measurements [67] or via ancillary probes [68–71]. Therefore, under strong-coupling conditions where the commutator $[\hat{H}_B, \hat{H}_I]$ is non-negligible, work and heat are simultaneously measurable only if the system-bath interaction vanishes at the beginning and end of the evolution [62]. This is the relevant scenario for cyclic thermal machines, for example. Considering a relaxation dynamics in which the initial and final states of the system are in thermal equilibrium, the internal energy change of the system is

$$\Delta U = \langle \hat{H}_S \rangle_t - \langle \hat{H}_S \rangle_0. \tag{4.16}$$

For a Hamiltonian that is time independent during the relaxation process, all energy transferred during the evolution is in the form of heat exchanged with the bath. The mean heat absorbed by the bath is given by

$$\langle Q \rangle = \langle \hat{H}_B \rangle_t - \langle \hat{H}_B \rangle_0. \tag{4.17}$$

From the conservation of the total energy $\langle \hat{H} \rangle_t = \langle \hat{H} \rangle_0$ and the first law of thermodynamics Eq. (4.6), it follows that $\langle W \rangle$ is the average work performed on the entire system by switching the system-bath interaction on and off at the endpoints of the evolution,

$$\langle W \rangle = \langle \hat{H}_I \rangle_0 - \langle \hat{H}_I \rangle_t. \tag{4.18}$$

The average heat dissipated into the bath therefore comprises two contributions: the change in the system's internal energy and the system-bath interaction energy developed throughout the relaxation process.

4.4.1 Entropy production in a system interacting with a bath

For a protocol where the initial and final states of the system are equilibrium states, the total change in entropy of the open system is given by

$$\Delta S = S[\hat{\rho}_S(t)] - S[\hat{\rho}_S(0)], \tag{4.19}$$

where $S[\hat{\rho}] = -\mathrm{Tr}[\hat{\rho}\ln\hat{\rho}]$ is the von Neumann entropy of state $\hat{\rho}$. For quantum systems, the positivity of the entropy production $\langle\Sigma\rangle$ characterizing irreversible processes is due to the entropy contribution arising from correlations between system and bath [17]. It was shown that the irreversible entropy production can be written as the sum [72]

$$\langle\Sigma\rangle = I_{SB} + D(\hat{\rho}_B(t)||\hat{\rho}_B(0)) \tag{4.20}$$

with $\hat{\rho}_B(0)$ a thermal state in Gibbs form. Here $I_{SB} = S[\hat{\rho}_S] + S[\hat{\rho}_B] - S[\hat{\rho}]$ is the mutual information between system and bath, and $D(\hat{\rho}_B(t)||\hat{\rho}_B(0))$ the relative entropy between the bath state at time t and its initial state, defined as $D(\hat{\rho}||\hat{\sigma}) = \mathrm{Tr}[\hat{\rho}(\ln\hat{\rho} - \ln\hat{\sigma})]$, which is always a non-negative quantity. It has been shown that in open quantum systems with small Hilbert space dimension, such as a qubit, the displacement of the environment from equilibrium $D(\hat{\rho}_B(t)||\hat{\rho}_B(0))$ dominates the irreversible entropy production [72]. Furthermore, the relative entropy of the bath can be divided into two terms, $D(\hat{\rho}_B(t)||\hat{\rho}_B(0)) = D_{env} + I_{env}$, where D_{env} is a sum of relative entropies of the modes or levels composing the bath, and I_{env} is the mutual information between the degrees of freedom of the bath, arising from the building of inter-bath correlations. For large baths, it has been shown that I_{env} is the dominant contribution to the relative entropy of the environment. Therefore, even in non-dissipative protocols, it is possible to have a significative contribution to the irreversible entropy production due to the building of correlations between the bath degrees of freedom.

4.4.2 Thermalization of an open quantum system

The thermal equilibrium discrete Boltzmann probabilities Eq. (4.9) corresponds in quantum mechanics to a thermal equilibrium density matrix in Gibbs form,

$$\hat{\rho}_{eq} = \frac{\exp(-\beta \hat{H})}{Z}, \tag{4.21}$$

where $Z = \mathrm{Tr}[\exp(-\beta \hat{H})]$ is the partition function and $\hat{H}$ the system Hamiltonian. Due to the coupling with the bath, the equilibrium state of an open quantum system, if a state towards which the system evolves to and remains in exists, is not necessarily a thermal state in the form of Eq. (4.21). More generally, the equilibrium state of the open system is given by $\hat{\bar{\rho}}_S = \mathrm{Tr}_B[\hat{\bar{\rho}}]$, where $\hat{\bar{\rho}} = \lim_{T\to\infty} \frac{1}{T} \int_0^T \hat{\rho}\,(t)\, dt$ [35]. The total system equilibrium state is by definition a steady state, that is, a state that is unchanged by the time evolution

$$\mathcal{L}\hat{\bar{\rho}} = 0, \tag{4.22}$$

from the quantum equivalent of the Liouville equation Eq. (2.8).

4.4.3 Decoherence

In open quantum systems, the interaction between system and environment leads to the phenomenon of decoherence [7, 73], which destroys the relative phase between quantum states in superposition so that they can no longer be observed to interfere. Decoherence is not only a major limiting factor for entanglement-enhanced metrology [74] and scalable quantum computation [75, 76], but is also fundamental for the quantum measurement process and the emergence of classical reality [77, 78]. Moreover, the dynamics of decoherence can now be studied in carefully controlled experiments [79–84] and harnessed for nondestructive measurements using auxiliary probes [68, 69, 85–90].

Decoherence frequently occurs as a byproduct of thermalization, where an open system equilibrates by exchanging energy with its environment. Even for small

quantum systems initially far from equilibrium, it is well known that thermalization dynamics is tightly constrained by the laws of thermodynamics [17, 91]. Pure decoherence occurs when the energy of the open quantum system is strictly conserved and thermalization is inhibited. It arises when $[\hat{H}_I, \hat{H}_S] = 0$, so that the system Hamiltonian $\hat{H}_S$ is a constant of motion. The most general interaction that satisfies this constraint is

$$\hat{H}_I = \sum_n g_n \hat{\Pi}_n \otimes \hat{V}_n \tag{4.23}$$

where $\hat{\Pi}_n = |n\rangle\langle n|$ is a projector onto the eigenstate of $\hat{H}_S$ with eigenvalue ε_n, $\hat{V}_n$ is a generic operator acting on the bath, and g_n is a coupling constant. In the eigenbasis of $\hat{H}_S$, the reduced state $\hat{\rho}_S(t) = \mathrm{Tr}_B[\hat{\rho}(t)]$ has matrix elements $\hat{\rho}_S^{mn}(t) = \langle m|\hat{\rho}_S(t)|n\rangle$ given by [92]

$$\hat{\rho}_S^{mn}(t) = e^{-i(\varepsilon_m - \varepsilon_n)t} \left\langle e^{i\hat{H}_n t} e^{-i\hat{H}_m t} \right\rangle_B \hat{\rho}_S^{mn}(0). \tag{4.24}$$

We defined

$$\hat{H}_n = \hat{H}_B + g_n \hat{V}_n, \tag{4.25}$$

which describes the bath dynamics conditioned on state $|n\rangle$. Eq. (4.24) states that the diagonal matrix elements ($m = n$) are constant, while the off-diagonal elements ($m \neq n$) are proportional to the overlap $\langle e^{i\hat{H}_n t} e^{-i\hat{H}_m t}\rangle_B$, which decays in time whenever $\hat{H}_m \neq \hat{H}_n$ so that the bath carries information on the open system's state.

4.4.4 Distributions of heat and work

As discussed in Sec. 4.3, nonequilibrium dynamics in the quantum regime can give rise to significant fluctuations of thermodynamic quantities. It is therefore crucial to go beyond average values and consider the full probability distribution of the absorbed heat and work. By definition, the heat transfer is the energy change that would be registered by projective energy measurements on the bath at the beginning and end of the process. We denote by $\hat{\Pi}_n^B = |E_n\rangle\langle E_n|$ the projector onto the eigen-

state $|E_n\rangle$ of $\hat{H}_B$ with eigenvalue E_n. The heat distribution is then defined by

$$P(Q) = \sum_{m,n} p_n p_{n\to m} \delta(Q + E_n - E_m), \tag{4.26}$$

where $p_n = \mathrm{Tr}[(\mathbb{I} \otimes \hat{\Pi}_n^B)\hat{\rho}(0)]$ is the probability of measuring initial energy E_n, and $p_{n\to m} = \mathrm{Tr}[\hat{\Pi}_m^B \hat{U}(t)(\hat{\rho}_S(0) \otimes \hat{\Pi}_n^B)\hat{U}^\dagger(t)]$ is the conditional probability for the transition $E_n \to E_m$ [93]. A time evolution as in Eq. (2.6) is here assumed. The fluctuating heat exchange can be characterised by the statistical moments

$$\langle Q^n \rangle = \int_{-\infty}^{\infty} dQ\, P(Q) Q^n \tag{4.27}$$

$$= (-i)^n \frac{d^n}{du^n} \chi(u) \Big|_{u=0}. \tag{4.28}$$

The characteristic function $\chi(u)$ is defined as

$$\chi(u) = \int_{-\infty}^{\infty} dQ\, P(Q) e^{iuQ}, \tag{4.29}$$

where u is referred to as the counting field parameter. On the other hand, the work distribution $P(W)$ has the same form as the distribution in Eq. (4.26), where the work variable W replaces the heat variable Q. If one considers the work distribution of the bath independently of the open system, the conditional probability of the transition $E_n \to E_m$ is in this case given by $p_{n\to m} = \mathrm{Tr}[\hat{\Pi}_m^B(\mathbb{I} \otimes \hat{U}_B(t))(\hat{\rho}_S(0) \otimes \hat{\Pi}_n^B)(\mathbb{I} \otimes \hat{U}_B^\dagger(t))]$, where by $\hat{U}_B(t)$ we denote the time evolution operator of the bath density matrix, $\hat{\rho}_B(t) = \hat{U}_B(t)\,\hat{\rho}_B(0)\hat{U}_B^\dagger(t)$ [67].

It is possible to experimentally measure the probability distributions of thermodynamic quantities. The probability distribution of work performed on a system has been experimentally measured, for example, for the case of a two-dimension quantum harmonic oscillator with angular momentum [94].

Part II

Quantum heat statistics

5 | Introduction

Part I of this thesis introduced the TEMPO algorithm as a method to solve non-Marko-vian dynamics, and discussed the importance of non-Markovianity in the context of irreversible thermodynamic processes that involve heat dissipation. The question that remains unanswered is then: how do we model heat transfer, when analytical solutions are not available? This question has experimental and practical importance. A crucial limiting factor for the performance of quantum devices is the transfer of heat to and from their surroundings. A detailed understanding of heat transfer is therefore essential to optimise control protocols while minimising wasteful dissipation [95–97]. More generally, heat flux is a fundamental source of irreversibility and entropy production in open quantum systems [17, 40]. Entropy production limits the efficiency of heat engines and refrigerators [98], determines the energy cost of information erasure [99] and feedback control [100], constrains current fluctuations far from equilibrium [101–105], and can be directly measured in well controlled quantum settings [106–108]. However, modelling heat transfer in strongly coupled systems is a difficult theoretical problem because it requires access to the energetics of the bath. On the contrary, the majority of techniques for describing open quantum systems either neglect the environment's dynamics completely or treat it via an effective or approximate description [12]. An accurate, tractable method to predict the fluctuations of heat transfer in generic open quantum systems is still lacking.

The main research work of this thesis, which will be introduced now in Part II, focuses on this problem. Here, we find a solution by developing an efficient nu-

merical method to compute heat statistics using the path integral formulation of dissipative quantum mechanics [30]. Previous research has shown that the probability distributions of heat and work can be formally derived within this framework [93, 109, 110]. However, a direct evaluation of the corresponding path integral is only possible for a few exactly solvable models, while numerical approaches based on the quasi-adiabatic path integral (QuAPI) method [13, 14] require careful fine-tuning to avoid error accumulation [15, 111]. We solve this problem by generalising the TEMPO algorithm [16] to calculate the characteristic function of energy changes in the bath, equivalent to the Fourier transform of the heat probability distribution. This algorithm exploits a tensor-network representation of the QuAPI propagator to describe complicated non-Markovian evolutions efficiently [112]. As a result, we obtain a flexible and accurate tool to describe fluctuating heat transfer in generic, strongly coupled open quantum systems, which can be extended to deal with time-dependent Hamiltonians [113] or multiple baths [111]. The code we developed as an extension of the existing algorithm [114] is applied to the simulation of the spin-boson model, which describes quantum dots [115], ultracold atomic impurities [116] and superconducting circuits [117], to name just a few examples.

We demonstrate our approach by applying it to the non-equilibrium quantum thermodynamics of this important model. We first verify the accuracy of our method by comparison with the exact solution in the limit of the independent boson model. Then we compute the time-dependent heat transfer and its fluctuations across a range of parameters in the unbiased spin-boson model, including the challenging low-temperatu-re and strong-coupling regimes. We interpret our results using the notion of generalised equilibration in strong-coupling thermodynamics [62], and develop analytical models that quantitatively explain the mean heat exchange in the high-temperature and low-temperature limits. We also show numerically that the heat distribution obeys a fluctuation-dissipation relation (FDR) in the high-temperature limit, which is similar to the well-known FDR of the work distribution [44].

The second research project presented in this thesis is a study of heat dissipation in pure decoherence [92]. Following the full counting statistics approach developed for the extension of the TEMPO algorithm, we apply it to a model consisting of a single qubit coupled to a fermionic bath, undergoing a pure decoherence process. At first glance, the lack of direct energy exchange between system and heat bath seems to render the thermodynamics of pure decoherence trivial, even meaningless. We will show that this is not the case: quantum dephasing noise generated by a thermal environment is generally accompanied by nontrivial heat dissipation. Indeed, we prove under generic conditions that decoherence without dissipation is equivalent to static, classical phase noise: a highly restrictive situation that does not describe most realistic environments. We also demonstrate that the corresponding heat probability distribution obeys an integral fluctuation relation, and is entirely distinct from the work distribution associated with the initial system-bath interaction quench [118–120].

6 | Full counting statistics approach to heat transfer

This chapter introduces the full counting statistics approach and derives a modified discretized influence functional, equivalent in the absence of a counting field u to the one in Eq. (3.14). This result is derived for an open quantum system interacting with a bath modelled by an infinite collection of harmonic oscillators and coupled linearly to the system, with generic total Hamiltonian given by

$$\hat{H} = \frac{\hat{p}_s^2}{2m_s} + \hat{V}(S) + \sum_j \left[\frac{\hat{P}_j^2}{2m_j} + \frac{1}{2} m_j \omega_j^2 \left(\hat{Q}_j - \frac{c_j \hat{S}}{m_j \omega_j^2} \right)^2 \right]. \tag{6.1}$$

Here S is the eigenvalue of a quantum particle's coordinate operator $\hat{S}$, $\hat{V}(S)$ a generic nonlinear potential that depends on the particle coordinate only, $\hat{p}_s$ the particle momentum operator and m_s its mass. The momentum and position operators for the bath are $\hat{P}_j$ and $\hat{Q}_j$ respectively, for each mode j. c_j is the coupling constant between the system and the bath mode j, ω_j is the mode's angular frequency and m_j the mass of the j-th bath particle. The coordinate and momentum operators of the bath can be written in terms of creation and annihilation operators, $\hat{a}_j^\dagger$ and $\hat{a}_j$ respectively, as $\hat{P}_j = i\sqrt{m_j \omega_j / 2}\left(\hat{a}_j^\dagger - \hat{a}_j\right)$ and $\hat{Q}_j = \sqrt{2 m_j \omega_j}^{-1}\left(\hat{a}_j + \hat{a}_j^\dagger\right)$. The interaction Hamiltonian $\hat{H}_I = \hat{S}\sum_j c_j \hat{Q}_j$ and the free bath Hamiltonian can be then written as

$$\hat{H}_B = \sum_j \omega_j \hat{a}_j^\dagger \hat{a}_j, \tag{6.2}$$

$$\hat{H}_I = \hat{S} \otimes \sum_j g_j \left(\hat{a}_j + \hat{a}_j^\dagger \right), \tag{6.3}$$

where $g_j = \left(\sqrt{2m_j\omega_j}\right)^{-1} c_j$. The bath is characterized by its spectral density function, defined in Eq. (3.17). The overall Hamiltonian is given by Eq. (2.2). The total density matrix evolves in time through the time evolution operators in Eq. (2.6), and we assume the open system and the bath to be initially uncorrelated at the start of the process $t_0 = 0$, where the initial state of the bath is a Gibbs state.

6.1 Characteristic function of heat and work

The characteristic function of heat is defined by Eq. (4.29) and introduced in Sec. 4.4.4 as the Fourier transform of the probability distribution of heat $P(Q)$. In quantum mechanics, from the definition of the probability distribution Eq. (4.26) one obtains [65]

$$\chi(u) = \mathrm{Tr}\left[e^{iu\hat{H}_B} \hat{U}(t) e^{-iu\hat{H}_B} \hat{\rho}(0) \hat{U}^\dagger(t) \right]. \tag{6.4}$$

It is convenient to define a modified time evolution operator as

$$\hat{V}_u(t) = e^{i\hat{H}_B u/2} \hat{U}(t) e^{-i\hat{H}_B u/2}. \tag{6.5}$$

This allows the rewriting of Eq. (6.4) as $\chi(u) = \mathrm{Tr}\left[\hat{\rho}(t,u)\right]$, with the modified density matrix

$$\hat{\rho}(t,u) = \hat{V}_u(t) \hat{\rho}(0) \hat{V}_{-u}^\dagger(t). \tag{6.6}$$

The initial condition we assume is $\hat{\rho}(0,u) = \hat{\rho}(0)$. Defining $\hat{\rho}_S(t,u) = \mathrm{Tr}_B\left[\hat{\rho}(t,u)\right]$ as the reduced modified system density matrix, we have

$$\chi(u) = \mathrm{Tr}_S\left[\hat{\rho}_S(t,u)\right]. \tag{6.7}$$

The form in Eq. (6.7) facilitates the calculation of the heat statistics by means of path-integral techniques. The characteristic function of work done on the overall system, on the other hand, is given by [67]

$$\vartheta(v) = \mathrm{Tr}\left[e^{iv\hat{H}(t)}\hat{U}(t)\, e^{-iv\hat{H}(0)}\hat{\rho}(0)\hat{U}^{\dagger}(t)\right], \tag{6.8}$$

where we have defined v as the work counting field.

6.1.1 Properties of the characteristic function

We can see that the characteristic function of heat presents symmetries that will prove useful in our numerical calculations. Specifically, from the definition in Eq. (4.29), it is clear that

$$\chi^{*}(u) = \chi(-u). \tag{6.9}$$

since the probability distribution $P(Q)$ is a real function. This implies that the real and imaginary parts of $\chi(u)$ have the symmetries

$$\begin{aligned} Re(\chi(u)) &= Re(\chi(-u)), \\ Im(\chi(u)) &= -Im(\chi(-u)). \end{aligned} \tag{6.10}$$

It is also clear from Eq. (6.4) that $\chi(0) = 1$.

6.1.2 First and second moments of the fluctuating heat exchange

From Eq. (4.28), the first moment of exchanged heat is given by

$$\langle Q \rangle = -i\,\frac{d}{du}\chi(u)\bigg|_{u=0}. \tag{6.11}$$

In our method we perform a numerical differentiation in order to calculate the first and second moments of the heat distribution. In order to do that, we have to choose a suitable small value of u which we define to be u_ϵ. Note however that the counting

field is not a numerical parameter of the TEMPO algorithm, but a variable of the characteristic function. Then the average heat can be calculated numerically as

$$\langle Q \rangle = -i\frac{\chi(u_\epsilon) - \chi(0)}{u_\epsilon} + \mathcal{O}(u_\epsilon). \tag{6.12}$$

with an error of the order $\mathcal{O}(u_\epsilon)$. From the symmetries in Eq. (6.10), it is clear that $dRe(\chi(u))/du|_{u=0} = 0$ and $Im(\chi(0)) = 0$. Thus the mean heat depends only on the imaginary part of the characteristic function and is given by its linear slope in an interval $[u_\epsilon, 0]$,

$$\langle Q \rangle = \frac{Im(\chi(u_\epsilon))}{u_\epsilon} + \mathcal{O}(u_\epsilon). \tag{6.13}$$

Similarly, we can calculate numerically the second moment of heat as

$$\langle Q^2 \rangle = -2\frac{Re(\chi(u_\epsilon)) - 1}{u_\epsilon^2} + \mathcal{O}(u_\epsilon^2). \tag{6.14}$$

The variance of the heat is $\langle\langle Q^2 \rangle\rangle = \langle Q^2 \rangle - \langle Q \rangle^2$.

6.2 Reduced modified system density matrix time evolution

In the following, we construct the time evolution of an open system reduced density matrix $\hat{\rho}_S(t,u)$, modified with the counting field. In the interaction picture, the modified density matrix Eq. (6.6) is $\hat{\tilde{\rho}}(t,u) = e^{i(\hat{H}_S+\hat{H}_B)t}\hat{\rho}(t,u)e^{-i(\hat{H}_S+\hat{H}_B)t}$. Writing explicitly the form of the time evolution operators $\hat{V}_u(t)$ in Eq. (6.5), and having that $[\hat{H}_S, \hat{H}_B] = 0$, we can see the only term transformed by the operators $e^{\pm i\hat{H}_B u/2}$ is $e^{-i\hat{H}_I t}$. We can then define a modified interaction Hamiltonian as $\hat{H}_I(u) = e^{i\hat{H}_B u/2}\hat{H}_I e^{-i\hat{H}_B u/2}$. For an interaction of the form defined by Eq. (6.3), the annihilation operators $\hat{a}_j$ transform more explicitly as $e^{i\hat{H}_B u/2}\hat{a}_j e^{-i\hat{H}_B u/2} = \hat{a}_j + i\frac{u}{2}\left[\hat{H}_B, \hat{a}_j\right] + \mathcal{O}\left(u^2\right)$, where we have expanded the operators up to the second order in the counting field u. In order to calculate the commutator $[\hat{H}_B, \hat{a}_j]$, we notice that the bosonic

bath free Hamiltonian Eq. (6.2) can be written as $\hat{H}_B = \sum_j \omega_j(\hat{a}_j^\dagger \hat{a}_j + \hat{a}_j \hat{a}_j^\dagger)/2$. It is then easy to see that the commutator is $[\hat{H}_B, \hat{a}_j] = \sum_n \omega_n \left(\left[\hat{a}_n^\dagger \hat{a}_n, \hat{a}_j\right] + \left[\hat{a}_n \hat{a}_n^\dagger, \hat{a}_j\right] \right)/2$. Applying the commutation rule $\left[\hat{A}\hat{B}, \hat{C}\right] = \hat{A}\left[\hat{B}, \hat{C}\right] + \left[\hat{A}, \hat{C}\right]\hat{B}$, it follows that $\left[\hat{H}_B, \hat{a}_j\right] = -\omega_j \hat{a}_j$ and, similarly, $\left[\hat{H}_B, \hat{a}_j^\dagger\right] = \omega_j \hat{a}_j^\dagger$. In conclusion, we can identify the transformations of the bath operators $\hat{a}_j$ and $\hat{a}_j^\dagger$ as, respectively, $e^{i\hat{H}_B u/2}\hat{a}_j e^{-i\hat{H}_B u/2} = \hat{a}_j e^{-i\frac{u}{2}\omega_j}$ and $e^{i\hat{H}_B u/2}\hat{a}_j^\dagger e^{-i\hat{H}_B u/2} = \hat{a}_j^\dagger e^{i\frac{u}{2}\omega_j}$. It follows that the explicit form of the modified interaction Hamiltonian is,

$$\hat{H}_I(u) = \hat{S} \otimes \sum_j g_j \left(\hat{a}_j e^{-i\frac{u}{2}\omega_j} + \hat{a}_j^\dagger e^{i\frac{u}{2}\omega_j} \right). \tag{6.15}$$

Eq. (6.15), in the interaction picture $\hat{\tilde{H}}_I(t,u) = e^{i(\hat{H}_S+\hat{H}_B)t}\hat{H}_I(u)e^{-i(\hat{H}_S+\hat{H}_B)t}$, becomes

$$\hat{\tilde{H}}_I(t,u) = \hat{S}(t) \otimes \sum_j g_j \left(\hat{a}_j e^{-i\omega_j t} e^{-i\frac{u}{2}\omega_j} + \hat{a}_j^\dagger e^{i\omega_j t} e^{i\frac{u}{2}\omega_j} \right). \tag{6.16}$$

On the other hand, the master equation for the modified density matrix in the interaction picture is $(d/dt)\hat{\tilde{\rho}}(t,u) = \mathcal{L}_I(t,u)\hat{\tilde{\rho}}(t,u)$, similarly to what we discussed in Sec. 3.4.2. Considering that the time evolution operator $V_u(t)$ can be written in terms of Eq. (6.15) as $V_u(t) = \exp[-i\left(\hat{H}_S + \hat{H}_B + \hat{H}_I(u)\right)t]$, it follows from Eq. (6.6) that

$$\hat{\tilde{\rho}}(t,u) = e^{-i\left(\hat{\tilde{H}}_I^L(t,u) - \hat{\tilde{H}}_I^R(t,-u)\right)t}\hat{\tilde{\rho}}(0,u), \tag{6.17}$$

where we have used the superoperator formalism from Eqs. (3.23)-(3.24). We find that the interaction Liouvillian superoperator in the presence of counting field is

$$\mathcal{L}_I(t,u) = -i\left(\hat{\tilde{H}}_I^L(t,u) - \hat{\tilde{H}}_I^R(t,-u)\right). \tag{6.18}$$

As for the unmodified reduced density matrix $\hat{\rho}_S(t)$, the solution for the modified reduced density matrix is

$$\hat{\tilde{\rho}}_S(t,u) = I(t,u)\hat{\rho}_S(0), \tag{6.19}$$

where $I(t,u)$ is the modified influence functional

$$I(t,u) = \left\langle \overleftarrow{T} \left[\int_0^t dt' \mathcal{L}_I\left(t',u\right) \right] \right\rangle_B . \tag{6.20}$$

The time-ordering symbol $\overleftarrow{T}$ reorders superoperators such that time increases from right to left. Since the interaction Hamiltonian $\hat{H}_I$ in Eq. (6.3) is linear and the assumed thermal state of the bath is Gaussian, analogously to Eq. (3.30) for the unmodified reduced density matrix, we can write

$$I(t,u) = \overleftarrow{T} \exp\left[\int_0^t dt' \int_0^{t'} dt'' \left\langle \mathcal{L}_I(t',u)\mathcal{L}_I(t'',u) \right\rangle_B \right], \tag{6.21}$$

using a time-ordered cumulant expansion up to second order [33].

The modified influence functional determines the time evolution of $\hat{\rho}_S(t,u)$. In the following we will focus on the calculation of the correlation function in Eq. (6.21), using the interaction Liouvillian operator we derived in Eq. (6.18).

6.3 Modified influence functional for a bosonic bath

We analytically evaluate the term $\langle \mathcal{L}_I(t',u)\mathcal{L}_I(t'',u)\rangle_B$ in Eq. (6.21). The discretized form of this correlation function is coded in our extension of the TEMPO algorithm in order to implement simulations of heat statistics. We notice that the modified interaction Hamiltonian $\hat{\tilde{H}}_I(t,u)$ in Eq. (6.16) can be written as the sum of two terms,

$$\begin{aligned} \hat{\tilde{H}}_I(t,u) = {} & \hat{S}\left(t\right) \sum_j g_j \cos\left(\frac{u}{2}\omega_j\right) \left(\hat{a}_j e^{-i\omega_j t} + \hat{a}_j^\dagger e^{i\omega_j t} \right) \\ & - i\hat{S}\left(t\right) \sum_j g_j \sin\left(\frac{u}{2}\omega_j\right) \left(\hat{a}_j e^{-i\omega_j t} - \hat{a}_j^\dagger e^{i\omega_j t} \right). \end{aligned} \tag{6.22}$$

We define

$$B_1(t,u) = \sum_j g_j \cos\left(\frac{u}{2}\omega_j\right)\left(\hat{a}_j e^{-i\omega_j t} + \hat{a}_j^\dagger e^{i\omega_j t}\right), \tag{6.23}$$

$$B_2(t,u) = -i\sum_j g_j \sin\left(\frac{u}{2}\omega_j\right)\left(\hat{a}_j e^{-i\omega_j t} - \hat{a}_j^\dagger e^{i\omega_j t}\right), \tag{6.24}$$

so that the modified interaction Hamiltonian can be compactly written as

$$\hat{\tilde{H}}_I(t,u) = \hat{S}(t) B_1(t,u) + \hat{S}(t) B_2(t,u). \tag{6.25}$$

The interaction Hamiltonian has thus been divided into the sum of the two Hamiltonians

$$H_{I,1}(t,u) = \hat{S}_z B_1(t,u), \tag{6.26}$$

$$H_{I,2}(t,u) = \hat{S}_z B_2(t,u). \tag{6.27}$$

We note that, given the cosine and sine functions in the interaction parts dependent on the counting field, Eqs. (6.23) and (6.24), it holds that $H_{I,1}(t,-u) = H_{I,1}(t,u)$ and $H_{I,2}(t,-u) = -H_{I,2}(t,u)$. In light of this new notation, the Liouvillian operator defined in Eq. (6.18) is

$$\mathcal{L}_I(t,u) = -i\left(H_{I,1}^-(t,u) + H_{I,2}^+(t,u)\right), \tag{6.28}$$

where we have used Eq. (3.25) and Eq. (3.26). The exponent of the modified influence functional in Eq. (6.21) can then be written as

$$\begin{aligned}
&\left\langle \mathcal{L}_I(t',u)\,\mathcal{L}_I(t'',u)\right\rangle_B = \\
&-\left\langle H_{I,1}^-(t',u)\,H_{I,1}^-(t'',u)\right\rangle_B - \left\langle H_{I,2}^+(t',u)\,H_{I,2}^+(t'',u)\right\rangle_B \\
&-\left\langle H_{I,1}^-(t',u)\,H_{I,2}^+(t'',u)\right\rangle_B - \left\langle H_{I,2}^+(t',u)\,H_{I,1}^-(t'',u)\right\rangle_B .
\end{aligned} \tag{6.29}$$

Using the decomposition defined in Eq. (6.26) and Eq. (6.27), and rules (3.25 - 3.28), we can write $H^{\pm}_{I,j}(t,u) = (\hat{S}(t)B_j(t,u))^L \pm (\hat{S}(t)B_j(t,u))^R$, with $j = 1,2$. Applying the properties $(AB)^L = A^L B^L$ and $(AB)^R = A^R B^R$, it is possible to separate the superoperator acting on the system operators from those acting on the reservoir operators. Each term in Eq. (6.29) can then be calculated explicitly:

$$\begin{aligned}
\left\langle H^{-}_{I,1}(t',u)\, H^{+}_{I,2}(t'',u)\right\rangle_B &= \frac{1}{4}\hat{S}^{-}(t)\left(\hat{S}^{+}(t)\left\langle B^{+}_1(t',u)\, B^{+}_2(t'',u)\right\rangle_B\right. \\
&\quad \left. +\hat{S}^{-}(t)\left\langle B^{+}_1(t',u)\, B^{-}_2(t'',u)\right\rangle_B\right), \qquad (6.30)\\
\left\langle H^{+}_{I,2}(t',u)\, H^{-}_{I,1}(t'',u)\right\rangle_B &= \frac{1}{4}\hat{S}^{+}(t)\left(\hat{S}^{+}(t)\left\langle B^{+}_2(t',u)\, B^{-}_1(t'',u)\right\rangle_B\right. \\
&\quad \left. +\hat{S}^{-}(t)\left\langle B^{+}_2(t',u)\, B^{+}_1(t'',u)\right\rangle_B\right), \qquad (6.31)\\
\left\langle H^{-}_{I,1}(t',u)\, H^{-}_{I,1}(t'',u)\right\rangle_B &= \frac{1}{4}\hat{S}^{-}(t)\left(\hat{S}^{+}(t)\left\langle B^{+}_1(t',u)\, B^{-}_1(t'',u)\right\rangle_B\right. \\
&\quad \left. +\hat{S}^{-}(t)\left\langle B^{+}_1(t',u)\, B^{+}_1(t'',u)\right\rangle_B\right), \qquad (6.32)\\
\left\langle H^{+}_{I,2}(t',u)\, H^{+}_{I,2}(t'',u)\right\rangle_B &= \frac{1}{4}\hat{S}^{+}(t)\left(\hat{S}^{+}(t)\left\langle B^{+}_2(t',u)\, B^{+}_2(t'',u)\right\rangle_B\right. \\
&\quad \left. +\hat{S}^{-}(t)\left\langle B^{+}_2(t',u)\, B^{-}_2(t'',u)\right\rangle_B\right). \qquad (6.33)
\end{aligned}$$

Through the rules in Eqs. (3.25 - 3.26) we can calculate all the bath correlation functions appearing in Eqs. (6.30 - 6.33). It can be noted that given the definition $\langle\bullet\rangle_B \equiv \mathrm{Tr}[\bullet\hat{\rho}_B(0)]$ in interaction picture, for any two superoperators α and β, it holds that $\langle\alpha^{-}\beta^{\pm}\rangle_B = Tr_B\left[\left[\alpha,\beta^{\pm}\hat{\rho}_B(0)\right]\right] = 0$. Therefore the superoperators $B^{-}_1(t',u)$ and $B^{-}_2(t',u)$ in Eqs. (6.30 - 6.33) produce null terms, $B(t,u)$ being the only operator that contains degrees of freedom of the bath B. We then only need to evaluate the non-null correlations $\langle B^{+}_m(t',u)\, B^{+}_n(t'',u)\rangle_B$ and $\langle B^{+}_m(t',u)\, B^{-}_n(t'',u)\rangle_B$, with $m,n = 1,2$,

$$\left\langle B^{+}_m(t',u)\, B^{\pm}_n(t'',u)\right\rangle_B = 2\left\langle B_m(t',u)\, B_n(t'',u)\right\rangle_B \pm 2\left\langle B_n(t'',u)\, B_m(t',u)\right\rangle_B. \qquad (6.34)$$

Since $\langle B_n(t'',u)\,B_m(t',u)\rangle_B = \langle B_m(t',u)\,B_n(t'',u)\rangle_B^*$, we have that

$$\left\langle B_m^+(t',u)\,B_n^+(t'',u)\right\rangle_B = 4Re\left[\mathrm{Tr}_B\left[B_m(t',u)\,B_n(t'',u)\,\hat{\tilde{\rho}}_B(0)\right]\right], \tag{6.35}$$

$$\left\langle B_m^+(t',u)\,B_n^-(t'',u)\right\rangle_B = 4iIm\left[\mathrm{Tr}_B\left[B_m(t',u)\,B_n(t'',u)\,\hat{\tilde{\rho}}_B(0)\right]\right]. \tag{6.36}$$

With the definitions of functions $B_1(t,u)$ and $B_2(t,u)$ in Eqs. (6.23 - 6.24), we can explicitly calculate the functions in Eqs. (6.35 - 6.36) using the properties of the bosonic operators. Specifically, we know that $Tr_B\left[\hat{a}_k^\dagger\hat{a}_j\hat{\tilde{\rho}}_B(0)\right] = \left\langle\hat{N}_j\right\rangle_{t=0}\delta_{kj}$, where $\hat{N}_j = \hat{a}_k^\dagger\hat{a}_j$ is the bosonic number operator of mode j, whose average at time $t=0$, for a Planck distribution of bosons occupying the energy level $\hbar\omega_j$, is

$$\left\langle\hat{N}_j\right\rangle_{t=0} = \frac{1}{\exp\left[\beta_0\omega_j\right]-1} = \frac{\exp\left[-\beta_0\omega_j/2\right]}{2\sinh\left[\beta_0\omega_j/2\right]}, \tag{6.37}$$

where β_0 is the inverse temperature of the bath at initial time $t=0$.

We find that, for $m\neq n$, $m,n=1,2$,

$$\left\langle B_1^+(t',u)\,B_2^+(t'',u)\right\rangle_B = -\left\langle B_2^+(t',u)\,B_1^+(t'',u)\right\rangle_B = -4Re\left[\mathcal{C}(t',t'',u)\right], \tag{6.38}$$

$$\left\langle B_1^+(t',u)\,B_2^-(t'',u)\right\rangle_B = -\left\langle B_2^+(t',u)\,B_1^-(t'',u)\right\rangle_B = -4iIm\left[\mathcal{C}(t',t'',u)\right], \tag{6.39}$$

where

$$\mathcal{C}(t',t'',u) = i\sum_j g_j^2\cos\left(\frac{u}{2}\omega_j\right)\sin\left(\frac{u}{2}\omega_j\right)\frac{\sinh\left[i\omega_j(t'-t'')-\beta_0\omega_j/2\right]}{\sinh\left[\beta_0\omega_j/2\right]}. \tag{6.40}$$

Similarly, for $m=n$, $m,n=1,2$, the calculation of Eqs. (6.35 - 6.36) leads to

$$\left\langle B_1^+(t',u)\,B_1^+(t'',u)\right\rangle_B = 4Re\left[\mathcal{A}_1(t',t'',u)\right], \tag{6.41}$$

$$\left\langle B_2^+(t',u)\,B_2^+(t'',u)\right\rangle_B = 4Re\left[\mathcal{A}_2(t',t'',u)\right], \tag{6.42}$$

$$\left\langle B_1^+(t',u)\,B_1^-(t'',u)\right\rangle_B = 4iIm\left[\mathcal{A}_1(t',t'',u)\right], \tag{6.43}$$

$$\left\langle B_2^+(t',u)\,B_2^-(t'',u)\right\rangle_B = 4iIm\left[\mathcal{A}_2(t',t'',u)\right], \tag{6.44}$$

where

$$\mathcal{A}_1\left(t',t'',u\right)=\sum_j g_j^2\cos^2\left(\frac{u}{2}\omega_j\right)\frac{\cosh\left[i\omega_j\left(t'-t''\right)-\beta_0\omega_j/2\right]}{\sinh\left[\beta_0\omega_j/2\right]}, \tag{6.45}$$

$$\mathcal{A}_2\left(t',t'',u\right)=\sum_j g_j^2\sin^2\left(\frac{u}{2}\omega_j\right)\frac{\cosh\left[i\omega_j\left(t'-t''\right)-\beta_0\omega_j/2\right]}{\sinh\left[\beta_0\omega_j/2\right]}. \tag{6.46}$$

In terms of the spectral density function $J(w)$ defined in Eq. (3.17), functions $\mathcal{C}(t',t'',u)$, $\mathcal{A}_1(t',t'',u)$ and $\mathcal{A}_2(t',t'',u)$ can be written as

$$\mathcal{C}\left(t',t'',u\right)=i\int_0^\infty d\omega J\left(\omega\right)\cos\left(\frac{u}{2}\omega\right)\sin\left(\frac{u}{2}\omega\right)\frac{\sinh\left[i\omega\left(t'-t''\right)-\beta_0\omega/2\right]}{\sinh\left[\beta_0\omega/2\right]}, \tag{6.47}$$

$$\mathcal{A}_1\left(t',t'',u\right)=\int_0^\infty d\omega J\left(\omega\right)\cos^2\left(\frac{u}{2}\omega\right)\frac{\cosh\left[i\omega\left(t'-t''\right)-\beta_0\omega/2\right]}{\sinh\left[\beta_0\omega/2\right]}, \tag{6.48}$$

$$\mathcal{A}_2\left(t',t'',u\right)=\int_0^\infty d\omega J\left(\omega\right)\sin^2\left(\frac{u}{2}\omega\right)\frac{\cosh\left[i\omega\left(t'-t''\right)-\beta_0\omega/2\right]}{\sinh\left[\beta_0\omega/2\right]}. \tag{6.49}$$

Eqs. (6.47 - 6.48) allow for the calculation of the bath correlation terms appearing in $\left\langle\mathcal{L}_I\left(t',u\right)\mathcal{L}_I\left(t'',u\right)\right\rangle_B$ in Eq. (6.29). The full exponent of the modified influence functional Eq. (6.21), is then calculated by integrating Eqs. (6.47 - 6.48) and defining the correlation functions

$$\eta^\alpha(t,u)=\int_0^t dt'\int_0^{t'}dt''\alpha\left(t',t'',u\right), \tag{6.50}$$

where $\alpha=\mathcal{C},\mathcal{A}_1,\mathcal{A}_2$. The three resulting correlation functions are

$$\begin{aligned}\eta^{\mathcal{C}}(t,u)=&\int_0^\infty d\omega\frac{J(\omega)}{2\omega^2}\sin(u\omega)\\&\times\left[\coth\left(\frac{\omega}{2T}\right)\left[\sin(\omega t)-\omega t\right]-i\left[1-\cos(\omega t)\right]\right],\end{aligned} \tag{6.51}$$

$$\begin{aligned}\eta^{\mathcal{A}_1}(t,u)=&\int_0^\infty d\omega\frac{J(\omega)}{\omega^2}\cos^2\left(\frac{u\omega}{2}\right)\\&\times\left[\coth\left(\frac{\omega}{2T}\right)\left[1-\cos(\omega t)\right]+i\left[\sin(\omega t)-\omega t\right]\right],\end{aligned} \tag{6.52}$$

$$\eta^{\mathcal{A}_2}(t,u) = \int_0^\infty d\omega \frac{J(\omega)}{\omega^2} \sin^2\left(\frac{u\omega}{2}\right) \times \left[\coth\left(\frac{\omega}{2T}\right)[1-\cos(\omega t)] + i\,[\sin(\omega t) - \omega t]\right]. \tag{6.53}$$

In order to obtain a discretized modified influence functional in the form of Eq. (3.14) for the original TEMPO algorithm, we discretize the correlation functions Eqs. (6.51 - 6.53), and define, equivalently to Eq. (3.15),

$$\eta^{\alpha}_{k-k'}(u) = \begin{cases} \int_{t_{k-1}}^{t_k}\int_{t_{k'-1}}^{t_{k'}} \alpha\,(t'-t'',u)\,dt''dt' & k \neq k' \\ \\ \int_{t_{k-1}}^{t_k}\int_{t_{k-1}}^{t'} \alpha\,(t'-t'',u)\,dt''dt' & k = k', \end{cases} \tag{6.54}$$

where $\eta^{\alpha}_{k-k'}(u) = \eta^{\alpha}(t_k - t_{k'}, u)$, and $\eta^{\alpha}(t,u) = \sum_{k=0}^{N}\sum_{k'=0}^{k}\eta^{\alpha}_{k-k'}(u)$. Following the method illustrated in Sec. 3.3 and developed in Ref. [15], we simply discretize time in N intervals of equal length Δ, so that $t_k = k\Delta$. We again use the notation $\left|s_k^{\pm}\right\rangle$ for the eigenstates of $\hat{S}$, where the superscript $+(-)$ is used to label eigenvectors inserted on the left (right) of the reduced system density matrix.

The path integral for $\hat{\rho}_S(t,u)$ is constructed by inserting resolutions of the identity $\hat{\mathbb{I}} = \sum_{s_k^{\pm}}\left|s_k^{\pm}\right\rangle\left\langle s_k^{\pm}\right|$ in the eigenbasis of the system operator $\hat{S}$ at each time step in Eq. (6.19). In the interaction picture, the free propagators do not appear and we obtain the modified influence functional in the form

$$I\left(\left\{s_k^{\pm}\right\},u\right) = \prod_{k=0}^{N}\prod_{k'=0}^{k} I_{\Delta k}(s_k^{\pm}, s_{k'}^{\pm}, u), \tag{6.55}$$

$$I_{\Delta k}\left(s_k^{\pm}, s_{k'}^{\pm}, u\right) = \exp\left[-\sum_{q,q'=\pm} s_k^{q}\eta^{qq'}_{k-k'}(u)s_{k'}^{q'}\right]. \tag{6.56}$$

Here, $\Delta k = k - k'$ and $\eta^{qq'}_{k-k'}(u)$ are the discretized correlation functions

$$\eta^{++}_{k-k'}(u) = \eta^{\mathcal{A}_1}_{k-k'}(u) + \eta^{\mathcal{A}_2}_{k-k'}(u) = \left[\eta^{--}_{k-k'}(u)\right]^* \tag{6.57}$$

$$\eta^{-+}_{k-k'}(u) = \eta^{\mathcal{A}_2}_{k-k'}(u) - \eta^{\mathcal{A}_1}_{k-k'}(u) + 2\eta^{\mathcal{C}}_{k-k'}(u) \tag{6.58}$$

$$\eta^{+-}_{k-k'}(u) = \left[\eta^{\mathcal{A}_2}_{k-k'}(u) - \eta^{\mathcal{A}_1}_{k-k'}(u) - 2\eta^{\mathcal{C}}_{k-k'}(u)\right]^*. \tag{6.59}$$

Our expression for $I\left(\{s^{\pm}_k\}, u\right)$ matches the one recently derived in Ref. [111] and it is straightforward to verify that, for $u = 0$, it reduces to the original influence functional described in Ref. [13]. From Eq. (3.22), the reduced modified density matrix element at final time t_N is

$$\left\langle s^+_N\right| \hat{\rho}_S(t,u) \left|s^-_N\right\rangle = \sum_{s^{\pm}_0, s^{\pm}_1 \ldots s^{\pm}_{N-1}} F\left(\{s^{\pm}_k\}\right) I\left(\{s^{\pm}_k\}, u\right) \left\langle s^+_0\right| \hat{\rho}'_S(0) \left|s^-_0\right\rangle. \tag{6.60}$$

Here, $\hat{\rho}'_S(0) = e^{-i\hat{H}_S\Delta/2}\hat{\rho}_S(0)e^{i\hat{H}_S\Delta/2}$ is a modified initial condition, and

$$F\left(\{s^{\pm}_k\}\right) = \prod_{k=1}^{N} G(s^{\pm}_k, s^{\pm}_{k-1}) \tag{6.61}$$

is a product of free propagators for the system, with

$$G(s^{\pm}_k, s^{\pm}_{k-1}) = \left\langle s^+_k\right| e^{-i\hat{H}_S\Delta_k} \left|s^+_{k-1}\right\rangle \left\langle s^-_{k-1}\right| e^{i\hat{H}_S\Delta_k} \left|s^-_k\right\rangle, \tag{6.62}$$

where $\Delta_k = \Delta$ for $k < N$ and $\Delta_N = \Delta/2$.

The form of Eq. (6.55) emphasises that the environment introduces memory into the evolution by coupling the system coordinate to itself at different times. Crucially, however, the correlation functions $\eta^{\alpha}(t,u)$ decay to zero for sufficiently large t and therefore the memory time of the environment is finite. We are therefore able to implement the modified influence functional Eq. (6.56) into TEMPO, and calculate the time evolution of $\hat{\rho}_S(t,u)$ for any given time t in the presence of counting field. Through Eq. (6.7) our modified algorithm is able to numerically calculate the characteristic function of heat. The ADT iterative propagation scheme described in

Sec. 3.3.3 remains unchanged, with the essential replacement of the original influence functional with the modified one in the propagator tensor Eq. (3.19).

7 | Simulation of the non-Markovian spin-boson model dynamics

In the original work by Strathearn *et al.* in Ref. [16], the TEMPO algorithm is applied to the paradigmatic spin-boson model. Aside from setting the environmental parameters, the TEMPO algorithm requires the input of three additional parameters: the discretization time-step Δ, the memory cutoff length K, and the precision parameter p for performing singular value decompositions of the system's ADT, such that $\lambda_C = \lambda_{max} 10^{-p/10}$ is the cut-off value (see Sec. 3.4). For the spin-boson model, Ref. [16] finds that it is sufficient to set $\Delta = 0.06$, $K = 200$, and $p = 60$ in the original TEMPO algorithm in order to achieve convergence in the dynamics of a single spin-1/2 coupled to a bosonic bath with Ohmic spectral density, at temperature $T = 0$ and up to the strong coupling regime. When setting the counting field parameter $u = 0$ in the modified influence functional we derived in Eq. (6.56), it is easy to verify from Eqs. (6.51 - 6.53) that $\eta^{\mathcal{C}}(t,0) = 0$, $\eta^{\mathcal{A}_2}(t,0) = 0$ and $\eta^{\mathcal{A}_1}(t,0)$ is equal to the autocorrelation function $C(t)$ in Eq. (3.16) for the unmodified TEMPO. The first step in our analysis of the heat statistics of the spin-boson model is to verify that our modified code reproduces the results shown in Ref. [16], as a general check, when we set $u = 0$. Since we will be simulating heat statistics for a bath with temperatures up to $T = 5\Omega$, where Ω is a unit we will define in terms of the parameters of the system Hamiltonian, we verify the TEMPO parameter ranges that allow for the convergence of the system observables for temperatures $T > 0$.

7.1 The spin-boson model

In the spin-boson model, the terms in the total Hamiltonian $\hat{H}$ Eq. (2.2) take the form

$$\hat{H}_S = \omega_0 \hat{S}_z + \Omega \hat{S}_x, \tag{7.1}$$

$$\hat{H}_B = \sum_j \omega_j \hat{a}_j^\dagger \hat{a}_j, \tag{7.2}$$

$$\hat{H}_I = \hat{S}_z \sum_j g_j \left(\hat{a}_j + \hat{a}_j^\dagger \right). \tag{7.3}$$

Above, $\hat{S}_z$ and $\hat{S}_x$ are the spin operators for the system. We focus on an Ohmic spectral density function of the form

$$J(\omega) = 2\alpha\omega e^{-\omega/\omega_C}, \tag{7.4}$$

where α is a dimensionless system-environment coupling constant and ω_C is a cut-off frequency. The bath is characterised by a correlation time $\tau_C = 2\pi/\omega_C$. The frequency and temperature are both defined in units of Ω, which for simplicity we will here set to $\Omega = 1$. This model presents a quantum phase transition at zero bath temperature at the critical value of the coupling constant $\alpha_{critical}$. As in Ref. [16], in the following we set the initial state of the spin to be the eigenstate $|\uparrow\rangle$ of the spin operator $\hat{S}_z$, such that $\hat{S}_z|\uparrow\rangle = 1/2|\uparrow\rangle$, and $\hat{\rho}_S(0) = |\uparrow\rangle\langle\uparrow|$. Fig. 7.1 and Fig. 7.2 show the Ohmic spectral density in Eq. (7.4) for fixed frequency cutoff $\omega_C = 5$ and fixed coupling strength $\alpha = 1$ respectively. From Fig. 7.1 it is clear that the frequency at which $J(\omega)$ presents a peak remains unchanged by the coupling strength, while the magnitude of the peak is proportional to α. Changing the cutoff frequency, on the other hand, affects the frequency range at which $J(\omega)$ becomes negligible, which happens at lower ω for smaller ω_C. This means the correlation functions Eqs. (6.51 - 6.53) decay after a timescale set by $1/\omega_C$, and the bath no longer affects the dynamics of the spin. The spectral density function has in all cases a peak at $\omega = \omega_C$.

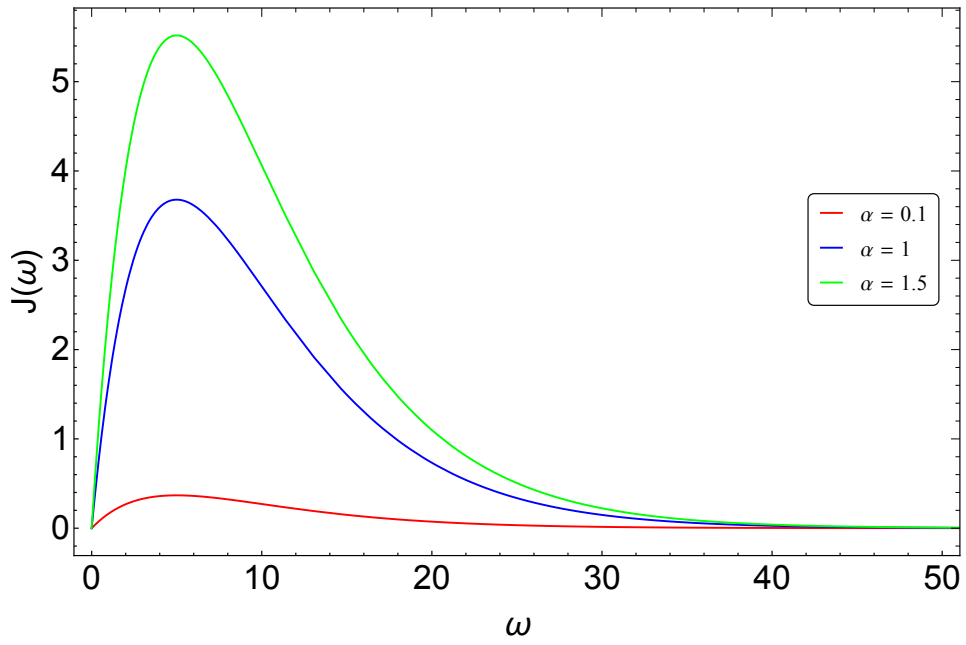

Figure 7.1: Ohmic spectral density function of the bath $J(\omega)$ for fixed frequency cutoff $\omega_C = 5$, and three different values of the coupling strength α.

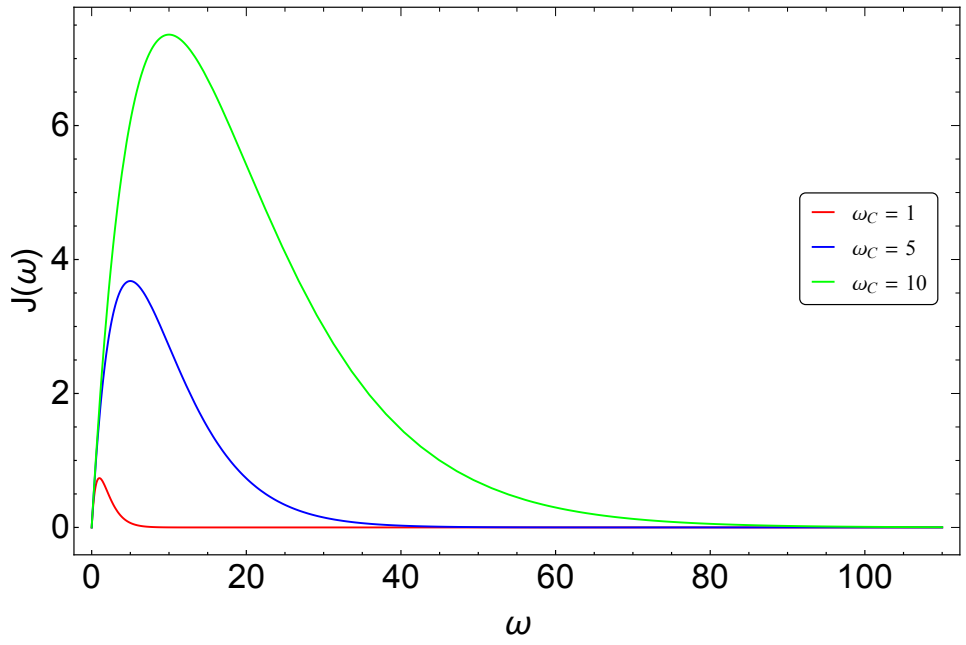

Figure 7.2: Ohmic spectral density function of the bath $J(\omega)$ for fixed coupling strength $\alpha = 1$, and three different values of frequency cutoff ω_C.

7.2 Correlation function and memory depth

In order to fix the correct memory length that has to be taken into account during the unmodified system dynamics, it is important to evaluate at what time the correlation function decays and the effects of the environment are no longer relevant and can be ignored. We rewrite the correlation function $\mathcal{A}_1(t', t'', , 0)$ as a function of the memory depth time $K\Delta$, by setting $(t' - t'') = K\Delta$ in Eq. (6.48). Separating the real and imaginary part of the correlation function, we have

$$Re[\mathcal{A}_1](K\Delta) = \begin{cases} 2\alpha \int_0^\infty \omega e^{-\frac{\omega}{\omega_C}} \coth\left(\frac{\beta_0 \omega}{2}\right) \cos(K\Delta\omega) & T \neq 0 \\ \\ 2\alpha \int_0^\infty \omega e^{-\frac{\omega}{\omega_C}} \cos(K\Delta\omega) & T = 0, \end{cases} \tag{7.5}$$

where we have used $\lim_{\beta_0 \to \infty} \coth(\beta_0 \omega/2) = 1$, and

$$Im[\mathcal{A}_1](K\Delta) = -2\alpha \int_0^\infty \omega e^{-\frac{\omega}{\omega_C}} \sin(K\Delta\omega), \tag{7.6}$$

independent of temperature. Figs. (7.3-7.4) show the real part of $\mathcal{A}_1$, for fixed system-environment coupling strength and for fixed bath temperature respectively. It can be noted that the memory depth time $K\Delta$ at which function $Re[\mathcal{A}_1]$ goes to zero does not have a strong dependence on temperature. It does, however, have a dependence on the frequency cutoff ω_C. $Re[\mathcal{A}_1]$ becomes negligible faster for higher values of the cutoff. In Fig. 7.4, for example, the orange curve ($\omega_C = 1$) has a value of $Re[\mathcal{A}_1] = 0.2$ for $K\Delta = 3$, while the green curve ($\omega_C = 20$) has a value of $Re[\mathcal{A}_1] = 0.01$ for the same memory depth. Identical observations can the made for the temperature independent imaginary part the correlation function, $Im[\mathcal{A}_1]$, shown in Fig. 7.5 for different values of ω_C and a fixed value of α. We notice that for a fixed frequency cutoff value $\omega_C = 5$, we would need a memory depth time $K\Delta > 3$ in order to achieve a negligible correlation function for the coupling value of $\alpha = 0.1$ in the range of temperatures $0 \leq T \leq 5$, within an approximation < 0.04.

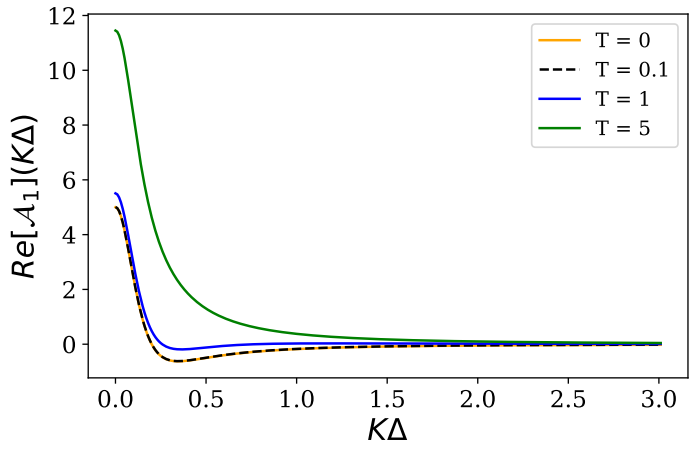

Figure 7.3: Real part of the bath correlation function $\mathcal{A}_1$, for four different values of bath temperature T, as a function of the memory depth time $K\Delta$ as defined in Eqs. (7.5). Here we have fixed $\alpha = 0.1$, $\omega_C = 5$.

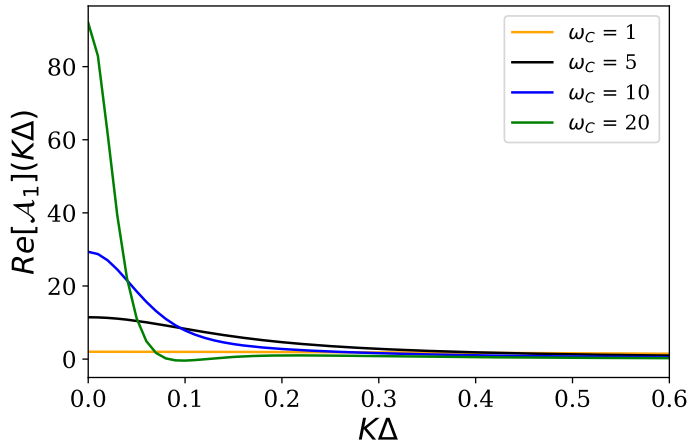

Figure 7.4: Real part of the bath correlation function $\mathcal{A}_1$, for four different values of frequency cutoff ω_C, as a function of the memory depth time $K\Delta$ as defined in Eqs. (7.5). Here we have fixed $T = 5$, $\alpha = 0.1$

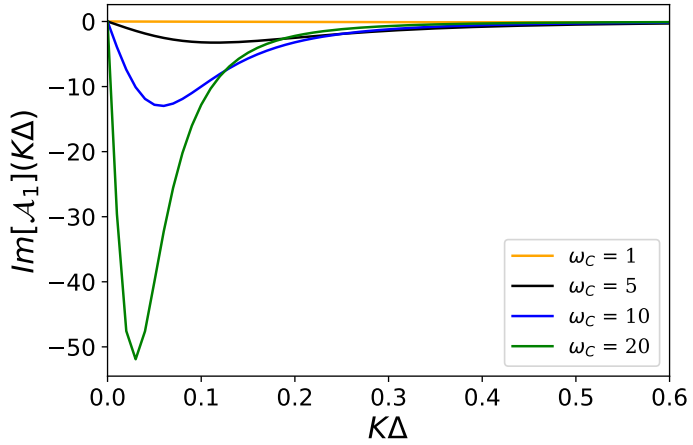

Figure 7.5: Imaginary part of the bath correlation function $\mathcal{A}_1$, for four different values of frequency cutoff ω_C, as a function of the memory depth time $K\Delta$ as defined in Eqs. (7.6). Here we have fixed $\alpha = 0.1$

7.3 Spin observables and TEMPO parameters

For $u = 0$, we use TEMPO to compute the dynamics of the spin observables $\langle \hat{S}_z \rangle$ and $\langle \hat{S}_x \rangle$ for different values of the algorithm parameters. We first consider the zero temperature case. In order to see how the Trotter error, introduced in the QuAPI method and shown in Eq. (3.10), affects the convergence of the observables, we fix the length of the memory propagated at each time-step $K\Delta$ to a constant value, and vary Δ. The first row in Fig. 7.6 shows different behaviour between $\langle \hat{S}_z \rangle$, where convergence arises for $\Delta > 0.01$, and $\langle \hat{S}_x \rangle$, where convergence arises for $\Delta < 0.1$, signalling the existence of a suitable range for the time-step value for fixed $K\Delta$.

Secondly, in order to check how the finite memory time affects the convergence of the observables, we fix the time-step Δ and increase K until the results converge. Fig. 7.6 shows that, for zero bath temperature, the average spin functions converge reasonably for $K > 200$, while lower values of the memory cutoff lead to an inaccurate dynamics (see second row, $K = 10$, blue line). The dynamics of $\langle \hat{S}_z \rangle$ calculated here at value $K = 200$ (red line, second row) matches the result obtained in Ref. [16] by Strathearn *et al.* with the original TEMPO algorithm, for the same values of K, α and ω_C.

Lastly, in order to check how the cutoff in the singular value decomposition affects the convergence of the observables, we fix K and Δ and increase p until convergence is achieved. The third row in Fig. 7.6 shows that best convergence is obtained for values of $p \geq 80$. Fig. 7.7 shows that a similar behaviour in the convergence of the spin observables is observed for finite temperature $T = 5$. Convergence of the spin dynamics is here obtained for $\Delta \sim 0.01$, $K \geq 200$ and $p \geq 80$.

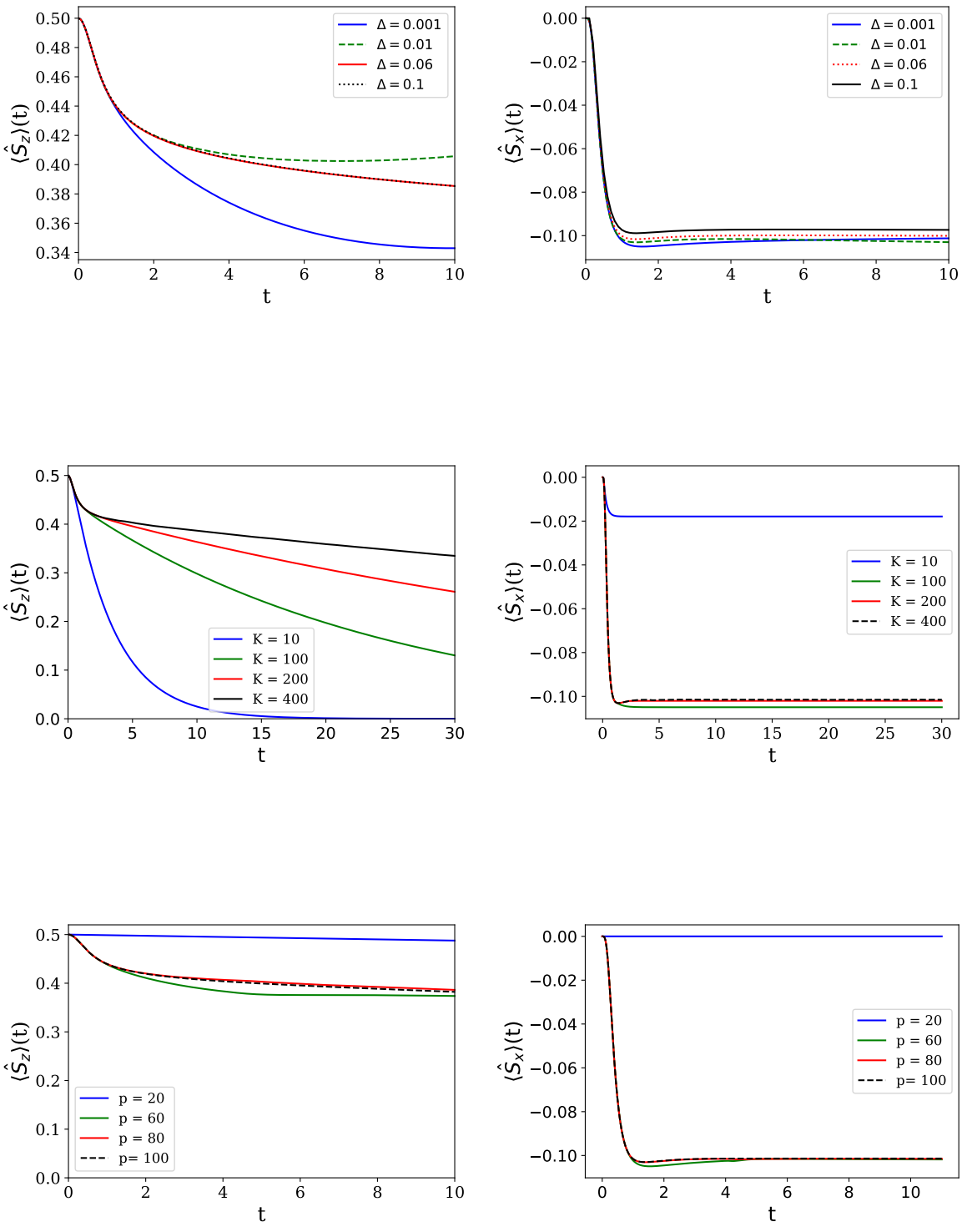

Figure 7.6: Dynamics of the mean values of the spin operators $\langle \hat{S}_z \rangle$ (left column) and $\langle \hat{S}_x \rangle$ (right column) for zero bath temperature, calculated with TEMPO for $u = 0$. The initial spin state is $|\psi(0)\rangle = |\uparrow\rangle$. Here $\omega_C = 5$ and $\alpha = 1$. First row: behaviour for different values of Δ, with fixed product $K\Delta = 3$ and $p = 80$. Second row: behaviour for different values of K, for fixed $p = 80$, $\Delta = 0.01$. Third row: behaviour for different values of p, for fixed $K = 400$, $\Delta = 0.01$.

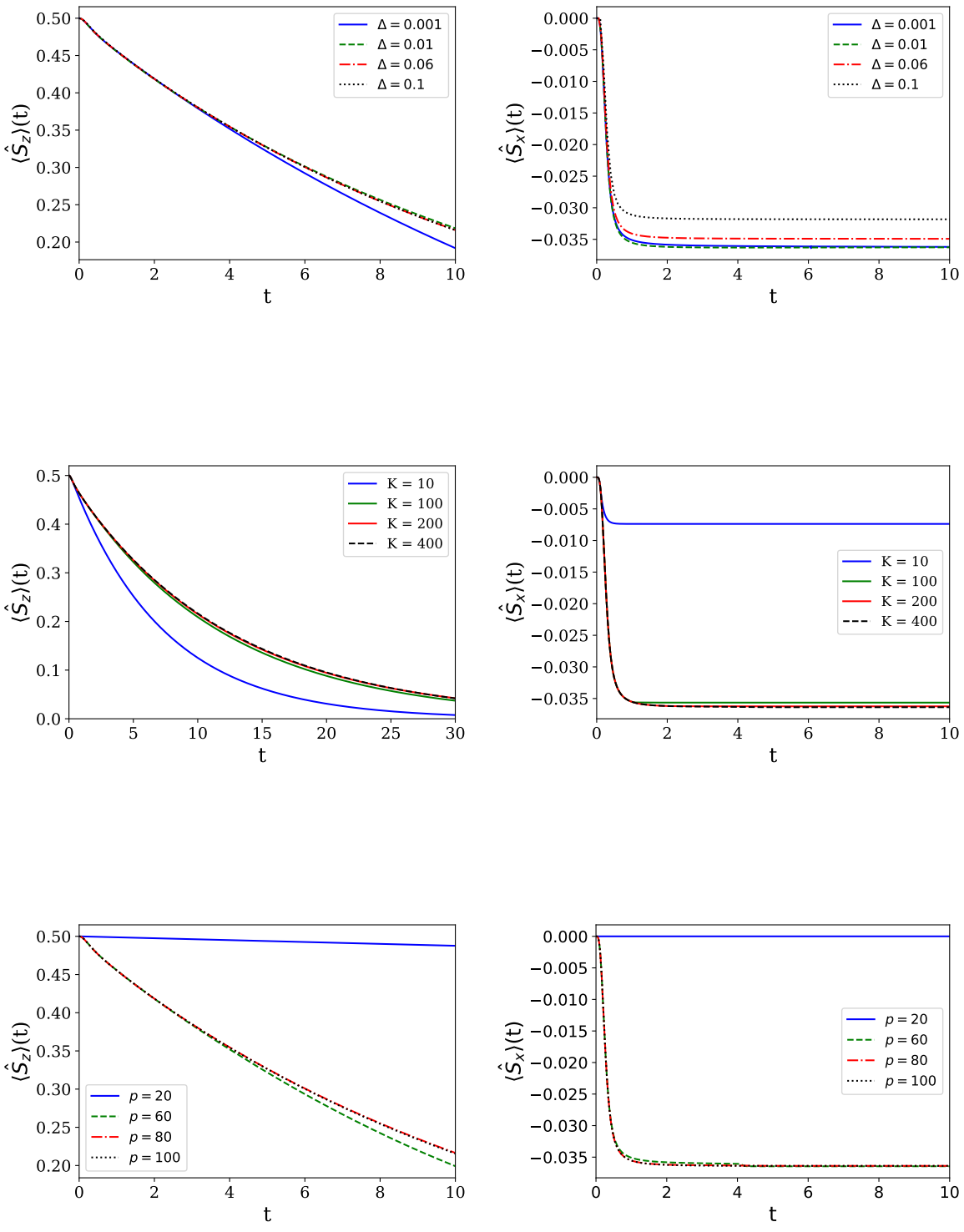

Figure 7.7: Dynamics of the mean values of the spin operators $\langle \hat{S}_z \rangle$ (left column) and $\langle \hat{S}_x \rangle$ (right column) for finite bath temperature $T = 5$, calculated with TEMPO for $u = 0$. The initial spin state is $|\psi(0)\rangle = |\uparrow\rangle$. Here $\omega_C = 5$ and $\alpha = 1$. First row: behaviour for different values of Δ, with fixed product $K\Delta = 3$ and $p = 80$. Second row: behaviour for different values of K, for fixed $p = 80$, $\Delta = 0.01$. Third row: behaviour for different values of p, for fixed $K = 400$, $\Delta = 0.01$.

8 | An application: Heat statistics of the spin-boson model

Although our method for the calculation of heat statistics is general, in the following we specialize to the spin-boson model describing a single spin one-half interacting with a bosonic bath of harmonic oscillators. We have presented this model and its characteristics in Chap. 7, where we defined the Hamiltonians of the overall system and bath in Eqs. (7.1 - 7.3). We have verified that in the absence of counting field, our modified TEMPO algorithm reproduces the correct dynamics of the spin observables and studied the convergence of such dynamics in relation to the TEMPO parameters. We now consider two different limits of the spin-boson model: the independent-boson model with $\Omega = 0$ and the unbiased spin-boson model with $\omega_0 = 0$ and $\Omega \neq 0$, with a focus on heat statistics. The independent-boson model is exactly solvable, allowing us to verify the accuracy of our numerical method. We then turn to the unbiased spin-boson model, an archetypal example of a non-integrable open quantum system. The experimental reasons that make the spin-boson model relevant have been discussed in the introduction Chap. 5. Another practical motivation for our focus on this model is that it represents a general setting known to be amenable to efficient tensor-network descriptions [121, 122]. Furthermore, the canonical open quantum system comprises a small, few-state system coupled to a bosonic bath, and the spin-boson model is the simplest case.

We start by studying the mean heat exchanged with the bath in the Markovian limit, for which an analytical solution is easily obtainable. We then apply our numer-

ical method for the calculation of heat statistics in non-Markovian regimes, where analytical solutions do not exist, after having verified the efficiency of the modified algorithm and TEMPO parameter ranges necessary for convergence through the solvable independent-boson model. Interestingly, our results show that the system-bath interaction energy makes a considerable contribution to the heat statistics, even in the weak-coupling and high-temperature regime where a Markovian description of the system dynamics alone is accurate. This underlines the need to interpret with care the standard Markovian description of quantum thermodynamics [123], which is based on properties of the open system alone.

In the following we choose a bosonic bath characterized by an Ohmic spectral density Eq. (7.4).

8.1 Exchanged heat in the Markovian limit

In order to gather a better understanding of the expected behaviour of the mean exchanged heat $\langle Q \rangle$ defined in Eq. (4.17), we study the Lindblad master equation for the reduced modified density matrix $\hat{\rho}_S(t,u)$ describing the Markovian limit for an unbiased spin-boson model. For the total Hamiltonian defined by Eqs. (7.1 - 7.3), the Lindblad master equation is [95]

$$\begin{aligned}\frac{\partial \hat{\rho}_S(t,u)}{\partial t} &= -i\left[\hat{H}_S, \hat{\rho}_S(t,u)\right] \\ &- \frac{\gamma_e}{2}\left[\{\hat{r}_+\hat{r}_-, \hat{\rho}_S(t,u)\} - 2e^{iu\Omega}\hat{r}_-\hat{\rho}_S(t,u)\,\hat{r}_+\right] \\ &- \frac{\gamma_a}{2}\left[\{\hat{r}_-\hat{r}_+, \hat{\rho}_S(t,u)\} - 2e^{-iu\Omega}\hat{r}_+\hat{\rho}_S(t,u)\,\hat{r}_-\right],\end{aligned} \tag{8.1}$$

where we have set $\omega_0 = 0$, $\hat{r}_+ = \hat{S}_z + i\hat{S}_y$ and $\hat{r}_- = \hat{S}_z - i\hat{S}_y$. Here γ_e and γ_a are the emission and absorption rates respectively, given by

$$\gamma_e = \pi\alpha\left(1 + \left\langle \hat{N}_\Omega \right\rangle_{t=0}\right)\Omega e^{-\Omega/\omega_C}, \tag{8.2}$$

$$\gamma_a = \pi\alpha\left\langle \hat{N}_\Omega \right\rangle_{t=0}\Omega e^{-\Omega/\omega_C}, \tag{8.3}$$

with $\langle \hat{N}_\Omega \rangle_{t=0}$ being the Planck distribution as defined by Eq. (6.37) for $\omega_j = \Omega$. From the Lindblad equation we can calculate the time derivative of the mean heat transferred between bath and system,

$$\frac{d\langle Q \rangle (t)}{dt} = \Omega \left[\gamma_e \rho_S^{\uparrow} (t,0) - \gamma_a \rho_S^{\downarrow} (t,0) \right]. \tag{8.4}$$

$\rho_S^{\uparrow}(t,0)$ and $\rho_S^{\downarrow}(t,0)$ are the diagonal elements of matrix $\hat{\rho}_S(t,0)$ in the eigenbasis of $\hat{H}_S$; that is, in the basis of eigenstates of operator $\hat{S}_x$. Setting an initial state for the spin, the Lindblad master equation Eq. (8.1) can be solved for $\hat{\rho}_S(t,u)$ for a fixed value of the counting field u. The characteristic function of heat is calculated through Eq. (6.7). This allows us to find the average heat exchanged through a numerical derivative, as in Eq. (6.13). Preliminary checks show that for a counting field parameter $u \leq 0.01$, the obtained results for $\langle Q \rangle (t)$ converge to one unique function of time. One could alternatively solve the Lindblad master equation and integrate Eq. (8.4) in time in order to find $\langle Q \rangle (t)$.

8.1.1 Asymptotic exchanged heat

In the following, we set the initial state of the spin to be $|\psi(0)\rangle = |\uparrow\rangle$, with $|\uparrow\rangle$ an eigenstate of $\hat{S}_z$. Fig. 8.1 shows the average heat exchanged in the Markovian limit, for a spin splitting fixed to $\Omega = 1$, and comparatively high temperature $T = 5$. It is clear that the system-bath coupling strength α does not affect the asymptotic value $\langle Q \rangle_\infty$ at which the exchanged heat equilibrates, but only affects the time frame at which this equilibration happens. Stronger coupling leads to a faster equilibration time. The Markovian solution is however of interest because in a generic non-Markovian, weak coupling limit, we expect the dynamics defined by the modified influence functional Eq. (6.21) to lead to an asymptotic solution $\langle Q \rangle_\infty$ that includes the average heat transfer described by the Markovian result, among other possible effects. We will see this is indeed the case. Fig. 8.2 shows that the spin splitting Ω, on the other hand, affects the asymptotic heat value, which increases, although not

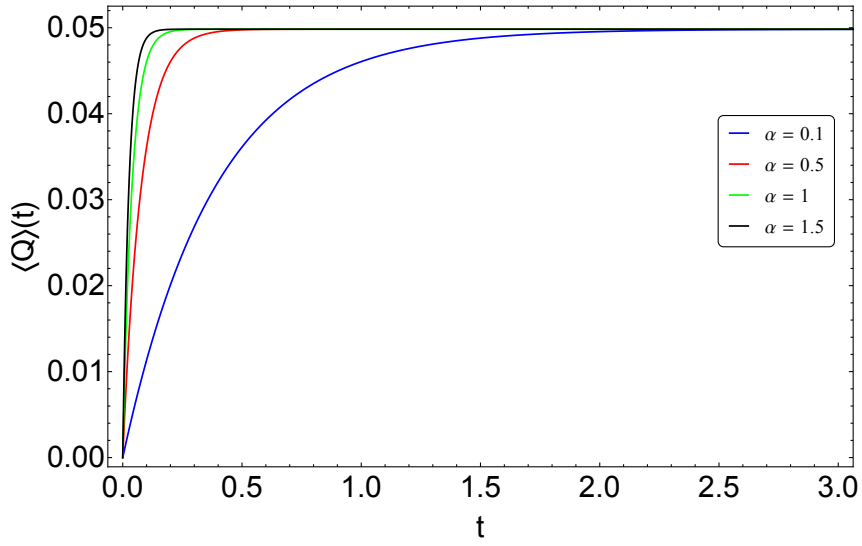

Figure 8.1: Average heat exchanged between bath and system in the Markovian limit, as a function of time, for four different values of the system-bath coupling strength. Here we have set $T = 5$, $\omega_C = 5$, $\Omega = 1$. The initial state of the system is $|\psi_0\rangle = |\uparrow\rangle$. The numerical derivative is taken at $u = 0.01$.

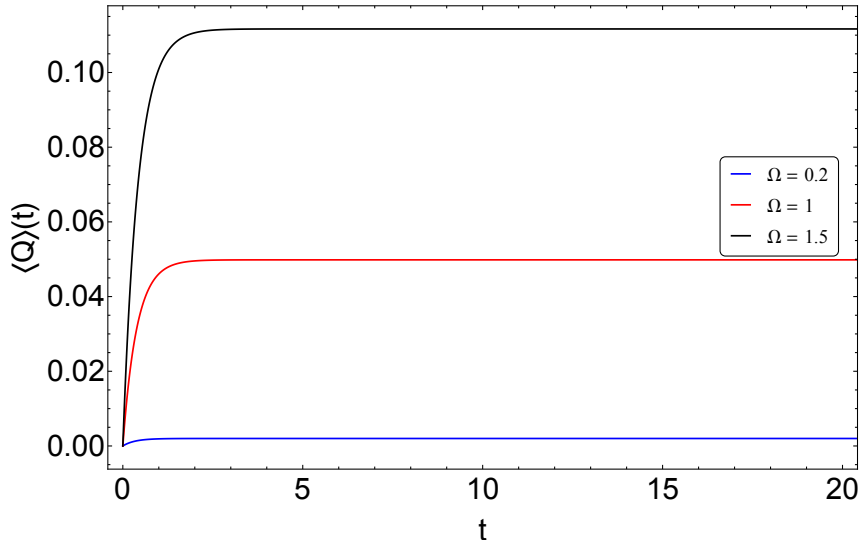

Figure 8.2: Average heat exchanged between bath and system in the Markovian limit, as a function of time, for three different values of the spin splitting. Here we have set $T = 5$, $\omega_C = 5$, $\alpha = 0.1$. The initial state of the system is $|\psi(0)\rangle = |\uparrow\rangle$. The numerical derivative is taken at $u = 0.01$.

linearly, with increasing value of Ω.

In the Markovian weak-damping limit, the spin evolves in time to a thermal steady-state in Gibbs form, $\hat{\rho}_S(\infty) = \exp[-\beta \hat{H}_S]/Z_S$, with $Z_S = \mathrm{Tr}_S[\exp(-\beta \hat{H}_S)]$. The asymptotic value of its energy $\langle \hat{H}_S \rangle_\infty = \mathrm{Tr}_S[\hat{\rho}_S(\infty)\hat{H}_S]$ is then easily calculated. The only contribution to the average heat change in the spin system $\langle Q_S \rangle_\infty = \langle \hat{H}_S \rangle_\infty - \langle \hat{H}_S \rangle_0$, is the heat transferred as it relaxes to a thermal state, which, in the absence of external work, is equal to the change in its internal energy. We therefore have

$$\langle Q_S \rangle_\infty = -\frac{\sqrt{\Omega^2 + \omega_0^2}}{2} \tanh\left[\frac{\sqrt{\Omega^2 + \omega_0^2}}{2T}\right] - \langle \psi(0)|\hat{H}_S|\psi(0)\rangle. \tag{8.5}$$

For an initial spin state $|\psi(0)\rangle = |\uparrow\rangle$, and parameters $\omega_0 = 0$, $\Omega = 1$ and $T = 5$ as in Fig. 8.1, we can calculate from Eq. (8.5) $\langle Q_S \rangle_\infty = -0.04983$. On the other hand, the numerical asymptotic solution for the average heat exchanged by the bath can be extrapolated from the data collected in Fig. 8.1, and amounts to $\langle Q \rangle_\infty = 0.04983$. We can see that in the Markovian limit, the only change in energy that occurs in the bath is caused by the transfer of heat from the system, $\langle Q \rangle_\infty = -\Delta U_\infty$. For an initial spin state $|\uparrow\rangle$, this amounts to

$$\langle Q \rangle_\infty = \frac{\Omega}{2} \tanh\left[\frac{\Omega}{2T}\right]. \tag{8.6}$$

We can verify that this conclusion holds true for different initial states of the spin. Fig. 8.3 shows $\langle Q \rangle(t)$ for an initial state of the spin $|\leftarrow\rangle = (-1, 1)$ and $|\rightarrow\rangle = (1, 1)$, both eigenstates of the spin operator $\hat{S}_x$ with eigenvalues $\pm 1/2$ respectively. The asymptotic heat exchanged by the bath is drastically different. Again, the data from Fig. 8.3 shows it is equal to $-\langle Q_S \rangle_\infty$. From Eq. (8.5), it amounts to

$$\langle Q \rangle_\infty = \frac{\Omega}{2} \tanh\left[\frac{\Omega}{2T}\right] - \frac{\Omega}{2} \tag{8.7}$$

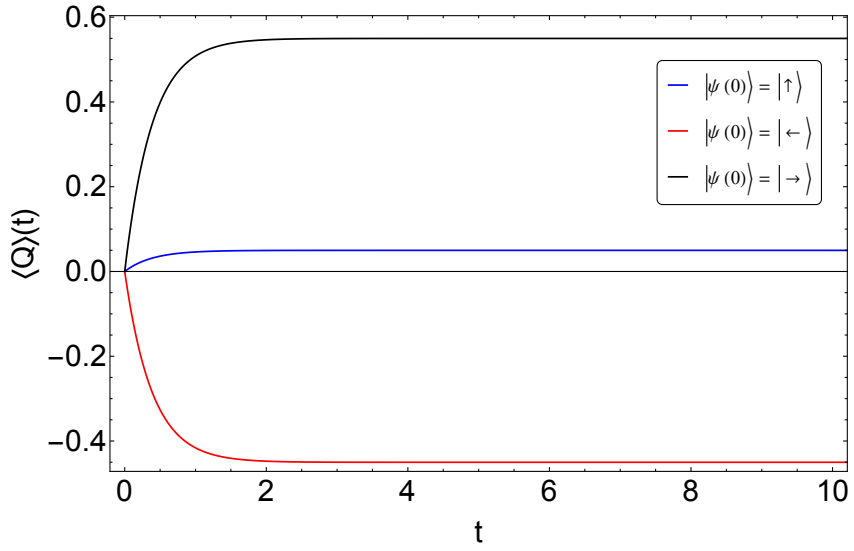

Figure 8.3: Average heat exchanged between bath and system in the Markovian limit, as a function of time, for three different initial states of the spin. Here we have set $T = 5$, $\omega_C = 5$, $\alpha = 0.1$, and $\Omega = 1$. The numerical derivative is taken at $u = 0.01$.

for initial state $|\psi(0)\rangle = |\leftarrow\rangle$, and

$$\langle Q\rangle_\infty = \frac{\Omega}{2}\tanh\left[\frac{\Omega}{2T}\right] + \frac{\Omega}{2} \tag{8.8}$$

for initial state $|\psi(0)\rangle = |\rightarrow\rangle$. From both the data and the analytical prediction of Eqs. (8.7 - 8.8), the asymptotic values are $\langle Q\rangle_\infty = -0.45016$ and $\langle Q\rangle_\infty = 0.54983$ respectively, for $\Omega = 1$ and $T = 5$. Fig. 8.3, in particular, reveals that in a Markovian set up with a system Hamiltonian as in Eq. (7.1), the total heat exchanged by the bath equals the sum of the energies that it takes for the initial system state to reach the energy level of the state $|\uparrow\rangle$ and the heat transferred from the system to the bath as it equilibrates to a thermal state Eq. (8.6). An initial system state $|\leftarrow\rangle$ has an energy lower than that of state $|\uparrow\rangle$ by an amount equal to $\Omega/2$, and therefore the bath transfers to the system a quantity of heat equal to $\Omega/2$. On the other hand, an initial system state $|\rightarrow\rangle$ has an energy higher than that of state $|\uparrow\rangle$ by an amount $\Omega/2$, and therefore the bath receives from the system a quantity of heat equal to $\Omega/2$.

These predictions derived from the Markovian limit will be useful in the explanation of the phenomena that drive non-Markovian heat transfers.

8.2 Independent boson model

The independent-boson (IB) model is described by Eqs. (7.1 - 7.3) with $\Omega = 0$. This model, for which we derive an analytical solution for the characteristic function of heat, will serve us as a way to verify the accuracy of our method.

The Hamiltonian can be diagonalised by a polaron transformation, which takes the general form

$$\hat{P} = \exp\left[\hat{S}_z \sum_j \frac{f_j}{\omega_j}\left(\hat{a}_j - \hat{a}_j^\dagger\right)\right]. \tag{8.9}$$

This describes a spin-dependent displacement of each bath oscillator by an amount proportional to f_j. The choice $f_j = g_j$ diagonalises the IB Hamiltonian as $\hat{P}^\dagger \hat{H} \hat{P} = \hat{H}_0 - \frac{1}{2}E_r$, where $\hat{H}_0 = \hat{H}_S + \hat{H}_B$ is the free Hamiltonian and we have defined the reorganisation energy

$$E_r = \frac{1}{2}\int_0^\infty d\omega \, \frac{J(\omega)}{\omega} = \alpha\omega_C, \tag{8.10}$$

for an Ohmic spectral density, which determines the shift in ground-state energy due to the system-bath interaction. In the IB model, $[\hat{H}, \hat{H}_S] = 0$, meaning that the local energy of the spin is conserved and $\Delta U = 0$. Therefore, the heat dissipated into the bath is associated purely with the system-bath interaction.

8.2.1 Average heat and variance for the independent boson model

Using the transformation defined by Eq. (8.9), we write the unitary time evolution operator as

$$\hat{U}(t) = \hat{P} e^{-i\hat{H}_0 t}\hat{P}^\dagger \tag{8.11}$$

$$= e^{-i\hat{H}_0 t}\left(e^{i\hat{H}_0 t/2}\tilde{P}(t/2)\tilde{P}^\dagger(-t/2)e^{-i\hat{H}_0 t/2}\right), \tag{8.12}$$

where the tilde denotes an operator in the interaction picture with respect to $\hat{H}_0$, i.e.,

$$\begin{aligned}\tilde{P}(t) &= e^{i\hat{H}_0 t}\hat{P}e^{-i\hat{H}_0 t} \\ &= \exp\left[\hat{S}_z \sum_j \frac{g_j}{\omega_j}\left(e^{-i\omega_j t}\hat{a}_j - e^{i\omega_j t}\hat{a}_j^\dagger\right)\right].\end{aligned} \tag{8.13}$$

Using the Baker-Campbell-Hausdorff formula, $e^A e^B = \exp(A + B + \frac{1}{2}[A, B] + \ldots)$, and neglecting an irrelevant phase factor, we obtain $\hat{U}(t) = \hat{U}_0(t)\hat{U}_I(t)$, where $\hat{U}_0(t) = e^{-i\hat{H}_0 t}$ is the free propagator and

$$\hat{U}_I(t) = \exp\left[2\hat{S}_z \sum_j \left(\alpha_j(t)\hat{a}_j^\dagger - \alpha_j^*(t)\hat{a}_j\right)\right] \tag{8.14}$$

is the interaction-picture propagator, which describes a spin-dependent displacement for each mode of magnitude

$$\alpha_j(t) = \frac{g_j}{2\omega_j}\left(1 - e^{i\omega_j t}\right). \tag{8.15}$$

The time evolution of the bath density matrix $\hat{\rho}_B(t)$ is

$$\hat{\rho}_B(t) = Tr_S\left[\hat{U}_I(t)\,\hat{\rho}_S(0) \otimes \hat{\rho}_B(0)\,\hat{U}_I^\dagger(t)\right]. \tag{8.16}$$

Expanding the trace over the spin degrees of freedom in the basis of eigenstates of $\hat{S}_z$, $\{|\uparrow\rangle, |\downarrow\rangle\}$, we see that the action of the time evolution operator $\hat{U}_I(t)$ is

$$\hat{U}_I^\dagger(t)\,|\downarrow\rangle = \exp\left[\sum_i \left(\alpha_i(t)\,\hat{a}_i^\dagger - \alpha_i^*(t)\,\hat{a}_i\right)\right]|\downarrow\rangle \tag{8.17}$$

$$\hat{U}_I^\dagger(t)\,|\uparrow\rangle = \exp\left[-\sum_i \left(\alpha_i(t)\,\hat{a}_i^\dagger - \alpha_i^*(t)\,\hat{a}_i\right)\right]|\uparrow\rangle, \tag{8.18}$$

which is the action of a product of displacement operators $\hat{D}(x_i) = e^{x_i \hat{a}^\dagger - x_i^* \hat{a}}$ for each bosonic mode, where in this case $x_i = \alpha_i(t)$. We can define the bath operator

$$\hat{D}_B(t) = \exp\left[\sum_i \left(\alpha_i(t)\,\hat{a}_i^\dagger - \alpha_i^*(t)\,\hat{a}_i\right)\right], \tag{8.19}$$

and write the time evolution of $\hat{\rho}_B(t)$ as

$$\begin{aligned}\hat{\rho}_B(t) = &\left(\hat{D}_B^\dagger(t)\,\hat{\rho}_B(0)\,\hat{D}_B(t) - \hat{D}_B(t)\,\hat{\rho}_B(0)\,\hat{D}_B^\dagger(t)\right)\langle\downarrow|\,\hat{\rho}_S(0)\,|\downarrow\rangle \\ &+ \hat{D}_B(t)\,\hat{\rho}_B(0)\,\hat{D}_B^\dagger(t).\end{aligned} \tag{8.20}$$

It is easy to see that the action of the bath displacement operator $\hat{D}_B(t)$ on the bath free Hamiltonian $\hat{H}_B$ is given by

$$\hat{D}_B(t)\,\hat{H}_B\hat{D}_B^\dagger(t) = \hat{H}_B - \sum_i \omega_i\left(\alpha_i(t)\,\hat{a}_i^\dagger + \alpha_i^*(t)\,\hat{a}_i\right) + \mathcal{O}\left(g_i^2\right), \tag{8.21}$$

$$\hat{D}_B^\dagger(t)\,\hat{H}_B\hat{D}_B(t) = \hat{H}_B + \sum_i \omega_i\left(\alpha_i(t)\,\hat{a}_i^\dagger + \alpha_i^*(t)\,\hat{a}_i\right) + \mathcal{O}\left(g_i^2\right). \tag{8.22}$$

Here we have expanded the operator $\hat{D}_B(t)$ up the the second order in the coupling strength constant g_i, and used the commutation rules $[\hat{H}_B, \hat{a}_i^\dagger] = \omega_i\hat{a}_i^\dagger$ and $[\hat{H}_B, \hat{a}_i] = -\omega_i\hat{a}_i$. The coefficients of any given even power of g_i in the further Taylor series expansion of Eqs. (8.21-8.22) are the same function, with same sign. The coefficients of any given odd power of g_i are the same function, but appear with opposite sign. However the odd power coefficients consist of an odd number of annihilation and creation operators, and therefore their mean value $\langle\bullet\rangle_B$ is zero. On the other hand the terms with an even power of g_i in the Taylor series expansion cancel each other when subtracted, and it follows that

$$\left\langle\hat{D}_B(t)\,\hat{H}_B\hat{D}_B^\dagger(t)\right\rangle_B - \left\langle\hat{D}_B^\dagger(t)\,\hat{H}_B\hat{D}_B(t)\right\rangle_B = 0. \tag{8.23}$$

Using this result and the time evolution of $\hat{\rho}_B(t)$ Eq. (8.20), it is easy to calculate the mean heat exchanged by the bath $\langle Q\rangle(t) = \langle \hat{H}_B\rangle_t - \langle \hat{H}_B\rangle_0$,

$$\langle Q\rangle(t) = \left\langle \hat{D}_B^\dagger(t)\, \hat{H}_B \hat{D}_B(t)\right\rangle_B - \langle \hat{H}_B\rangle_0. \tag{8.24}$$

This is not surprising, as one would expect the heat exchanged by the bosonic bath to be independent of the initial state of the system, in a pure dephasing, independent boson model. We expand the first term, noting that the displacement operator $\hat{D}_B(t)$ acts on the bosonic modes as

$$\hat{D}_B^\dagger(t)\, \hat{a}_i \hat{D}_B(t) = \hat{a}_i + \alpha_i(t)\,, \tag{8.25}$$

$$\hat{D}_B^\dagger(t)\, \hat{a}_i^\dagger \hat{D}_B(t) = \hat{a}_i^\dagger + \alpha_i^*(t)\,. \tag{8.26}$$

It follows that $\left\langle \hat{D}_B^\dagger(t)\, \hat{H}_B \hat{D}_B(t)\right\rangle_B = \sum_i \omega_i |\alpha_i(t)|^2 + \langle \hat{H}_B\rangle_0$. Eq. (8.24) leads then to $\langle Q\rangle(t) = \sum_i \omega_i |\alpha_i(t)|^2$. Using the definition of the displacement coefficients $\alpha_i(t)$ Eq. (8.15), and the definition of the spectral density function Eq. (3.17), we find the mean heat for the independent boson model to be

$$\langle Q\rangle = \frac{1}{2}\int_0^\infty d\omega \frac{J(\omega)}{\omega}\left[1-\cos(\omega t)\right], \tag{8.27}$$

which is strictly positive and independent of temperature. Interestingly, these properties are shared by all odd cumulants of the heat distribution in the IB model. For an Ohmic spectral density, we have $\langle Q\rangle = \alpha\omega_C^3 t^2/(1+\omega_C^2 t^2)$, which monotonically approaches the reorganisation energy in the long-time limit:

$$\langle Q\rangle_\infty = \alpha\omega_C = E_r. \tag{8.28}$$

The same passages that lead to the calculation of Eq. (8.27), lead to the exact analytical expression for the heat variance

$$\langle\langle Q^2 \rangle\rangle = \frac{1}{2}\int_0^\infty d\omega J(\omega)\left[1-\cos(\omega t)\right]\coth\left(\frac{\beta\omega}{2}\right). \tag{8.29}$$

Unlike the mean heat in Eq. (8.27), which is independent of temperature, the variance in Eq. (8.29) depends on the inverse temperature of the bath β.

8.2.2 Characteristic function for the independent boson model

We show that the heat characteristic function is independent of the state of the spin and given explicitly by

$$\begin{aligned}\ln\chi(u) = -\frac{1}{2}\int_0^\infty d\omega\,\frac{J(\omega)}{\omega^2}\left[1-\cos(\omega t)\right] \\ \times\left\{\left[1-\cos(\omega u)\right]\coth\left(\frac{\omega}{2T}\right) - i\sin(\omega u)\right\}.\end{aligned} \tag{8.30}$$

To do this we use the expression for the interaction-picture propagator $\hat{U}_I(t)$ from Eq. (8.14), in the definition of quantum characteristic function Eq. (6.4), where $\hat{U}(t) = \hat{U}_0(t)\hat{U}_I(t)$, obtaining $\chi(u) = \langle \bar{V}^\dagger_{-u}(t)\bar{V}_u(t)\rangle_0$. Here $\bar{V}_u(t) = e^{iu\hat{H}_B/2}\hat{U}_I(t)e^{-iu\hat{H}_B/2}$ is the modified interaction-picture evolution operator, given explicitly by

$$\bar{V}_u(t) = |\uparrow\rangle\langle\uparrow| \otimes \prod_j \hat{D}_B\left(\alpha_j e^{i\omega_j u/2}\right) + |\downarrow\rangle\langle\downarrow| \otimes \prod_j \hat{D}^\dagger_B\left(\alpha_j e^{i\omega_j u/2}\right), \tag{8.31}$$

where we have expanded the operator $\hat{S}_z$ into its eigenbasis. $\hat{D}_B(x)$ is the displacement operator for each bosonic mode. We can therefore divide the characteristic function into the sum of two terms, $\chi(u) = p_\uparrow\chi_\uparrow(u) + p_\downarrow\chi_\downarrow(u)$, where $p_\uparrow = \langle\uparrow|\hat{\rho}_S(0)|\uparrow\rangle$ and $p_\downarrow = \langle\downarrow|\hat{\rho}_S(0)|\downarrow\rangle$ denote the initial spin occupations and

$$\chi_\uparrow(u) = \prod_j \left\langle \hat{D}^\dagger_B\left(\alpha_j e^{-i\omega_j u/2}\right)\hat{D}_B\left(\alpha_j e^{i\omega_j u/2}\right)\right\rangle_0, \tag{8.32}$$

$$\chi_\downarrow(u) = \prod_j \left\langle \hat{D}_B\left(\alpha_j e^{-i\omega_j u/2}\right)\hat{D}^\dagger_B\left(\alpha_j e^{i\omega_j u/2}\right)\right\rangle_0. \tag{8.33}$$

These can be evaluated using the property $\hat{D}_B(x)\hat{D}_B(y) = e^{i\mathrm{Im}(xy^*)}\hat{D}_B(x+y)$ [124] and the thermal average $\langle \hat{D}(x)\rangle = \exp[-\frac{1}{2}|x|^2 \coth(\beta\omega/2)]$. We find that $\chi_\uparrow(u) = \chi_\downarrow(u)$ and therefore $\chi(u)$ is independent of the spin populations. The final result for $\chi(u)$ is quoted in Eq. (8.30), from which the n-th cumulant of the heat distribution can be derived via the formula

$$\langle\langle Q^n \rangle\rangle = (-i)^n \frac{d^n}{du^n} \ln \chi(u)\Big|_{u=0}. \tag{8.34}$$

Through Eq. (8.34) we equivalently find Eq. (8.27) and Eq. (8.29) calculated before. Explicitly, we obtain

$$\langle\langle Q^{2l-1} \rangle\rangle = \frac{1}{2}\int_0^\infty d\omega\, J(\omega)\omega^{2l-3}\left[1-\cos(\omega t)\right], \tag{8.35}$$

$$\langle\langle Q^{2l} \rangle\rangle = \frac{1}{2}\int_0^\infty d\omega\, J(\omega)\omega^{2l-2}\left[1-\cos(\omega t)\right]\coth\left(\frac{\beta\omega}{2}\right), \tag{8.36}$$

for integers $l > 0$. We see that all cumulants are positive and only the even cumulants depend on temperature.

8.2.3 Numerical and analytical solution: a comparison

For an Ohmic spectral density function, Eq. (8.27) depends on only two parameters, the coupling strength and the frequency cutoff. While ω_C sets the timescale of the heat transfer process, the mean exchanged heat scales linearly with α. At first glance, it is not obvious that for strong coupling our method will be able to give the correct prediction, as this regime is often difficult to reach numerically. It is therefore of interest to demonstrate the validity of the numerical method for different values of α. The mean heat is plotted as a function of evolution time for several different coupling strengths in Fig. 8.4. We use these results to validate the numerical modified TEMPO algorithm, the results of which are shown in the same plot. We find excellent agreement between our simulations and the exact solution for each value of α considered. A simple estimate of the accuracy of our approach is obtained by com-

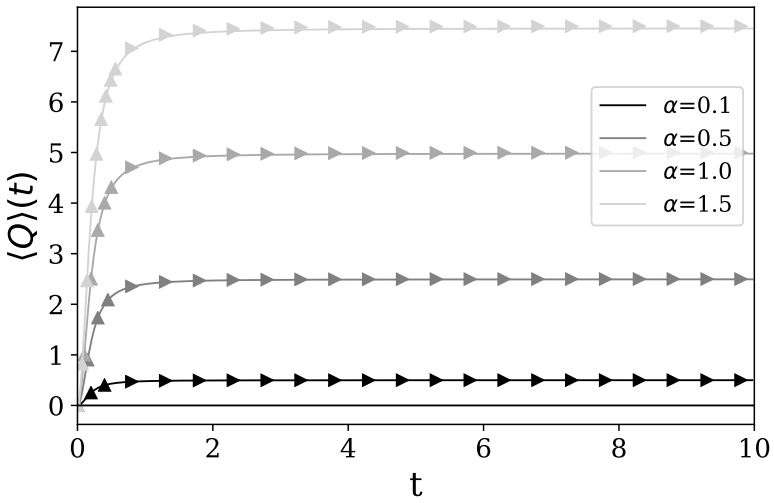

Figure 8.4: Mean heat dissipated into the bath as a function of time in the independent boson model, as given by Eq. (8.27) (triangles) and as calculated numerically (solid lines), for four different values of the coupling strength α. The spin splitting is $\omega_0 = 1$, the temperature is $T = 5$, and the bath cutoff is $\omega_C = 5$. The parameters controlling the numerical accuracy are $K\Delta = 5$, $\Delta = 0.01$, $p = 100$, and the derivative is taken at $u = 0.01$.

paring the asymptotic heat values to the exact result in Eq. (8.28). For the convergence parameters we have used, we find a relative discrepancy of $\delta Q/Q = 0.04\%$ in the case of $\alpha = 0.1$, which increases to $\delta Q/Q = 0.67\%$ in the case of $\alpha = 1.5$. These discrepancies could be further reduced by increasing the accuracy of TEMPO through changing the convergence parameters Δ, p and K.

To quantify the fluctuations of the exchanged heat, we consider the variance $\langle\langle Q^2 \rangle\rangle = \langle Q^2 \rangle - \langle Q \rangle^2$, given by Eq. (8.29). Unlike the mean heat in Eq. (8.27), which is independent of temperature, the variance in Eq. (8.29) depends on the inverse temperature of the bath β. We show that our method is accurate for both a lower and a comparable temperature $k_B T$ with respect to the energy scale of the system ω_0. Fig. 8.5 shows the variance as a function of time, for different values of temperature and coupling strength. The numerical predictions again match the analytical solutions given by Eq. (8.29). Note that in order to get a better match between the solutions for high coupling, $\alpha = 1.5$, the value of the counting field at which the numerical derivative of $\chi(u)$ is taken has been set to $u = 0.005$, compared to the value of $u = 0.01$ in the case of $\alpha = 0.1$. This suggests that high coupling strength cases require in general more computational precision than low coupling cases, although

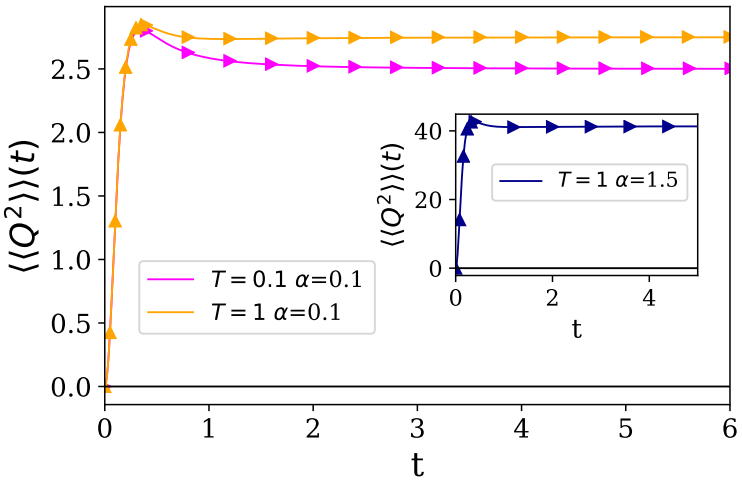

Figure 8.5: Variance of the heat dissipated into the bath as a function of time in the independent boson model. The solid lines are the second cumulant calculated numerically for the values of temperature and coupling strength indicated. The triangular markers are the corresponding analytical results given by Eq. (8.29). The spin splitting is set to $\omega_0 = 1$ and the bath cutoff is $\omega_C = 5$. The parameters controlling the numerical accuracy are $K\Delta = 5$, $\Delta = 0.01$, and $p = 100$. The derivative is taken at $u = 0.01$ for $\alpha = 0.1$ and at $u = 0.005$ for $\alpha = 1.5$.

not higher precision in the singular-value decomposition cutoff or time-step. The relative discrepancy in the asymptotic values between analytical and numerical solutions for $\langle\langle Q^2\rangle\rangle$ in the case of $T = 1$ are found to be $\delta Q^2/Q^2 = 0.12\%$ for $\alpha = 0.1$, and $\delta Q^2/Q^2 = 0.06\%$ for $\alpha = 1.5$. In the case of $T = 0.1$, $\alpha = 0.1$, the relative discrepancy is $\delta Q^2/Q^2 = 0.13\%$.

Overall we can conclude that, within the discussed discrepancies, our numerical method matches the analytical solution with great accuracy.

8.2.4 TEMPO memory depth

In Sec. 3.4 we have discussed the finite memory depth K of the TEMPO algorithm that allows it to efficiently propagate the ADT. We have also discussed in Sec. 7.2 how the correlation function in the absence of counting field vanishes with a memory depth time $K\Delta$ which depends on the bath parameters. We will now show how the memory depth affects the convergence of the mean heat and the variance of the heat distribution studied throughout this thesis.

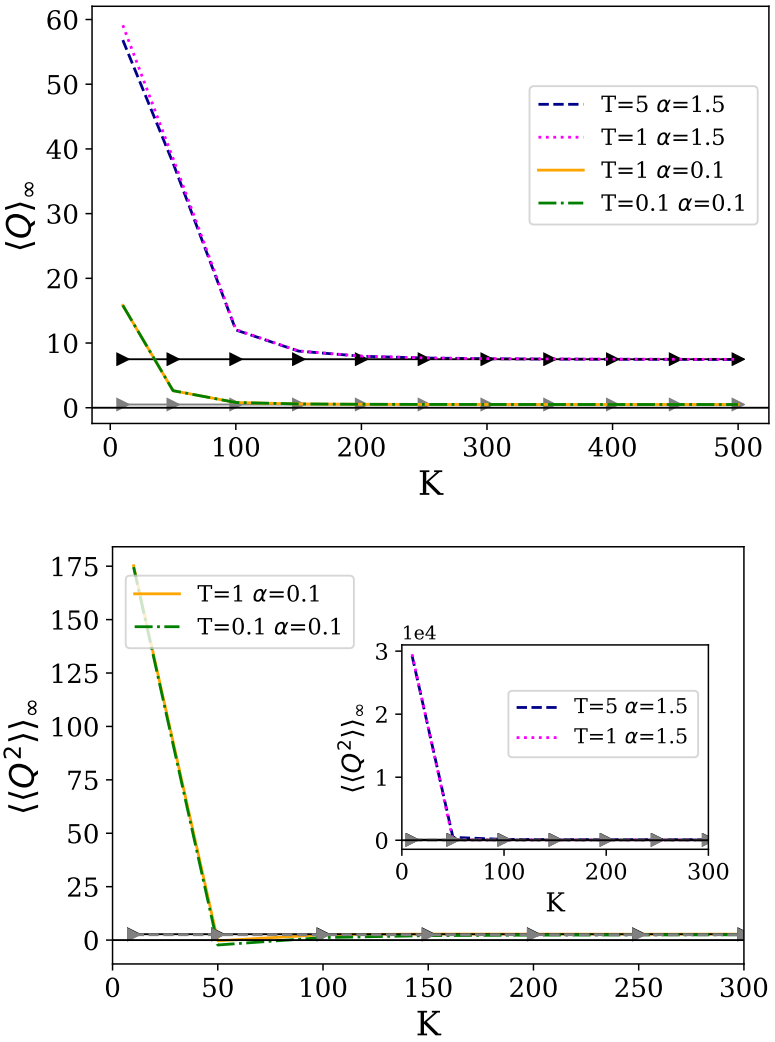

Figure 8.6: Upper figure: asymptotic mean heat for the independent-boson model as a function of K. Lower figure: asymptotic variance of the heat distribution for the independent-boson model as a function of K. Triangles represent the analytical solution given by Eq. (8.27) (upper figure) and Eq. (8.29) (lower figure) in the long time limit. The figures are plotted for different values of the temperature and coupling strength. The remaining parameters are set to $\omega_C = 5$, $\Delta = 0.01$, $p = 100$ and $u = 0.01$.

The form of the correlation functions in Eq. (6.51-6.53) sets the minimum value of $K\Delta$ needed. Indeed, $K\Delta$ has to be large enough to so that the discretized correlation functions are negligible. Preliminary calculations have shown that, for the values of temperature and coupling strength we will consider, this requirement is satisfied around the value $K\Delta = 5$. Fig. 8.6 shows that in the independent-boson model, for a fixed value of Δ, both the mean heat and the variance of the heat distribution reach the predicted asymptotic value for $K > 300$, for all the values of T and α depicted. For values $K < 100$, however, the asymptotic TEMPO result diverges greatly from the predicted one. This clearly shows how our method, which is able to operate at high values of the memory depth, has a much greater accuracy than other methods which operate in the region $K < 100$.

8.3 Unbiased spin-boson model

We now turn to the spin-boson model with $\Omega \neq 0$ in the Hamiltonian Eq. (7.1), focusing on the unbiased case where $\omega_0 = 0$. In this context, TEMPO has previously been used to pinpoint the localisation phase transition [16], which occurs when $T = 0$ and at a critical value of the coupling α [125, 126], and to study non-Markovian dynamics induced by spatially correlated environments [112]. Here we use our numerical method based on TEMPO to investigate the non-equilibrium thermodynamics of relaxation over a range of temperatures and coupling strengths. In the following, we take $\Omega = 1$, which defines our unit of energy.

8.3.1 Numerical derivative and counting field value

It has been discussed in Sec. 6.1.2 that in order to evaluate the statistical moments of the heat exchange, one needs to evaluate the derivative of the characteristic function at the point $u = 0$. The symmetries of $\chi(u)$ have been shown in Eq. (6.10) and are illustrated in Fig. 8.7, for both the independent-boson and spin-boson model. Note that in Fig. 8.7 it was not computationally possible to evaluate the character-

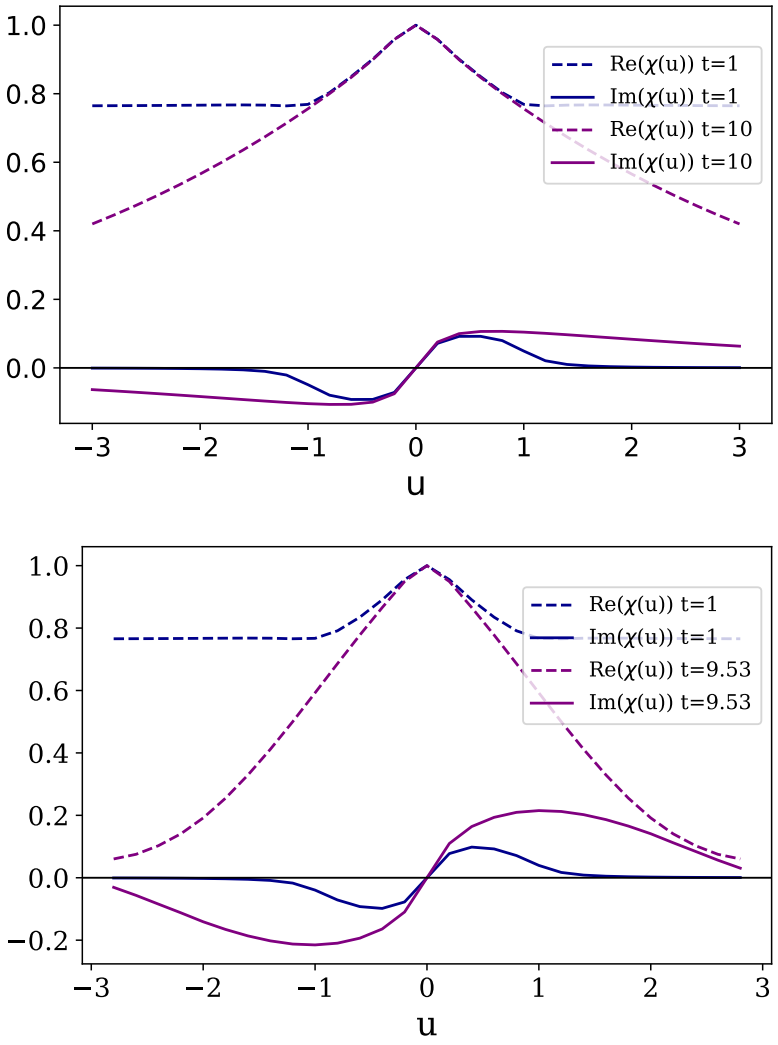

Figure 8.7: Upper figure: independent-boson model. Lower figure: spin-boson model. Real (dashed line) and imaginary (solid line) parts of the characteristic function, as a function of the counting field parameter u. $\chi(u)$ is evaluated for both a small time $t = 1$ (blue) and equilibrium times $t = 10$ for the IB model and $t = 9.53$ for the SB model (purple). The temperature is set to $T = 1$ and the coupling strength to $\alpha = 0.1$. The parameters controlling the numerical accuracy are $\omega_C = 5$, $K\Delta = 5$, $\Delta = 0.01$, and $p = 100$. The sampling of the function is taken at intervals of $\delta u = 0.2$.

istic function up to equilibrium time for values of u higher than those represented. In the case of the spin-boson model, $t = 9.53$ was the maximum time the TEMPO algorithm was able to reach for $u = 3$.

In our method we perform a numerical differentiation in order to calculate the first and second moments of the heat distribution, as shown in Eq. (6.13) and Eq. (6.14). In order to do that, we have to choose a suitable value of u. Note however that the counting field is not a numerical parameter of the TEMPO algorithm, but a variable of the characteristic function. The value u_ϵ of the counting field at which the numerical derivative has to be taken must be such that, within the interval $[0, u_\epsilon]$, the real part of the characteristic function can still be approximated by a constant function, and the slope of the imaginary part is linear. u_ϵ will depend on the model, as shown by comparing the two figures in Fig. 8.7, and on the physical parameters α, T and ω_C. Indeed, Fig. 8.5 shows an example where for $\alpha = 0.1$ it is sufficient to take $u = 0.01$, but for stronger coupling such as $\alpha = 1.5$ it is necessary to set $u = 0.005$ to achieve the same precision.

We have found that in order to achieve a function $\langle Q \rangle$ that is constant in the long time limit, for the parameters considered in this thesis the value of u_ϵ cannot be greater than $u_\epsilon = 0.01$. In general, decreasing the value of u_ϵ below $u_\epsilon = 0.005$ will increase the computational time but not improve significantly the precision of the result.

8.3.2 High temperature and weak coupling

We begin by studying the regime of weak coupling and relatively high temperature, with $\alpha = 0.1$ and $T = 5$. The mean heat transfer is plotted in Fig. 8.8 as a function of time, starting from a pure initial state, $\hat{\rho}_S(0) = |\psi(0)\rangle\langle\psi(0)|$. Specifically, we consider three different initial conditions: $|\psi(0)\rangle \in \{|\leftarrow\rangle, |\rightarrow\rangle, |\uparrow\rangle\}$, where $\hat{S}_x|\rightarrow\rangle = \frac{1}{2}|\rightarrow\rangle$, $\hat{S}_x|\leftarrow\rangle = -\frac{1}{2}|\leftarrow\rangle$ and $\hat{S}_z|\uparrow\rangle = \frac{1}{2}|\uparrow\rangle$. We also consider two values of the cutoff, $\omega_C = 5$ and $\omega_C = 50$.

Inspection of these results suggests that the heat transfer, $\langle Q \rangle$ is a sum of two

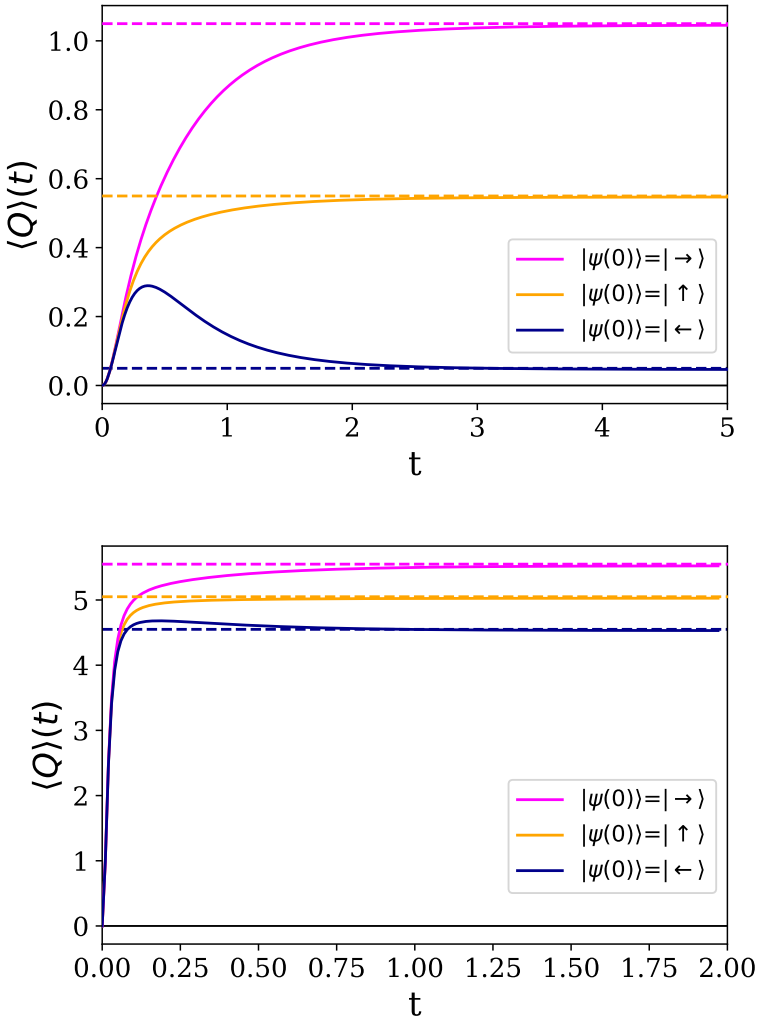

Figure 8.8: Heat transfer for the spin boson model in the high-temperature weak-coupling regime, with bath cut-off $\omega_C = 5$ (upper panel) and $\omega_C = 50$ (lower panel). Solid lines: numerical results for the mean heat $\langle Q \rangle (t)$ transferred to the bath as a function of time, for three different initial states of the system. Dashed lines: asymptotic approximation for $\langle Q \rangle_\infty$ given by Eq. (8.37). The environment parameters are set to $T = 5$ and $\alpha = 0.1$. The parameters controlling the numerical accuracy are $K\Delta = 5$, $\Delta = 0.01$, $p = 100$ and the derivative is taken at $u = 0.01$ for $\omega_C = 5$ and $u = 0.001$ for $\omega_C = 50$.

contributions. The first contribution is the heat transferred directly from the system as it relaxes to a thermal state $\hat{\rho}_S(\infty) \propto e^{-\beta \hat{H}_S}$. This is the contribution we discussed for the asymptotic Markovian limit in Sec. 8.1.1, whose corresponding change in internal energy ΔU_∞ is defined in Eq. (8.5). The second contribution to the mean heat transfer is associated with switching on the system-bath interaction, and is equivalent to the work done in a cyclic process. If we assume this contribution to be the reorganization energy E_r defined in Eq (8.10) as the asymptotic value of $\langle Q \rangle$ in the independent-boson model, we have the prediction

$$\langle Q \rangle_\infty = E_r + \frac{\Omega}{2} \tanh\left(\frac{\beta\Omega}{2}\right) + \langle \hat{H}_S \rangle_0. \tag{8.37}$$

This approximation shows near-perfect agreement with the long-time limit of the numerical results, as demonstrated by the dashed lines in Fig. 8.8. Notice that Eq. (8.5) is independent of the details of the bath spectral density (i.e. α and ω_C), while E_r does not depend in any way on the spin degrees of freedom. This indicates that, at high temperature and weak coupling, the displacement of the bath modes is not affected by the thermalization of the spin. Instead, these two processes give rise to independent and additive contributions to the mean heat transfer.

These distinct modes of heat transfer take place on different time scales. This is illustrated by the blue lines in both the $\omega_C = 5$ and $\omega_C = 50$ case of Fig. 8.8, corresponding to the low-energy initial state $|\psi(0)\rangle = |\leftarrow\rangle$. First, heat is transferred to the environment as the system-bath interaction forces the bath modes to rapidly adjust to their new equilibrium. This takes place over a time set by the inverse cutoff, $\omega_C^{-1} \approx 0.2$ for $\omega_C = 5$ and $\omega_C^{-1} \approx 0.02$ for $\omega_C = 50$. Then, the direction of heat flow reverses as the bath gives up energy in order to bring the spin to thermal equilibrium, which occurs on a slower timescale fixed by the inverse of the thermalization rate, which can be estimated as $\gamma \approx (\pi/4) J(\Omega) \coth(\beta\Omega/2)$ from standard weak-coupling theories, e.g., the secular Born-Markov master equation discussed in Sec. 2.3, giving $\gamma^{-1} \approx 0.8$ for $\omega_C = 5$ and $\gamma^{-1} \approx 0.65$ for $\omega_C = 50$. A comparison between the two different values of ω_C in Fig. 8.8 shows how a larger frequency cut-

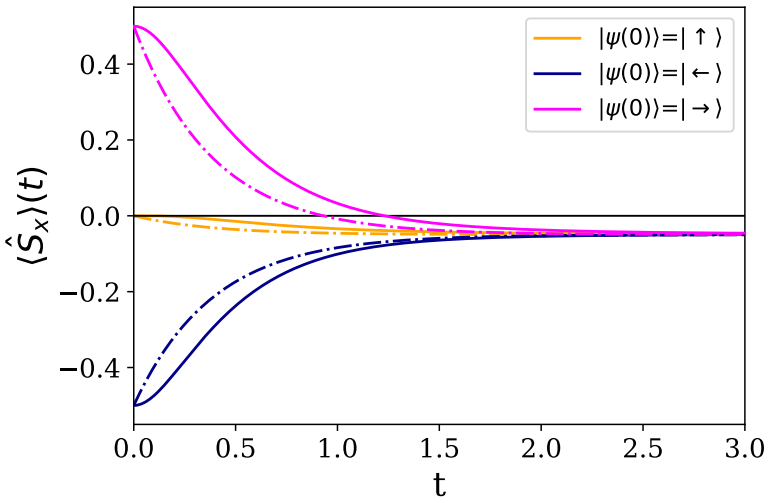

Figure 8.9: Expectation value $\langle \hat{S}_x \rangle(t)$ for the spin boson model at weak coupling and high temperature, for three different initial states of the system. The figure shows a comparison between the numerical results (solid lines) and the results obtained in the Born-Markov and weak-coupling approximation with the same parameters (dash-dotted lines of the same color as the corresponding initial states). The environment parameters are set to $T = 5$, $\alpha = 0.1$ and $\omega_C = 5$. The parameters controlling the numerical accuracy are $K\Delta = 5$, $\Delta = 0.01$, and $p = 100$.

off determines a shorter timescale for the heat transfer process, for fixed T and α. (E_r is ten times larger in the $\omega_C = 50$ case, so that the energy due to the displacement of the bath modes dominates over that due to the spin thermalization.) It is worth emphasising that the system-bath interaction energy gives a significant contribution to the heat transfer, even though the system dynamics is very well captured by a Markovian, weak-coupling description. Indeed, for the parameters considered in Fig. 8.8 and $\omega_C = 5$, the reorganisation energy is comparable to the natural energy scale of the spin, since $E_r = \Omega/2$. Nevertheless, Fig. 8.9 shows that in this regime the calculated spin dynamics (solid curves) matches the corresponding Born-Markov and weak-coupling approximated problem (dash-dotted curves), within the limits of such an approximation, the coupling strength being set to $\alpha = 0.1$. The discrepancy shown in Fig. 8.9 is $\lesssim 10\%$. We calculated the spin dynamics in the Born-Markov theory by solving the Lindblad master equation (8.1) for $u = 0$, and plotting $\langle \hat{S}_x \rangle(t) = \mathrm{Tr}_S[\hat{S}_x \hat{\rho}_S(t)]$.

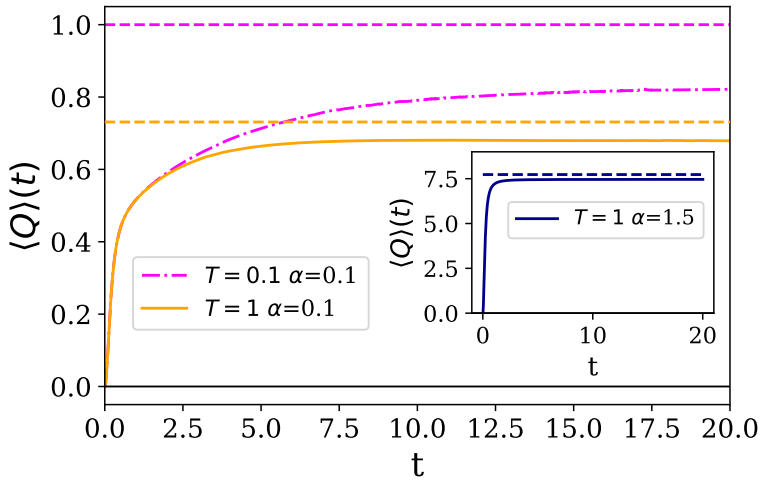

Figure 8.10: Mean heat $\langle Q \rangle (t)$ exchanged by the bath for the spin boson model in weak coupling at temperature $T = 1$ (solid line) and $T = 0.1$ (dash-dotted line), as a function of time, for an initial state of the system set to $|\uparrow\rangle$. Dashed lines: sum of the energy change in the system and the reorganisation energy of the bath for the corresponding temperatures and coupling strengths. Inset: same plot for temperature $T = 1$ and strong coupling. The parameters controlling the numerical accuracy are $K\Delta = 5$, $\Delta = 0.01$, $p = 100$ and the derivative is taken at $u = 0.01$. $\omega_C = 5$ for all the plots.

8.3.3 Lower temperature and stronger coupling

We now consider the heat transfer at intermediate and low temperatures. In Fig. 8.10 we show the mean heat transfer for temperatures $T = 1$ and $T = 0.1$, starting from the state $|\psi(0)\rangle = |\uparrow\rangle$. We see the same monotonic relaxation behaviour as was observed at high temperature (the orange curve in Fig. 8.8), albeit proceeding on a slower timescale as the temperature is reduced.

Outside of the high-temperature limit, the asymptotic value of $\langle Q \rangle$ can no longer be well approximated by Eq. (8.37), shown by the dashed lines in Fig. 8.10. We find that the the spin's internal energy change and the total heat transfer are smaller in magnitude than Eqs. (8.5) and (8.37) predict, as Fig. 8.10 and Fig. 8.11 both show, leading to

$$\langle Q \rangle_\infty < E_r + \frac{\Omega}{2} \tanh\left(\frac{\beta\Omega}{2}\right) + \langle \hat{H}_S \rangle_0. \tag{8.38}$$

This demonstrates that the tendency of the spin to minimise its local free energy defined by $\hat{H}_S$ competes with the displacing effect of $\hat{H}_I$ on the bath modes. As a

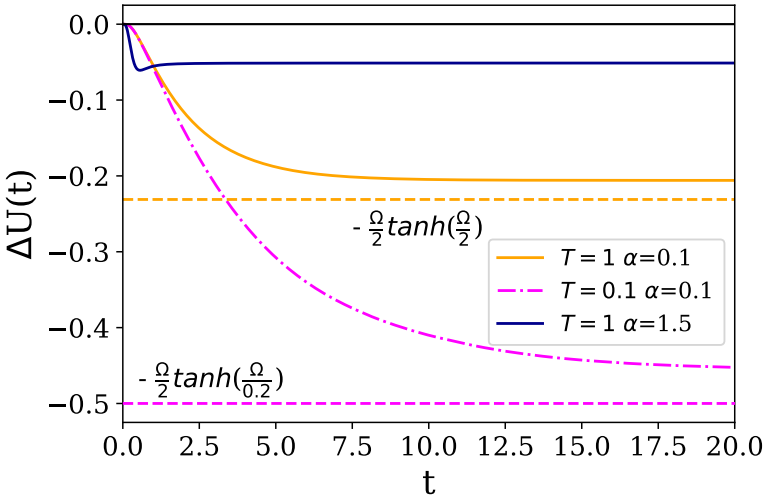

Figure 8.11: Variation of internal energy of the system $\Delta U\,(t)$ as a function of time for temperature $T = 1$, where the solid blue line is for $\alpha = 1.5$ and the solid orange line for $\alpha = 0.1$, and temperature $T = 0.1$, where the dash-dotted line is for $\alpha = 0.1$. Dashed lines: total internal energy change of system in the Markovian regime, $-\frac{\Omega}{2}\tanh\left(\frac{\Omega}{2T}\right)$, for $T = 1$ (dashed orange line) and $T = 0.1$ (dashed magenta line). The parameters controlling the numerical accuracy are $K\Delta = 5$, $\Delta = 0.01$ and $p = 100$. $\omega_C = 5$ for all the plots.

consequence of this interplay, both ΔU and $\langle W \rangle$ depend non-trivially on system-bath correlations generated during the relaxation process.

The effect of the correlations with the bath is indeed to decrease the magnitude of ΔU with respect to the value $-\frac{\Omega}{2}\tanh\left(\frac{\Omega}{2T}\right)$ predicted by Eq. (8.5), and represented in Fig. 8.11 by the dashed lines. Such discrepancy is starkly greater for stronger coupling.

In order to understand this, we note that at strong system-bath coupling the equilibrium state must be generalised to [62]

$$\hat{\rho}_S^{\mathrm{eq}} = \frac{\mathrm{Tr}_B\left[e^{-\beta\hat{H}}\right]}{\mathrm{Tr}\left[e^{-\beta\hat{H}}\right]}, \tag{8.39}$$

i.e. the reduction of a global thermal state. This takes into account correlations with the bath and reduces to the standard form $\hat{\rho}_S^{\mathrm{eq}} \propto e^{-\beta\hat{H}_S}$ in the weak-coupling limit. Assuming that the open quantum system couples to the bath locally in space, the interaction Hamiltonian is a local degree of freedom that is also expected to ther-

malise, in the sense that

$$\langle \hat{H}_I \rangle_\infty = \frac{\mathrm{Tr}\left[\hat{H}_I e^{-\beta \hat{H}}\right]}{\mathrm{Tr}\left[e^{-\beta \hat{H}}\right]}. \tag{8.40}$$

We emphasise that these thermalization conditions hold only for local subsystems: they do not imply that the system as a whole attains thermal equilibrium in the long-time limit.

8.3.4 System-bath correlations and variational theory of heat transfer

We estimate the effect of system-bath correlations on heat transfer using the variational approach pioneered by Silbey and Harris [127], which has been successfully applied to understand various static and dynamic properties of the spin-boson model [128–130]. The basic idea is to express the Hamiltonian in a different basis by applying a unitary transformation that mixes the system and bath degrees of freedom. Specifically, the Hamiltonian is diagonalized approximately using the polaron transformation in Eq. (8.9), with the displacements $\{fj\}$ interpreted as variational parameters. Applying the transformation $\hat{P}$, we arrive at $\hat{P}^\dagger \hat{H} \hat{P} = \hat{H}'_0 + \hat{H}'_I$, where it has been found in [127] that

$$\hat{H}'_0 = \Omega' \hat{S}_x + \sum_j \omega_j \hat{a}_j^\dagger \hat{a}_j + \sum_j \frac{f_j(f_j - 2g_j)}{4\omega_j}, \tag{8.41}$$

$$\hat{H}'_I = \Omega \left[\left(\hat{B} - B \right) \hat{S}_+ + \mathrm{h.c.} \right] + \hat{S}_z \sum_j (g_j - f_j)(\hat{a}_j + \hat{a}_j^\dagger). \tag{8.42}$$

Here $\hat{B} = \prod_k \hat{D}(f_k/\omega_k)$, or explicitly,

$$\hat{B} = \prod_j \exp\left[\frac{f_j}{\omega_j} \left(\hat{a}_j^\dagger - \hat{a}_j \right) \right], \tag{8.43}$$

and $B = \langle \hat{B} \rangle_0$, and using the displacement operator thermal average $\langle \hat{D}(x) \rangle_0 = \exp[-\frac{1}{2}|x|^2 \coth(\beta\omega/2)]$, one can write

$$B = \exp\left[-\frac{1}{2} \sum_j \frac{f_j^2}{\omega_j^2} \coth\left(\frac{\beta\omega_j}{2} \right) \right]. \tag{8.44}$$

The average defined here is relative to the variational Hamiltonian $\hat{H}_0'$,

$$\langle \bullet \rangle_0 = \frac{\mathrm{Tr}[\bullet e^{-\beta \hat{H}_0'}]}{Z_0}, \tag{8.45}$$

where $Z_0 = \mathrm{Tr}[e^{-\beta \hat{H}_0'}]$. We have defined $\hat{S}_+ = (\hat{S}_x + i\hat{S}_y)/2$ the spin raising operator, and $\Omega' = B\Omega$ is a renormalized tunneling amplitude.

We need to choose the set $\{f_j\}$ such that the Feynman-Bogoliubov upper bound on the free energy, $F = -T \ln \mathrm{Tr}[e^{-\beta \hat{H}}]$, is minimized, under the key assumption that the variational interaction Hamiltonian $\hat{H}_I'$ is small enough. The Feynman-Bogoliubov upper bound is defined as [127]

$$F \leq F_B = -T \ln Z_0' + \langle \hat{H}_I' \rangle_0 + \mathcal{O}(\langle \hat{H}_I'^2 \rangle_0), \tag{8.46}$$

where $\langle \hat{H}_I' \rangle_0 = 0$ by construction. This procedure is designed to give the optimal approximation with the free thermal state, $\exp[-\beta \hat{H}_0']/Z_0' \approx \exp[-\beta \hat{H}']/Z'$, where $\hat{H}' = \hat{P}^\dagger \hat{H} \hat{P}$, $Z' = \mathrm{Tr}[e^{-\beta \hat{H}'}]$, within the class of variational states defined by $\{f_j\}$. Writing explicitly Eq. (8.46), one can find that [127]

$$F_B = \sum_j \frac{f_j(f_j - 2g_j)}{4\omega_j} - T \ln\left[2\cosh\left(\frac{\beta\Omega'}{2} \right) \right]. \tag{8.47}$$

All terms $\mathcal{O}(\langle \hat{H}_I'^2 \rangle_0)$ are dropped since they are small by assumption.

The minimum of Eq. (8.47) is defined by $\partial F_B / \partial f_j = 0$, with solution $f_j = g_j \phi(\omega_j)$,

where

$$\phi(\omega) = \left[1 + \frac{\Omega'}{\omega} \tanh\left(\frac{\beta\Omega'}{2}\right) \coth\left(\frac{\beta\omega}{2}\right)\right]^{-1}, \tag{8.48}$$

$$\Omega' = \Omega \exp\left[-\frac{1}{2}\int_0^\infty d\omega \frac{J(\omega)}{\omega^2}\phi^2(\omega) \coth\left(\frac{\beta\omega}{2}\right)\right], \tag{8.49}$$

which must be solved self-consistently for Ω'. Using these results in Eq. (8.42) also shows self-consistently that $\hat{H}_I' = \mathcal{O}(\Omega)$. Eq. (8.46) can thus be interpreted as a formal expansion in powers of Ω/ω_c. That is, the variational approach treats the spin Hamiltonian $\hat{H}_S$ as a small perturbation with respect to the independent-boson Hamiltonian $\hat{H}_B + \hat{H}_I$, and becomes exact in the limit $\Omega \to 0$.

This equilibrium theory is not useful for the evaluation of the dynamics of the bath, which is far from equilibrium at all times. However, we find it useful in the evaluation of $\langle \hat{H}_B \rangle$. As discussed in Eq. (8.39) and Eq. (8.40), we can assume subsystem equilibration, which is known to be a correct assumption for exactly solvable models and expected for relatively weak coupling. If Eq. (8.39) holds true, then

$$\langle \hat{H}_S \rangle_\infty = \frac{\mathrm{Tr}\left[\hat{H}_S e^{-\beta\hat{H}}\right]}{\mathrm{Tr}\left[e^{-\beta\hat{H}}\right]}. \tag{8.50}$$

If the system is locally coupled to one part of an infinite bath, then the same assumption holds for the interaction Hamiltonian mean value, and Eq. (8.40) holds true. Then $\hat{H}_S$ and $\hat{H}_I$ can be considered operators on some augmented system S' which should approximately thermalize, with the assumption that the residual bath B' is approximately thermal at the same temperature. It follows from such reasoning and Eq. (8.50), under the assumption that we can approximate $\hat{P}^\dagger \hat{H} \hat{P} \approx \hat{H}_0'$ and therefore $e^{-\beta\hat{H}} \approx \hat{P} e^{-\beta\hat{H}_0'} \hat{P}^\dagger$, that

$$\langle \hat{H}_S \rangle_\infty \approx \frac{\mathrm{Tr}\left[\hat{H}_S \hat{P} e^{-\beta\hat{H}_0'} \hat{P}^\dagger\right]}{\mathrm{Tr}\left[\hat{P} e^{-\beta\hat{H}_0'} \hat{P}^\dagger\right]} = \frac{\mathrm{Tr}\left[\hat{P}^\dagger \hat{H}_S \hat{P} e^{-\beta\hat{H}_0'}\right]}{Z_0'} \tag{8.51}$$

$$= -\frac{\Omega'}{2} \tanh\left(\frac{\beta\Omega'}{2}\right). \tag{8.52}$$

Similarly, from Eq. (8.40),

$$\langle \hat{H}_I \rangle_\infty \approx \frac{\mathrm{Tr}\left[\hat{P}^\dagger \hat{H}_I \hat{P} e^{-\beta \hat{H}_0'}\right]}{Z_0'} = -\frac{1}{2}\int_0^\infty d\omega \, \frac{J(\omega)}{\omega}\phi(\omega). \tag{8.53}$$

Here Ω' is the renormalized tunneling matrix element defined in Eq. (8.49), and $E_r' = \frac{1}{2}\int d\omega J(\omega)\phi(\omega)/\omega$ the renormalized reorganization energy. From the conservation of the total energy $\langle \hat{H} \rangle_\infty = \langle \hat{H} \rangle_0$, we have that the asymptotic average heat exchanged by the bath $\langle Q \rangle_\infty = \langle \hat{H}_B \rangle_\infty - \langle \hat{H}_B \rangle_0$ is

$$\begin{aligned} \langle Q \rangle_\infty &= \langle \hat{H}_S \rangle_0 - \langle \hat{H}_S \rangle_\infty + \langle \hat{H}_I \rangle_0 - \langle \hat{H}_I \rangle_\infty = \\ &= E_r' + \frac{\Omega'}{2} \tanh\left(\frac{\beta\Omega'}{2}\right) + \langle \hat{H}_S \rangle_0, \end{aligned} \tag{8.54}$$

where $\langle \hat{H}_I \rangle_0 = 0$ for initial product states. This has the same form as Eq. (8.37).

The variational theory predicts that both the spin tunnelling matrix element and the reorganisation energy are reduced relative to their bare values, since $\Omega'/\Omega \leq 1$ and $\phi(\omega_j) \leq 1$. Physically, this occurs because the tunnelling between spin states $|\uparrow\rangle \leftrightarrow |\downarrow\rangle$ induced by $\hat{H}_S$ is suppressed by the spin-dependent mode displacements generated by $\hat{H}_I$, which reduce the effective overlap between the two spin states. The equilibrium state emerges from a balance of these two competing effects, which explains why both ΔU and $\langle Q \rangle$ are reduced at low temperature relative to Eqs. (8.5) and (8.37). We show in Fig. 8.12 that the variational theory gives a good quantitative approximation to the mean heat transfer at low temperature, $T = 0.1$, with the best agreement at weak coupling. At higher temperatures on the order of $T = 1$ and above, we find that the approximation breaks down completely because the renormalisation of the tunnelling amplitude is overestimated, leading to values $\Omega' \ll \Omega$. This failure is presumably due to the neglect of thermally activated transitions generated by $\hat{H}_I'$, which become relevant at temperatures $\beta\Omega' \lesssim 1$. On the other hand Fig. 8.12 shows that the additive ansatz given by Eq. (8.37) performs worse than the variational theory across all the coupling range.

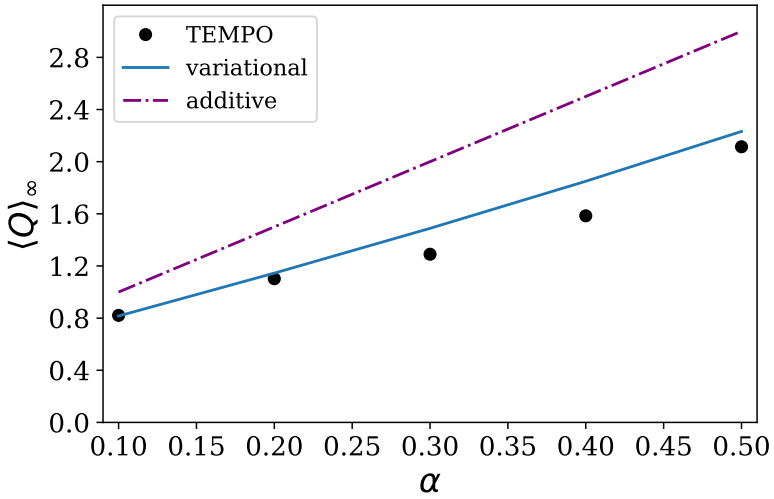

Figure 8.12: Long-time limit of the heat transfer for the spin boson model as a function of coupling strength, calculated using the path integral (circles), the additive theory (dash-dotted) and the variational method (line), for $T = 0.1$.

At very strong coupling, the variational theory performs well at all temperatures. In this regime, strong correlations with the bath lead to an almost maximally mixed equilibrium state of the spin, corresponding to a vanishing tunnelling rate in the variational frame, $\Omega' \to 0$. As a result, the heat transfer for an initial state $|\psi(0)\rangle = |\uparrow\rangle$ reduces to the bare reorganisation energy, E_r. This behaviour is shown in the inset of Fig. 8.10, where the solid curve converges to $\langle Q \rangle \approx E_r$ to a good approximation. The dynamics of the heat transfer is correspondingly fast in this regime since it depends only on the bath cutoff scale, ω_C.

8.3.5 Heat fluctuation-dissipation relation in the spin-boson model

As a final demonstration of our method, we study the temperature dependence of the heat fluctuations in the spin-boson model. Fig. 8.13 shows the asymptotic variance of the heat distribution at long times, starting from the initial state $|\psi(0)\rangle = |\uparrow\rangle$. We see that the fluctuations increase with temperature, and grow approximately linearly with T at high temperature.

This linear behaviour of $\langle\langle Q^2 \rangle\rangle_\infty$ can be understood as a manifestation of the fluctuation-dissipation relation (FDR) that is well known in the context of non-equilibrium work distributions. FDRs have been discussed in Sec. 4.3.1, and in

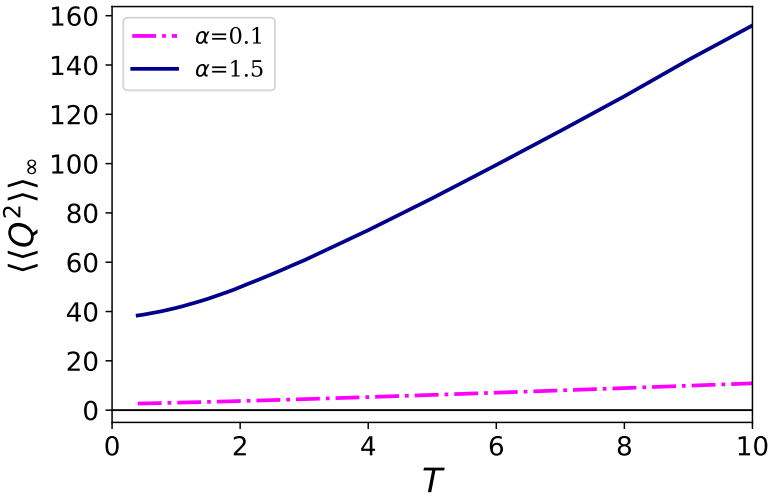

Figure 8.13: Variance of the heat distribution as a function of temperature in the spin-boson model, for both weak ($\alpha = 0.1$) and strong ($\alpha = 1.5$) coupling starting from the initial state $|\psi(0)\rangle = |\uparrow\rangle$. The parameters are $\omega_C = 5$, $K\Delta = 5$ and $\Delta = 0.01$, with $p = 100$ and $u = 0.005$ for $\alpha = 1.5$, and $p = 120$ and $u = 0.01$ for $\alpha = 0.1$.

particular Eq. (4.13) holds for Gaussian distributions of work W. In the case of the independent-boson model, $\hat{H}_S$ is a conserved quantity, which implies $\Delta U = 0$. From the first law of thermodynamics Eq. (4.6), it follows that $\langle Q \rangle = \langle W \rangle$ and heat is identical to work. The process is cyclic because the initial and final states of the open system are equilibrium states where $\hat{\rho}_S(t_f) = \hat{\rho}_S(0)$. Then from the definition of system entropy change Eq. (4.19), $\Delta S = 0$. The equilibrium free energy change is defined as $\Delta F = \Delta U - T\Delta S$, and therefore $\Delta F = 0$. It follows that we can write an equivalent FDR for the heat distribution from Eq. (4.13):

$$\langle\langle Q^2 \rangle\rangle = 2T\langle Q \rangle. \tag{8.55}$$

At high temperature, this relation holds at all times in the independent-boson model, as can be seen by comparing Eqs. (8.27) and (8.29) in the limit $\beta\omega_C \ll 1$. At low temperatures, the relation might fail at times too small for the open system to equilibrate.

In the spin-boson model, we no longer have equality between work and heat since $\Delta U \neq 0$. Nevertheless, we find numerically that the FDR (8.55) approximately holds at high temperatures, $\beta\omega_C \lesssim 1$, as shown in Fig. 8.14. This behaviour stems from the

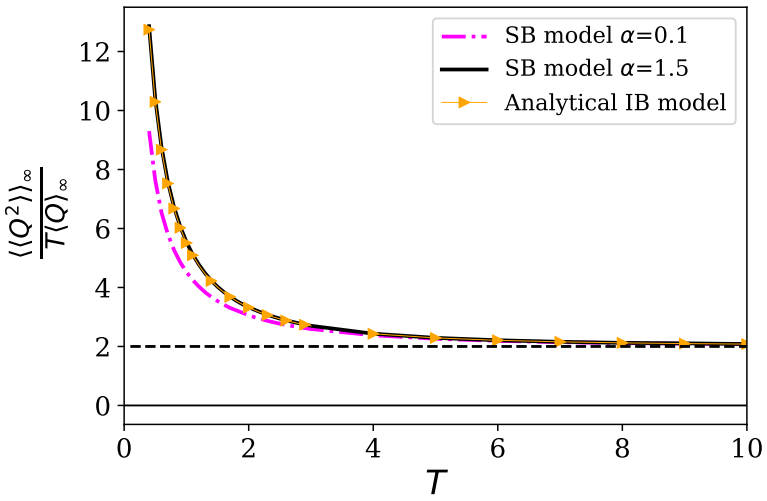

Figure 8.14: Asymptotic ratio of the variance to the mean heat as a function of temperature, showing the validity of the FDR for $T \gg \omega_C$. Dash-dotted and solid lines are the numerical results for the spin boson model, for the values of α indicated. The figure shows a comparison with the analytical solution for the independent boson model, which is independent of α (triangles). The FDR value of $\langle\langle Q^2\rangle\rangle_\infty / T\langle Q\rangle_\infty = 2$ is shown by the black dashed line. The parameters are the same as in Fig. 8.13.

fact that the spin's contribution to the heat fluctuations is limited by its finite energy splitting Ω, whereas the contribution of the spin-boson interaction energy can grow arbitrarily large. The heat fluctuations are thus dominated by independent-boson physics at high temperature. For strong coupling, where the spin energy scale Ω is negligible compared to the reorganisation energy E_r, we show in Fig. 8.14 that the heat fluctuations are essentially identical in the spin-boson and independent-boson models at all temperatures. One limitation encountered in the calculation of the data shown in Fig. 8.14, is that the TEMPO algorithm was not able to compute the variance up to equilibrium time for very low temperatures. Indeed, the lowest temperature shown is $T = 0.4$. Exploring the validity of the heat FDR in other scenarios, e.g. multipartite open quantum systems, is an interesting avenue for future work.

9 | Thermodynamics of decoherence

During any open dynamical process, correlations (both classical and non-classical) build between the environment and the quantum system, whether the environment is a measuring apparatus or a second quantum system, or both. The dynamics selects a set of preferred states in the Hilbert space of the quantum system, namely the eigenstates of an observable that is a constant of motion. In this process, the environment acts as a measurer of the conserved observable, destroying quantum coherence. Loss of quantum coherence means loss of phase information in the quantum system. In general, the probability density of a local measurement on the system will contain an interference or phase term, which depends on the overlap of the environment energy eigenstates [131]. For a large environment, interaction events between many degrees of freedom lead the overlap terms to decay in a time frame defined by a characteristic decoherence timescale τ_d. Consequently, the phase term decays and quantum coherence between different system eigenstates can no longer be measured. If the system is represented by a reduced density matrix in its energy eigenbasis, the diagonal elements are conserved, while off-diagonal elements, which depend on the phase information, are erased by decoherence. This process is also referred to as the quantum-to-classical transition, as information about quantum correlations is lost and quantum probability distributions approach classical probability distributions.

Decoherence as a phenomenon arising from the coupling of an open quantum system to a thermal bath is discussed in Sec. 4.4.3. This coupling leads a displaced system back to its thermal equilibrium during a thermalization process (see Sec. 4.4.2).

Thermalization is fundamental in thermodynamic protocols, making environment-induced decoherence an important aspect. While the study of heat transfer from an open system to a bath intuitively assumes an exchange of energy, in a pure decoherence process the system energy is conserved in the absence of dissipative phenomena. It could then seem that no heat is generated during a pure decoherence protocol. In the following, we show how, surprisingly, non-zero heat exchange is generated in this context [92].

9.1 Pure decoherence

We consider a pure dephasing (or pure decoherence) process, so that its effects on heat statistics can be distinguished from those arising from dissipation or stochastic fluctuations. The conservation of the open system energy $\Delta U = 0$ implies, from Eq. (4.6), that the heat exchanged is solely in the form of work performed on the system, $\langle Q \rangle = \langle W \rangle$. As there is no external force assumed to be acting on the open system, it could seem that $\langle Q \rangle = 0$ for a pure dephasing process. However, we show that this is not the case. Contrary to expectations, decoherence can lead to generation of heat. While the conservation of $\hat{H}_S$ does not imply $\langle Q \rangle = 0$, in order to have decoherence and heat exchange it is necessary that $\left[\hat{H}_B, \hat{H}_I\right] \neq 0$. We show that the origin of non-null heat exchange in pure dephasing processes arises from the interaction between system and bath. Decoherence is generated during the coupling process, which requires work to switch on and maintain the interaction. Such average work is then absorbed into the bath as heat when the system is decoupled from it at the end of the protocol.

9.2 Characteristic function of heat in pure decoherence processes

Following the standard two-point measurement scheme [65–67], the work W and heat Q of a quantum process are defined by a difference in energy obtained by projective measurements at the initial time, $t = 0$, and final time, $t = t_f$. Specifically, W pertains to measurements of the total Hamiltonian, $\hat{H}$, while Q corresponds to measurements of the bath Hamiltonian, $\hat{H}_B$, as already discussed in Sec. 4.4. In order for work and heat to be simultaneously measurable, therefore, the interaction energy must be negligible at the beginning and end of the evolution [62]. Here, we assume that the coupling is suddenly switched on at $t = 0$ and switched off at t_f, but other switching protocols yield similar results.

We write a very general equation for the characteristic function of heat of a bath interacting with an open quantum system, with overall Hamiltonian described by Eq. (2.2). Here the only assumptions are that $\left[\hat{H}_S, \hat{H}_I\right] = 0$, and that the initial state of the system is the product state Eq. (2.11). We show that the characteristic function of heat is a weighted sum of characteristic functions of work.

From Eq. (6.4) with $\hat{U}(t_f) = \exp[-it_f\hat{H}]$, we use $[\hat{H}_S, \hat{H}_I] = 0$ to cancel the terms $e^{\pm it_f\hat{H}_S}$ and write

$$\chi(u) = \mathrm{Tr}\left[e^{i\hat{H}_B t_f + i\sum_k g_k\hat{\Gamma}_k\otimes\hat{V}_k t_f} e^{iu\hat{H}_B} e^{-i\hat{H}_B t_f - i\sum_k g_k\hat{\Gamma}_k\otimes\hat{V}_k t_f} e^{-iu\hat{H}_B}\hat{\rho}_S(0)\otimes\hat{\rho}_B(0)\right]. \quad (9.1)$$

Here we used the most generic form of the interaction Hamiltonian defined in Eq. (4.23) for a process where $\Delta U = 0$. The generic open quantum system initial state can be written in the orthonormal eigenbasis of $\hat{H}_S$, $\{|n\rangle\}$, as $\hat{\rho}_S(0) = \sum_{i,j}\rho_S^{ij}(0)|i\rangle\langle j|$, where $\rho_S^{ij}(0) = \langle i|\hat{\rho}_S(0)|j\rangle$. Inserting a resolution of the identity in the eigenbasis of the quantum system energy in Eq. (9.1), and tracing over its

degrees of freedom S, it is straightforward to calculate

$$\chi(u) = \sum_n \mathrm{Tr}_B \left[\sum_m \sum_i \delta_{nm} e^{it_f \hat{H}_B + it_f g_n \hat{V}_n} e^{iu\hat{H}_B} \times \right.$$
$$\left. \delta_{mi} e^{-it_f \hat{H}_B - it_f g_m \hat{V}_m} e^{-iu\hat{H}_B} \rho_S^{in}(0) \hat{\rho}_B(0) \right], \tag{9.2}$$

where we have used $\langle n|\hat{\Pi}_k|m\rangle = \delta_{nk}\delta_{km}$ and $\langle n|m\rangle = \delta_{nm}$. Using the Kronecker delta properties, Eq. (9.2) simplifies to

$$\chi(u) = \sum_n p_n \mathrm{Tr}_B \left[e^{it_f \hat{H}_B + it_f g_n \hat{V}_n} e^{iu\hat{H}_B} e^{-it_f \hat{H}_B - it_f g_n \hat{V}_n} e^{-iu\hat{H}_B} \hat{\rho}_B(0) \right], \tag{9.3}$$

with $p_n = \rho_S^{nn}(0)$. It is straightforward to see from the definition of $\hat{H}_n$ Eq. (4.25) that

$$\chi(u) = \sum_n p_n \mathrm{Tr}_B \left[e^{it_f \hat{H}_n} e^{iu\hat{H}_0} e^{-it_f \hat{H}_n} e^{-iu\hat{H}_0} \hat{\rho}_B(0) \right]. \tag{9.4}$$

We obtain

$$\chi(u) = \sum_n p_n \chi_n(u), \tag{9.5}$$

where we have defined

$$\chi_n(u) = \langle e^{i\hat{H}_n t_f} e^{iu\hat{H}_B} e^{-i\hat{H}_n t_f} e^{-iu\hat{H}_B} \rangle_B. \tag{9.6}$$

A very similar calculation to the one leading to Eq. (9.4), leads to the expression for the time evolution of $\hat{\rho}_B(t_f)$. From $\hat{\rho}_B(t_f) = \mathrm{Tr}_S\left[\hat{U}(t_f)\hat{\rho}(0)\hat{U}^\dagger(t_f)\right]$, it follows that

$$\hat{\rho}_B(t_f) = \sum_n \langle n| e^{-it_f \hat{H}_B - it_f \sum_k g_k \hat{\Pi}_k \otimes \hat{V}_k}$$
$$\times \sum_{i,j} \rho_S^{i,j}(0) |i\rangle \langle j| \hat{\rho}_B(0) e^{it_f \hat{H}_B + it_f \sum_k g_k \hat{\Pi}_k \otimes \hat{V}_k} |n\rangle, \tag{9.7}$$

where we have again used the assumption $[\hat{H}_S, \hat{H}_{SB}] = 0$ and the decomposition of the system operator into the eigenbasis of $\hat{H}_S$. Using the orthonormality of the open

system energy eigenbasis, it follows that

$$\hat{\rho}_B(t_f) = \sum_n p_n e^{-it_f \hat{H}_n} \hat{\rho}_B(0)\, e^{it_f \hat{H}_n} \tag{9.8}$$

from which it is clear that $\hat{U}_B(t_f) = e^{-it_f \hat{H}_n}$ is the operator that defines the time evolution of the bath density matrix.

We recognise then $\chi_n(u)$ as the characteristic function of the work, as defined in Eq. (6.8), done on the bath in the following (fictitious) cyclic unitary process. The bath is initialised in the equilibrium state $\hat{\rho}_B(0)$ with Hamiltonian $\hat{H}_B$. The Hamiltonian is then suddenly perturbed as $\hat{H}_B \to \hat{H}_n = \hat{H}_B + g_n \hat{V}_n$ and the bath is allowed to evolve for a time t_f before the perturbation is switched off again.

9.3 Dissipated heat and work arising from interaction switching

The work done during the described cyclic process, w, is determined by the difference in energy that would be obtained by projective measurements of $\hat{H}_B$ at the start and finish of the evolution. This work is distributed according to the probability distribution (see Sec. 4.4.4)

$$P_n(w) = \sum_{j,k} \frac{e^{-\beta E_k}}{Z_B} |\langle E_j | e^{-i\hat{H}_n t_f} | E_k \rangle|^2 \delta\left(w - (E_j - E_k)\right), \tag{9.9}$$

where $|E_j\rangle$ is an eigenvector of $\hat{H}_B$ with eigenvalue E_j. Taking the Fourier transform of $P_n(w)$ in Eq. (9.9), we can verify that it results in Eq. (9.6) according to the definition of characteristic function Eq. (4.29). The heat probability distribution $P(Q)$, defined as the inverse Fourier transform of Eq. (9.4), is given by

$$P(Q) = \sum_n p_n P_n(w = Q). \tag{9.10}$$

The results shown in Eq. (9.5) and Eq. (9.10) express the dissipated heat as a sum over the work done in independent cyclic processes, each one conditioned on a state $|n\rangle$ of the open system and weighted by the probability $p_n = \langle n|\hat{\rho}_S(0)|n\rangle$ that the system is initially in that state. Accordingly, the bath dynamics is described by the unital map $\hat{\rho}_B(t_f) = \sum_n p_n e^{-i\hat{H}_n t_f}\hat{\rho}_B(0)e^{i\hat{H}_n t_f}$, with $e^{-i\hat{H}_n t_f}$ the physical time evolution operator for the bath conditional on the state $|n\rangle$. The average heat exchanged by the bath is the first moment of Eq. (9.10),

$$\langle Q\rangle = \sum_n p_n \langle w\rangle_n, \tag{9.11}$$

where $\langle w\rangle_n$ is the mean work associated to the conditional distribution P_n. Since the average work done in any thermodynamic cyclic process is non-negative, we conclude that $\langle Q\rangle \geq 0$. The free energy change vanishes for cyclic processes, $\Delta F = 0$, so that the Jarzynski equality discussed in Sec. 4.3.1 in this case becomes the integral fluctuation relation $\langle \exp(-\beta Q)\rangle = 1$. This also follows from Eq. (9.10) because each $P_n(w)$ obeys the Jarzynski equality, $\int dw e^{-\beta w} P_n(w) = 1$ [44, 67].

We also have that $\Delta S \geq 0$ because the evolution of the system density matrix in Eq. (4.24) is manifestly unital [132]. Therefore, pure decoherence processes obey a stronger bound on entropy production than the second law, since both terms in Eq. (4.7) are separately non-negative. We also note that the system entropy change ΔS is nonzero only when the system density matrix has initial coherences, while the entropy flux $\beta\langle Q\rangle$ depends only on the populations p_n. Therefore, the standard expression Eq. (4.7) represents a decomposition of the entropy production into contributions from initial coherences and populations in the energy eigenbasis, respectively [133–135].

9.4 Decoherence without heat dissipation and its connection to static phase noise

The evolution of the system coherences in time is intimately connected to the presence of non-trivial heat dissipation. Indeed, our results show that finite heat dissipation generically occurs in a pure decoherence process, unless $[\hat{H}_n, \hat{H}_B] = 0$ for all n. We show that decoherence processes that do not involve heat absorption by the bath are generically equivalent to classical, static phase noise.

From Eqs. (9.5) and (9.6) we see that a sufficient condition for vanishing heat dissipation is that $[\hat{H}_n, \hat{H}_B] = [\hat{V}_n, \hat{H}_B] = 0$ for all n. If the Hamiltonian $\hat{H}_B$ is non-degenerate, this further implies that $[\hat{V}_n, \hat{V}_m] = 0$ for all m, n. That is, the interaction operators $\{\hat{V}_n\}$ share a common eigenbasis with $\hat{H}_B$, i.e., $\hat{V}_n|E_j\rangle = V_n(E_j)|E_j\rangle$, with $V_n(E_j)$ denoting the eigenvalue of $\hat{V}_n$ corresponding to the energy eigenvector $|E_j\rangle$ of $\hat{H}_B$. Under these conditions, the overlap function $\langle e^{i\hat{H}_n t} e^{-i\hat{H}_m t}\rangle_B$ entering Eq. (4.24) can be written as

$$\left\langle e^{i\hat{H}_n t} e^{-i\hat{H}_m t} \right\rangle_B = \sum_j p(E_j) e^{i\left(V_n(E_j) - V_m(E_j)\right)t}, \tag{9.12}$$

which describes the average of a random phase shift that takes the value $V_n(E_j) - V_m(E_j)$ with probability $p(E_j) = e^{-\beta E_j}/Z_B$. This result can be reproduced by a simple noise model in which the dynamical bath is replaced by a random, time-independent Hamiltonian

$$\hat{H}_S = \sum_n (\varepsilon_n + \delta_n)|n\rangle\langle n|, \tag{9.13}$$

where the energy shift δ_n is a stochastic variable that takes the possible values $V_n(E_j)$ with corresponding probabilities $p(E_j)$. We can define a state

$$\begin{aligned}\hat{\rho}_S(t) &= \langle e^{-it\hat{H}_S}\hat{\rho}_S(0)e^{it\hat{H}_S}\rangle = \\ &= \sum_j p(E_j)e^{-it\sum_n(\varepsilon_n+V_n(E_j))|n\rangle\langle n|}\hat{\rho}_S(0)e^{it\sum_n(\varepsilon_n+V_n(E_j))|n\rangle\langle n|},\end{aligned} \tag{9.14}$$

which is an average over the noise distribution $p(E_m)$, whose matrix elements $\hat{\rho}_S^{mn}(t) = \langle m|\hat{\rho}_S(t)|n\rangle$ are given exactly by Eq. (4.24), with Eq. (9.12). We have therefore shown that the absence of heat dissipation implies that the dephasing noise is equivalent to a static, classical, random phase shift for each eigenstate of the open quantum system. This contrasts sharply with naturally occurring quantum dephasing noise, which is typically characterised by a nontrivial frequency spectrum [136–138]. Such time-dependent noise is a consequence of dynamical fluctuations of the bath, which arise when the absorption of energy drives it out of equilibrium.

We note that, since $[\hat{V}_n, \hat{H}_B] = 0$ for all n is only a sufficient condition, we cannot rule out the absence of heat dissipation when $[\hat{V}_n, \hat{H}_B] \neq 0$ for certain initial environment states, e.g., infinite-temperature states. Furthermore, the arguments above have assumed that $\hat{H}_B$ is nondegenerate. If we allow $\hat{H}_B$ to be degenerate, it is possible to construct models in which $[\hat{V}_n, \hat{H}_B] = 0$ for all n yet $[\hat{V}_n, \hat{V}_m] \neq 0$ for some m, n. Remarkably, such models can feature nontrivial decoherence for the open system despite the state of the bath being completely invariant under the dynamics.

9.5 An application: Qubit decoherence in a fermionic lattice environment

To exemplify the thermodynamics of decoherence, we now focus on a specific system comprising a qubit coupled to a noninteracting fermionic bath. Our setup is motivated by recent experiments that monitored the decoherence of two-level impu-

rity atoms embedded in a single-component atomic gas of ultracold fermions [81]. At low temperatures, the atoms interact via s-wave scattering. The fermions therefore do not interact with each other due to wavefunction antisymmetry, while the impurity-fermion interaction strength is proportional to the scattering length, which is generally different for each internal state of the impurity. For simplicity, we assume that the host Fermi gas is confined to the lowest band of a one-dimensional lattice potential, e.g., a species-selective optical lattice [139]. The Hamiltonian takes the form

$$\hat{H}_S = \frac{\epsilon}{2}\hat{\sigma}_z, \tag{9.15}$$

$$\hat{H}_B = -\frac{\Omega}{2}\sum_{j=1}^{L}\left(\hat{c}_j^\dagger \hat{c}_{j+1} + \hat{c}_{j+1}^\dagger \hat{c}_j\right), \tag{9.16}$$

$$\hat{H}_I = g\,|1\rangle\langle 1| \otimes \hat{c}_1^\dagger \hat{c}_1. \tag{9.17}$$

Here, $\hat{\sigma}_z$ is the Pauli spin operator for the qubit, with ϵ the energy level splitting, and $\hat{c}_j$ ($\hat{c}_j^\dagger$) is the fermionic annihilation (creation) operator for site j, with anticommutation relation $\{c_j, c_k^\dagger\} = \delta_{jk}$. $\hat{H}_B$ describes the tunnelling of fermions on the lattice, where Ω is the hopping amplitude and we impose periodic boundary conditions, $\hat{c}_{L+1} \equiv \hat{c}_1$. We take the thermodynamic limit by choosing the number of lattice sites $L = 500$ to be large enough so that all results are independent of L. We also fix the average fermion number $N = 250$ to half-filling, so that the Fermi energy equals Ω. Finally, $\hat{H}_I$ describes a collisional energy shift for the fermion localised on site $j = 1$, with coupling strength g to qubit state $|1\rangle$ and vanishing coupling when the qubit is in state $|0\rangle$. In the context of ultracold atoms, this can be achieved by tuning the corresponding scattering length to the zero crossing of a Feshbach resonance [140].

We consider a standard Ramsey interferometry protocol, following Refs. [88, 90, 141, 142]. The bath is initialised in thermal equilibrium with the qubit in its noninteracting state $|0\rangle$. At $t = 0$, a $\pi/2$-pulse prepares the qubit state $\hat{\rho}_S(0) = |+\rangle\langle+|$, with $|+\rangle = (|1\rangle + |0\rangle)/\sqrt{2}$ a superposition of the impurity eigenstates. According to Eq. (4.24), the qubit coherence evolves as $\hat{\rho}_S^{10}(t) = e^{-i\epsilon t}\nu(t)\hat{\rho}_S^{10}(0)$, where

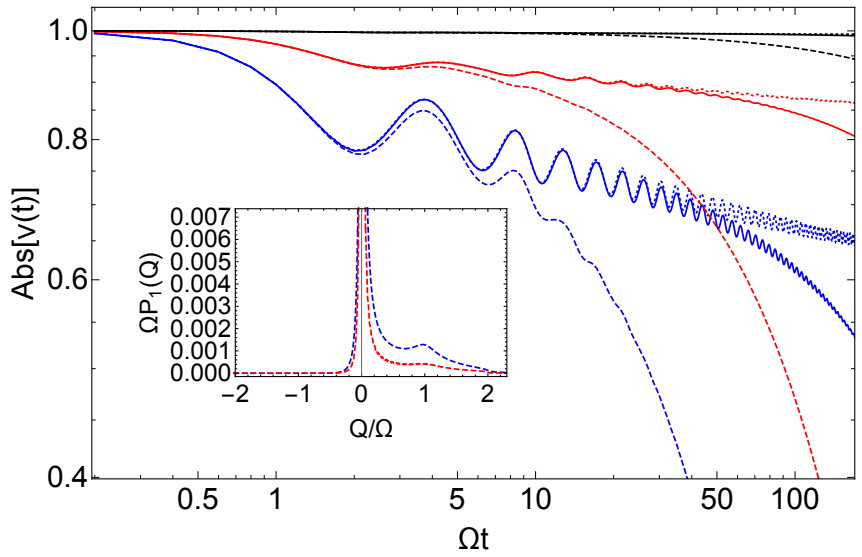

Figure 9.1: Decoherence functions for a qubit impurity in a 1D fermionic lattice. The value of the coupling is $g = 0.1\Omega$ (black lines), $g = 0.5\Omega$ (red lines) and $g = \Omega$ (blue lines), with temperature $T = 0$ (dotted lines), $T = 0.01\Omega$ (solid lines), and $T = 0.1\Omega$ (dashed lines). Axes are in logarithmic scale. Inset: Regular part of the heat distribution $P(Q) = \frac{1}{2}\delta(Q) + \frac{1}{2}P_1(Q)$ for $T = 0.1\Omega$, and $g = \Omega$ (blue, dashed), $g = 0.5\Omega$ (red, dashed).

$\nu(t) = \langle e^{i\hat{H}_0 t} e^{-i\hat{H}_1 t} \rangle_B$ is the decoherence function with

$$\hat{H}_0 = \hat{H}_B, \tag{9.18}$$

$$\hat{H}_1 = \hat{H}_B + g\hat{c}_1^\dagger \hat{c}_1. \tag{9.19}$$

This complex function may be experimentally extracted by applying a second $\pi/2$-pulse with a variable phase and measuring the final qubit populations [81, 84, 89].

9.5.1 Functional determinant approach and decoherence function

The decoherence function $\nu(t) = \langle e^{i\hat{H}_0 t} e^{-i\hat{H}_1 t} \rangle_B$ for a bath of fermionic modes can be computed exactly through the functional determinant approach [143–145], which expresses the average of a product of many-body exponential operators in terms of single-particle quantities through the Levitov formula [143],

$$\left\langle e^{\hat{Y}_1} e^{\hat{Y}_2} ... e^{\hat{Y}_N} \right\rangle_B = \det\left[1 - \hat{n} + \hat{n} e^{\hat{y}_1} e^{\hat{y}_2} ... e^{\hat{y}_N}\right], \tag{9.20}$$

where $\hat{Y}_i$ are bilinear many-body fermionic operators, $\hat{y}_i$ are their corresponding single-particle operators, and $\hat{n}$ is the single-particle occupation number operator. In particular, the decoherence function is found from

$$\nu(t) = \det\left[1 - \hat{n} + \hat{n}e^{i\hat{h}_0 t}e^{-i\hat{h}_1 t}\right], \tag{9.21}$$

where $\hat{n} = \left(e^{\beta(\hat{h}_0-\mu)}+1\right)^{-1}$ is the single-particle occupation number operator, μ is the chemical potential and $\hat{h}_0$ and $\hat{h}_1$ are the single-particle counterparts of the Hamiltonians $\hat{H}_0$ and $\hat{H}_1$. The absolute value of $\nu(t)$ is shown in Fig. 9.1 for different temperatures and coupling constants.

The decoherence function crosses over from power-law to exponential decay after the thermal timescale β. This behavior is a manifestation of the Fermi-edge singularity [146, 147] associated with Anderson's orthogonality catastrophe [148]. Decoherence arises because collisions with the impurity excite particle-hole pairs in the gas, gradually reducing the overlap between the perturbed and unperturbed states of the environment. These excitations are initially restricted to the vicinity of the Fermi surface due to the Pauli exclusion principle, generating the slow power-law decoherence seen in Fig. 9.1 for $t \ll \beta$. Thermal broadening of the Fermi surface eventually leads to the onset of exponential decay when $t \gtrsim \beta$. At stronger coupling, we also observe oscillations of the qubit coherence (blue curves in Fig. 9.1), indicating a highly non-Markovian (nondivisible) evolution [20]. We therefore see that nontrivial decoherence emerges here as a direct consequence of the dissipation of energy into the fermionic bath.

9.5.2 Heat dissipation in pure decoherence

The characteristic function of heat follows from Eqs. (9.5) and (9.6) as

$$\chi(u) = \frac{1}{2} + \frac{1}{2}\left\langle e^{it_f\hat{H}_1}e^{iu\hat{H}_0}e^{-it_f\hat{H}_1}e^{-iu\hat{H}_0}\right\rangle_B. \tag{9.22}$$

The first, constant term $\chi_0 = 1$ pertains to the $|0\rangle$ component of the qubit's initial superposition state, which leads to exactly zero heat dissipation, i.e., $P_0(Q) = \delta(Q)$. The second term $\chi_1(u) = \left\langle e^{it_f \hat{H}_1} e^{iu\hat{H}_0} e^{-it_f \hat{H}_1} e^{-iu\hat{H}_0} \right\rangle_B$ in Eq. (9.22) corresponds to the interacting state $|1\rangle$ and can be expressed as a functional determinant. We show how the identity in Eq. (9.20) can be used to exactly compute $\chi_1(u)$.

The unperturbed energy eigenbasis $\{|E_n\rangle\}_{n=1}^{L}$ of $\hat{H}_0$ and the perturbed energy eigenbasis $\left\{\left|E'_j\right\rangle\right\}_{j=1}^{L'}$ of $\hat{H}_1$ have in general size L and L' respectively. We define $\hat{M} = \sum_m |E_m\rangle \langle E'_m|$ an unitary operator represented by an $L \times L'$ matrix whose elements are $m_{kj} = \langle E'_k | E_j \rangle$. The operator $\hat{M}$ transforms between the perturbed and unperturbed basis. When applying Eq. (9.20) to function $\chi_1(u)$, we consider that the determinant is evaluated in the unperturbed basis, and transform $\hat{h}_1$ from its diagonal basis to the basis of eigenvalues of $\hat{h}_0$. Therefore we have

$$\chi_1(u) = \det\left[1 - \hat{n} + \hat{n}\left(\hat{M}^\dagger e^{i\hat{h}_1 t_f}\hat{M}\right) e^{iu\hat{h}_0}\left(\hat{M}^\dagger e^{-i\hat{h}_1 t_f}\hat{M}\right) e^{-iu\hat{h}_0}\right]. \tag{9.23}$$

The probability distribution $P_1(Q)$ associated to this second term is shown in the inset of Fig. 9.1, for a fixed temperature and two different values of the coupling constant. The divergence near $Q = 0$ is a hallmark of the Fermi edge singularity, which is centred around zero energy as a consequence of the cyclic nature of the process. For stronger coupling, there is also a feature near the Fermi energy $Q = \Omega$, which can be attributed to the creation of particle-hole excitations at the bottom of the band [142]. The mean heat $\langle Q \rangle$ is shown in Fig. 9.2 as a function of time for the same parameters as Fig. 9.1. We observe that $\langle Q \rangle$ grows with protocol time for short evolutions, $\Omega t_f \lesssim 1$, and then executes long-lasting oscillations around a finite value for relatively long protocols $\Omega t_f \gg 1$ before eventually settling to a constant. These intermediate-time oscillations can be understood as a consequence of the finite bandwidth of the fermionic lattice, and are more prominent for strong coupling, $g \gtrsim \Omega$. The temperature dependence of the mean heat absorbed at asymptotically long times is shown in Fig. 9.3, for two different values of the coupling constant. As its temperature increases, the bath absorbs less heat during the decoherence pro-

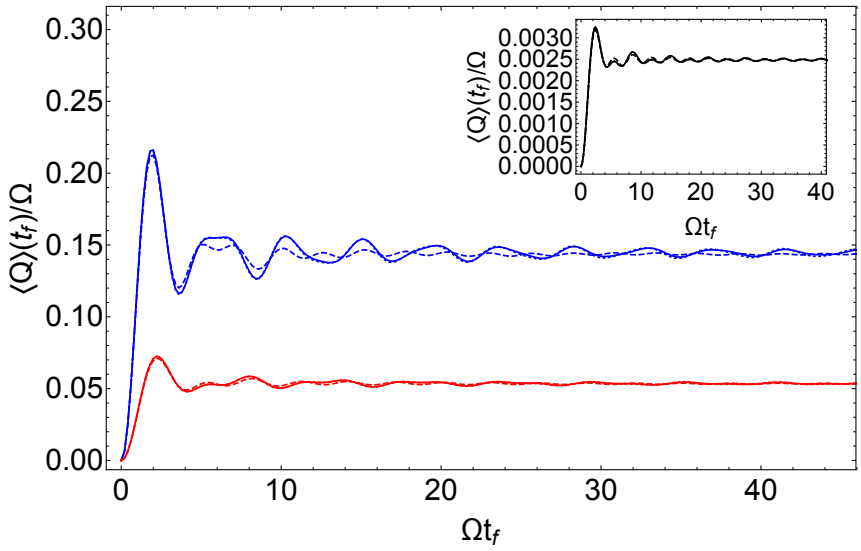

Figure 9.2: Heat transfer as a function of time for a qubit in a 1D fermionic lattice. The values of the coupling are $g = 0.1\Omega$ (black lines), $g = 0.5\Omega$ (red lines) and $g = \Omega$ (blue lines), with temperatures $T = 0$ (dotted lines), $T = 0.01\Omega$ (solid lines), and $T = 0.1\Omega$ (dashed lines).

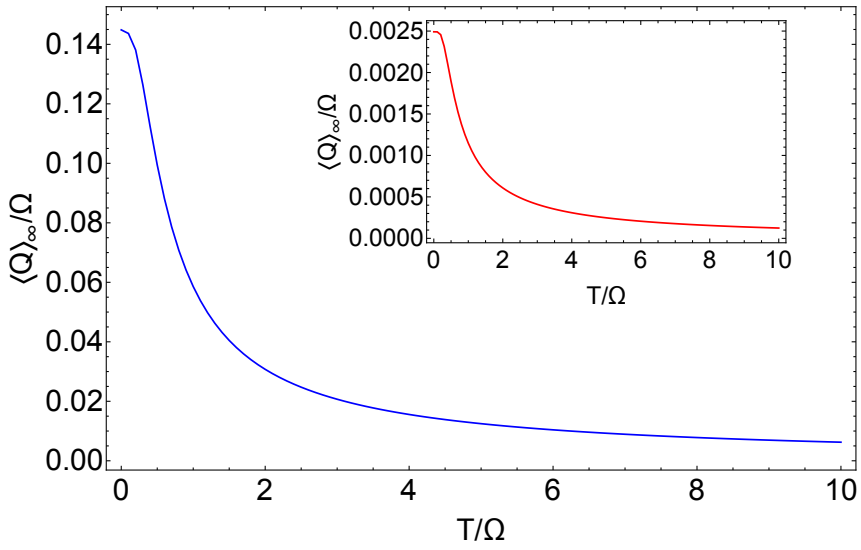

Figure 9.3: Long-time limit of the heat transfer as a function of temperature for a qubit in a 1D fermionic lattice, with couplings $g = \Omega$ (blue lines) and $g = 0.1\Omega$ (inset, red lines).

cess, which reflects the reduced disturbance of the high-temperature Fermi sea by the impurity perturbation.

9.6 Energy costs of projective measurements in pure decoherence processes

After investigating the heat dissipation due to a pure decoherence process in which a system relaxes to a thermal state, we study the thermodynamic cost of performing a measurement on the system at a given time of its relaxation evolution. Quantum feedback control exploits protocols of this kind, where measurements on the system are performed in order to retrieve information and determine its consequent evolution [149]. In this context, the maximum work that can be extracted from the thermal bath by the feedback control procedure has been studied [100]. Work extraction due to information gain is shown to be consistent with the second law of thermodynamics, which can be generalized to include quantum feedback control [132]. Here we are interested specifically in pure decoherence processes, and how measurements affect the average heat dissipated by the bath. In the following, we only lay out the theoretical framework for calculating the characteristic function of heat in the presence of feedback, but further, in-depth study will be the subject of future work.

9.6.1 One measurement on the open system

We define $\{\hat{P}_v\}$ a set of linear operators acting on the Hilbert space of the open system and satisfying the completeness condition $\sum_v \hat{P}_v^\dagger \hat{P}_v = \mathbb{1}_S$. Such a set defines a measurement on the system S. We assume $\hat{\rho}(t)$ evolves in time through Eq. (2.6) and a factorized initial state. We perform an instantaneous measurement on the open system at a certain time $0 < t_1 < t_f$ of the evolution, so that the overall density

matrix $\hat{\rho}(t)$ becomes

$$\hat{\rho}\left(t_1\right) \rightarrow \hat{\rho}'\left(t_1\right) = \frac{\left(\hat{P}_v \otimes \mathbb{1}_B\right) \hat{\rho}\left(t_1\right) \left(\hat{P}_v \otimes \mathbb{1}_B\right)^\dagger}{p_1\left(v\right)} = \frac{\left(\hat{P}_v \otimes \mathbb{1}_B\right) \hat{U}\left(t_1\right) \left(\hat{\rho}_S\left(0\right) \otimes \hat{\rho}_B\left(0\right)\right) \hat{U}^\dagger\left(t_1\right) \left(\hat{P}_v \otimes \mathbb{1}_B\right)^\dagger}{p_1\left(v\right)}, \tag{9.24}$$

where

$$p_1\left(v\right) = \mathrm{Tr}\left[\left(\hat{P}_v \otimes \mathbb{1}_B\right) \hat{U}\left(t_1\right) \left(\hat{\rho}_S\left(0\right) \otimes \hat{\rho}_B\left(0\right)\right) \hat{U}^\dagger\left(t_1\right) \left(\hat{P}_v \otimes \mathbb{1}_B\right)^\dagger\right] \tag{9.25}$$

is the probability of the outcome v. After a time $t > t_1$,

$$\hat{\rho}\left(t_f\right) = \hat{U}\left(t_f - t_1\right) \hat{\rho}'(t_1) \hat{U}^\dagger\left(t_f - t_1\right). \tag{9.26}$$

The characteristic function of heat after one measurement, $\chi^1(u)$, is defined by Eq. (6.4), where the unitary time evolution operator is replaced by the operator $\hat{V}_v(t_f, t_1) = \hat{U}\left(t_f - t_1\right) \left(\hat{P}_v \otimes \mathbb{1}_B\right) \hat{U}\left(t_1\right)$, so that

$$\chi^1(u) = \frac{1}{p_1\left(v\right)} \mathrm{Tr}\left[e^{iu\hat{H}_B} \hat{V}_v(t_f, t_1) e^{-iu\hat{H}_B} \left(\hat{\rho}_S\left(0\right) \otimes \hat{\rho}_B\left(0\right)\right) \hat{V}_v^\dagger(t_f, t_1)\right]. \tag{9.27}$$

For a pure decoherence process, $[\hat{H}_S, \hat{H}_I] = 0$, so that expanding the operators $\hat{V}_v(t_f, t_1)$ in Eq. (9.27) the terms $e^{\pm i t_1 \hat{H}_S}$ and $e^{\pm i(t_f - t_1)\hat{H}_S}$ cancel each other inside the trace. We expand the initial state of the open system in the eigenbasis of $\hat{H}_S$, $\hat{\rho}_S\left(0\right) = \sum_{i,j} \rho_S^{i,j}\left(0\right) \left|i\right\rangle \left\langle j\right|$, and expand the trace over the degrees of freedom of the system. Writing $\hat{H}_I$ as the most general interaction Hamiltonian for a pure decoherence process as defined in Eq. (4.23), the calculations that follow from Eq. (9.27) are identical to the ones discussed in Sec. 9.2 leading to Eq. (9.4). Using the orthonormality of the energy eigenbasis of the open system $\left\langle j \right| \left. m \right\rangle = \delta_{jm}$, and $\left\langle n\right| \hat{\Pi}_l \left|m\right\rangle = \delta_{nl}\delta_{lm}$,

we have the final result for the characteristic function of heat

$$\chi^1(u) = \frac{1}{p_1(v)} \sum_{m,n,t} \langle m| \hat{P}_v^\dagger |n\rangle \langle n| \hat{P}_v |t\rangle \rho_S^{t,m}(0) \times \left\langle e^{it_1\hat{H}_m} e^{i(t_f-t_1)\hat{H}_n} e^{iu\hat{H}_0} e^{-i(t_f-t_1)\hat{H}_n} e^{-it_1\hat{H}_t} e^{-iu\hat{H}_0} \right\rangle_B, \tag{9.28}$$

with

$$p_1(v) = \sum_{m,n,t} \langle m| \hat{P}_v^\dagger |n\rangle \langle n| \hat{P}_v |t\rangle \rho_S^{t,m}(0) \left\langle e^{it_1\hat{H}_m} e^{-it_1\hat{H}_t} \right\rangle_B. \tag{9.29}$$

Here we have used the definitions $\hat{H}_0 = \hat{H}_B$ and $\hat{H}_n = \hat{H}_B + g_n\hat{V}_n$.

Eqs (9.28 - 9.29) define a general characteristic function of heat where the operator $\hat{P}_v$ can be replaced with any measurement. The averages $\langle \bullet \rangle_B$ can easily be numerically computed with the functional determinant approach used in Sec. 9.5.1. Calculations of average heat $\langle Q \rangle$ can be derived, for example, for the qubit in a fermionic lattice environment model introduced in Eqs. (9.15 - 9.17).

9.6.2 N measurements on the open system

The result in Eqs (9.28 - 9.29) can be extended to an arbitrary number N of measurements taken on the system respectively at times $t_1 < t_2 < ... < t_N$. The overall density matrix at the N-th measurement is calculated iteratively as

$$\hat{\rho}'(t_N) = \frac{\left(\prod_{j=N}^{1} \hat{V}_{v_j}(t_j, t_{j-1})\right) \hat{\rho}(0) \left(\prod_{j=1}^{N} \hat{V}_{v_j}^\dagger(t_j, t_{j-1})\right)}{p_N(v_N \mid v_1, v_2 ... v_{N-1})}, \tag{9.30}$$

where $\hat{V}_{v_j}(t_j, t_{j-1}) = \left(\hat{P}_{v_j} \otimes \mathbb{1}_B\right) \hat{U}(t_j - t_{j-1})$, and we set $t_0 = 0$. The probability of outcome v_N of the N-th measurement, conditioned to the previous $N-1$ outcomes $v_1, v_2 ... v_{N-1}$, is

$$p_N(v_N \mid v_1, v_2 ... v_{N-1}) = \frac{1}{p_{N-1}(v_{N-1} \mid v_1, v_2 ... v_{N-2})} \times \mathrm{Tr}\left[\left(\prod_{j=N}^{1} \hat{V}_{v_j}(t_j, t_{j-1})\right) \hat{\rho}(0) \left(\prod_{j=1}^{N} \hat{V}_{v_j}^\dagger(t_j, t_{j-1})\right)\right]. \tag{9.31}$$

At the final time t_f, the density matrix is

$$\hat{\rho}\left(t_f\right) = \hat{U}\left(t_f - t_N\right)\hat{\rho}'(t_N)\hat{U}^{\dagger}\left(t_f - t_N\right), \tag{9.32}$$

from which it follows, after calculations similar to the ones leading to Eq. (9.28), that the characteristic function of heat is

$$\begin{aligned}\chi^N(u) = &\frac{1}{p_N\left(v_N \mid v_1, \ldots v_{N-1}\right)} \sum_{n_0, n_1 \ldots n_N} \sum_{k_{N-1} \ldots k_0} \rho_S^{k_0, n_0}(0) \times \\ &\left(\prod_{j=1}^{N} \left\langle n_{j-1}\right| \hat{P}_{v_j}^{\dagger} \left|n_j\right\rangle\right) \left\langle n_N\right| \hat{P}_{v_N} \left|k_{N-1}\right\rangle \left(\prod_{j=N-1>0}^{1} \left\langle k_j\right| \hat{P}_{v_j} \left|k_{j-1}\right\rangle\right) \times \\ &\left\langle \prod_{j=1}^{N} \left(e^{i\left(t_j - t_{j-1}\right)\hat{H}_{n_{j-1}}}\right) e^{i\left(t_f - t_N\right)\hat{H}_{n_N}} e^{iu\hat{H}_0} e^{-i\left(t_f - t_N\right)\hat{H}_{n_N}} \prod_{j=N}^{1} \left(e^{-i\left(t_j - t_{j-1}\right)\hat{H}_{k_{j-1}}}\right) e^{-iu\hat{H}_0} \right\rangle_B .\end{aligned} \tag{9.33}$$

The expanded conditional probability outcome is

$$\begin{aligned}p_N\left(v_N \mid v_1, \ldots v_{N-1}\right) = &\frac{1}{p_{N-1}\left(v_{N-1} \mid v_1, \ldots v_{N-2}\right)} \sum_{n_0, n_1 \ldots n_N} \sum_{k_{N-1} \ldots k_0} \rho_S^{k_0, n_0}(0) \\ &\times \left(\prod_{j=1}^{N} \left\langle n_{j-1}\right| \hat{P}_{v_j}^{\dagger} \left|n_j\right\rangle\right) \left\langle n_N\right| \hat{P}_{v_N} \left|k_{N-1}\right\rangle \left(\prod_{j=N-1>0}^{1} \left\langle k_j\right| \hat{P}_{v_j} \left|k_{j-1}\right\rangle\right) \\ &\times \left\langle \prod_{j=1}^{N} \left(e^{i\left(t_j - t_{j-1}\right)\hat{H}_{n_{j-1}}}\right) \prod_{j=N}^{1} \left(e^{-i\left(t_j - t_{j-1}\right)\hat{H}_{k_{j-1}}}\right) \right\rangle_B ,\end{aligned} \tag{9.34}$$

which can be calculated recursively starting from Eq. (9.29).

10 | Conclusions and Future Work

Part I of this thesis described the known theory of open quantum systems and its connection to quantum thermodynamics. It introduced a methodology to numerically simulate non-Markovian dynamics and described the TEMPO algorithm.

In Part II, we showed our research work and its results. We discussed how a better understanding of dissipation in open quantum systems is a fundamental goal of quantum thermodynamics as well as being crucial for quantum device engineering. We have shown that this goal can be successfully addressed by an extension of the TEMPO algorithm [114] to evaluate the characteristic function of the heat distribution. We have demonstrated the validity and flexibility of our approach by calculating the mean and variance of the heat transfer in the spin-boson model over a range of temperatures and system-bath coupling strengths. Our results clearly demonstrate the importance of system-environment correlations at low temperatures. Even at high temperature and weak coupling, we find significant contributions to the heat statistics from the system-environment interaction energy that are not captured by the standard weak-coupling master equation. This indicates that system-reservoir interactions are an important source of dissipation that must be accounted for when designing thermodynamic protocols [150–155], even in the weak-coupling regime.

Our approach to calculating heat statistics can be extended in several promising directions. It is straightforward to adapt the method to situations with a time-dependent system Hamiltonian, which would enable the characterisation of heat statistics for driven open systems. This problem, which is theoretically challenging even for Markovian environments outside of the slow-driving regime, has nu-

merous applications in quantum control, such as quantum information processing [156] and erasure [157], enhanced engine cycles through thermodynamic shortcuts [97, 158], and tailored quantum light sources [95, 159]. It is also possible to incorporate multiple baths within our framework by combining the corresponding influence functionals together [160]. This would allow the study of the full counting statistics of quantum heat transport in non-equilibrium steady states [111], including highly non-Markovian regimes. In general, we expect that the method presented here will facilitate further research into the non-equilibrium quantum thermodynamics of strongly coupled open systems.

Secondly, we discussed the importance of heat dissipation in a pure decoherence process. Decoherence and heat dissipation are commonly considered to be complementary manifestations of irreversibility in open quantum systems. Our results show that these two processes are in fact inextricably linked: environment-induced decoherence comes at a fundamental energetic cost. This heat dissipation is a subtle aspect of decoherence that, to our knowledge, has not yet been investigated in the literature on quantum thermodynamics. Beyond their foundational implications, our findings are directly relevant for current efforts to harness decoherence for nondestructive measurements of noise in quantum devices. The unavoidable dissipation of energy implies an intrinsic disturbance due to such measurements [161], which can be quantitatively assessed using the general framework developed here.

The experimentally relevant example of an impurity immersed in an ultra-cold Fermi gas [81] highlights the rich physics which is unveiled by considering the thermodynamics of decoherence. However, our framework can equally well be applied to a range of other situations, such as ultracold bosonic environments where dephasing impurities have recently been realized [84, 89], as well as strongly interacting systems. Starting from this work, further investigations of the peculiar thermodynamic features of decoherence and associated properties in diverse physical settings are possible.

Bibliography

[1] H. P. Breuer and F. Petruccione, *The Theory of Open Quantum Systems* (Oxford University Press, 2002).

[2] R. F. Bader, Advances in Quantum Chemistry **57**, 285 (2009).

[3] N. V. Prokof'ev and P. C. E. Stamp, Reports on Progress in Physics **63**, 669 (2000).

[4] M. Popovic, B. Vacchini, and S. Campbell, Phys. Rev. A **98**, 012130 (2018).

[5] E. O'Reilly and A. Olaya-Castro, Nat. Commun. **5**, 3012 (2014).

[6] A. Shabani, M. Mohseni, S. Jang, A. Ishizaki, M. Plenio, P. Rebentrost, A. Aspuru-Guzik, J. Cao, S. Lloyd, and R. Silbey, in *Quantum Effects in Biology* (Cambridge University Press, 2014) pp. 14—52.

[7] W. H. Zurek, Physics Today **44**, 36 (1991).

[8] J. Rossnagel, S. T. Dawkins, K. N. Tolazzi, O. Abah, E. Lutz, F. Schmidt-Kaler, and K. Singer, Science **352**, 325 (2016).

[9] B. Vacchini, A. Smirne, E. M. Laine, J. Piilo, and H. P. Breuer, New J. Phys. **13**, 093004 (2011).

[10] B. Bylicka, M. Tukiainen, D. Chruściński, J. Piilo, and S. Maniscalco, Sci. Rep. **6**, 27989 (2016).

[11] S. Hamedani Raja, M. Borrelli, R. Schmidt, J. P. Pekola, and S. Maniscalco, Phys. Rev. A **97**, 032133 (2018).

[12] I. de Vega and D. Alonso, Rev. Mod. Phys. **89**, 015001 (2017).

[13] N. Makri and D. E. Makarov, J. Chem. Phys. **102**, 4600 (1995).

[14] N. Makri and D. E. Makarov, J. Chem. Phys. **102**, 4611 (1995).

[15] A. Strathearn, B. W. Lovett, and P. Kirton, New J. Phys. **19**, 093009 (2017).

[16] A. Strathearn, P. Kirton, D. Kilda, J. Keeling, and B. W. Lovett, Nat. Commun. **9**, 3322 (2018).

[17] M. Esposito, K. Lindenberg, and C. V. den Broeck, New J. Phys. **12**, 013013 (2010).

[18] P. Strasberg, G. Schaller, T. Brandes, and M. Esposito, Phys. Rev. X **7**, 021003 (2017).

[19] M. Esposito, M. A. Ochoa, and M. Galperin, Phys. Rev. Lett. **114**, 080602 (2015).

[20] H. P. Breuer, E. M. Laine, J. Piilo, and B. Vacchini, Rev. Mod. Phys. **88**, 021002 (2016).

[21] Á. Rivas, S. F. Huelga, and M. B. Plenio, Rep. Prog. Phys. **77**, 094001 (2014).

[22] V. Gorini, A. Kossakowski, and E. C. G. Sudarshan, Journal of Mathematical Physics **17**, 821 (1976).

[23] H. P. Breuer, E. M. Laine, and J. Piilo, Phys. Rev. Lett. **103**, 210401 (2009).

[24] D. von Lindenfels, O. Gräb, C. T. Schmiegelow, V. Kaushal, J. Schulz, M. T. Mitchison, J. Goold, F. Schmidt-Kaler, and U. G. Poschinger, Phys. Rev. Lett. **123**, 080602 (2019).

[25] D. Gelbwaser-Klimovsky, N. Erez, R. Alicki, and G. Kurizki, Phys. Rev. A **88**, 022112 (2013).

[26] G. Thomas, N. Siddharth, S. Banerjee, and S. Ghosh, Phys. Rev. E **97**, 062108 (2018).

[27] G. A. Barrios, F. Albarrán-Arriagada, F. A. Cárdenas-López, G. Romero, and J. C. Retamal, Phys. Rev. A **96**, 052119 (2017).

[28] R. P. Feynman and A. R. Hibbs, *Quantum Mechanics and Path Integrals* (McGraw-Hill, 1965).

[29] R. P. Feynman and L. M. Brown, *Feynman's Thesis: a New Approach to Quantum Theory* (World Scientific, 2005).

[30] R. P. Feynman and F. L. Vernon, Annals of Physics **24**, 118 (1963).

[31] H. F. Baker, Proc. London Math. Soc. **3**, 24 (1905).

[32] U. Schollwöck, Annals of Physics **326**, 96 (2011).

[33] R. Kubo, J. Phys. Soc. Japan **17**, 1100 (1962).

[34] J. I. Cirac, D. Pérez-García, N. Schuch, and F. Verstraete, Rev. Mod. Phys. **93**, 045003 (2021).

[35] J. Goold, M. Huber, A. Riera, L. del Rio, and P. Skrzypczyk, J. Phys. A: Math. Theor. **49**, 143001 (2016).

[36] S. R. de Groot and P. Mazur, *Non-Equilibrium Thermodynamics* (North-Holland, 1962).

[37] R. Clausius, *The Mechanical Theory of Heat* (Macmillan, London, 1879).

[38] R. Fitzpatrick, *Thermodynamics and Statistical Mechanics* (World Scientific, 2020).

[39] S. Deffner and E. Lutz, Phys. Rev. Lett. **105**, 170402 (2010).

[40] S. Deffner and E. Lutz, Phys. Rev. Lett. **107**, 140404 (2011).

[41] W. Wu and J. Wang, Frontiers in Physics **8** (2020).

[42] B. Altaner, M. Polettini, and M. Esposito, Phys. Rev. Lett. **117**, 180601 (2016).

[43] F. Corberi, E. Lippiello, and M. Zannetti, Journal of Statistical Mechanics: Theory and Experiment **2007**, P07002 (2007).

[44] C. Jarzynski, Phys. Rev. Lett. **78**, 2690 (1997).

[45] G. Benenti, G. Casati, K. Saito, and R. S. Whitney, Phys. Rep. **694**, 1 (2017).

[46] F. Binder, L. A. Correa, C. Gogolin, J. Anders, and G. Adesso, *Thermodynamics in the Quantum Regime* (Springer International Publishing, 2018).

[47] M. T. Mitchison, Contemporary Physics **60**, 164 (2019).

[48] J. V. Koski, V. F. Maisi, J. P. Pekola, and D. V. Averin, Proc. Nat. Acad. Sci. **111**, 13786 (2014).

[49] J. V. Koski, A. Kutvonen, I. M. Khaymovich, T. Ala-Nissila, and J. P. Pekola, Phys. Rev. Lett. **115**, 260602 (2015).

[50] M. Josefsson, A. Svilans, A. M. Burke, E. A. Hoffmann, S. Fahlvik, C. Thelander, M. Leijnse, and H. Linke, Nature Nanotech. **13**, 920 (2018).

[51] G. Maslennikov, S. Ding, R. Hablützel, J. Gan, A. Roulet, S. Nimmrichter, J. Dai, V. Scarani, and D. Matsukevich, Nature Commun. **10** (2019).

[52] A. Ronzani, B. Karimi, J. Senior, Y.-C. Chang, J. T. Peltonen, C. Chen, and J. P. Pekola, Nature Phys. **14**, 991 (2018).

[53] J. P. S. Peterson, T. B. Batalhão, M. Herrera, A. M. Souza, R. S. Sarthour, I. S. Oliveira, and R. M. Serra, Phys. Rev. Lett. **123**, 240601 (2019).

[54] J. Klatzow, J. N. Becker, P. M. Ledingham, C. Weinzetl, K. T. Kaczmarek, D. J. Saunders, J. Nunn, I. A. Walmsley, R. Uzdin, and E. Poem, Phys. Rev. Lett. **122**, 110601 (2019).

[55] H. E. D. Scovil and E. O. Schulz-DuBois, Phys. Rev. Lett. **2**, 262 (1959).

[56] P. Santhanam, D. J. Gray, and R. J. Ram, Phys. Rev. Lett. **108**, 097403 (2012).

[57] K. E. Dorfman, D. V. Voronine, S. Mukamel, and M. O. Scully, Proc. Nat. Acad. Sci. **110**, 2746 (2013).

[58] C. Creatore, M. A. Parker, S. Emmott, and A. W. Chin, Phys. Rev. Lett. **111**, 253601 (2013).

[59] N. Killoran, S. F. Huelga, and M. B. Plenio, J. Chem. Phys. **143**, 155102 (2015).

[60] A. Fruchtman, R. Gómez-Bombarelli, B. W. Lovett, and E. M. Gauger, Phys. Rev. Lett. **117**, 203603 (2016).

[61] C. Jarzynski, Phys. Rev. X **7**, 011008 (2017).

[62] P. Talkner and P. Hänggi, Rev. Mod. Phys. **92**, 041002 (2020).

[63] M. Pezzutto, M. Paternostro, and Y. Omar, New J. Phys. **18**, 123018 (2016).

[64] G. Zicari, M. Brunelli, and M. Paternostro, Phys. Rev. Research **2**, 043006 (2020).

[65] M. Esposito, U. Harbola, and S. Mukamel, Rev. Mod. Phys. **81**, 1665 (2009).

[66] M. Campisi, P. Hänggi, and P. Talkner, Rev. Mod. Phys. **83**, 771 (2011).

[67] P. Talkner, E. Lutz, and P. Hänggi, Phys. Rev. E **75**, 050102 (2007).

[68] L. Mazzola, G. De Chiara, and M. Paternostro, Phys. Rev. Lett. **110**, 230602 (2013).

[69] R. Dorner, S. R. Clark, L. Heaney, R. Fazio, J. Goold, and V. Vedral, Phys. Rev. Lett. **110**, 230601 (2013).

[70] A. J. Roncaglia, F. Cerisola, and J. P. Paz, Phys. Rev. Lett. **113**, 250601 (2014).

[71] J. Goold, U. Poschinger, and K. Modi, Phys. Rev. E **90**, 020101 (2014).

[72] K. Ptaszyński and M. Esposito, Phys. Rev. Lett. **123**, 200603 (2019).

[73] W. H. Zurek and J. P. Paz, Phys. Rev. Lett. **72**, 2508 (1994).

[74] S. F. Huelga, C. Macchiavello, T. Pellizzari, A. K. Ekert, M. B. Plenio, and J. I. Cirac, Phys. Rev. Lett. **79**, 3865 (1997).

[75] P. W. Shor, Phys. Rev. A **52**, R2493 (1995).

[76] G. M. Palma, K.-A. Suominen, and A. K. Ekert, Proc. Royal Soc. Lond. A **452**, 567 (1996).

[77] E. Joos and H. D. Zeh, Zeitschrift für Physik B Condensed Matter **59**, 223 (1985).

[78] W. H. Zurek, Rev. Mod. Phys. **75**, 715 (2003).

[79] C. J. Myatt, B. E. King, Q. A. Turchette, C. A. Sackett, D. Kielpinski, W. M. Itano, C. Monroe, and D. J. Wineland, Nature **403**, 269 (2000).

[80] L. Ratschbacher, C. Sias, L. Carcagni, J. M. Silver, C. Zipkes, and M. Köhl, Phys. Rev. Lett. **110**, 160402 (2013).

[81] M. Cetina, M. Jag, R. S. Lous, I. Fritsche, J. T. M. Walraven, R. Grimm, J. Levinsen, M. M. Parish, R. Schmidt, M. Knap, and E. Demler, Science **354**, 96 (2016).

[82] Z.-D. Liu, H. Lyyra, Y.-N. Sun, B.-H. Liu, C.-F. Li, G.-C. Guo, S. Maniscalco, and J. Piilo, Nature Commun. **9**, 3453 (2018).

[83] T. K. Unden, D. Louzon, M. Zwolak, W. H. Zurek, and F. Jelezko, Phys. Rev. Lett. **123**, 140402 (2019).

[84] M. G. Skou, T. G. Skov, N. B. Jørgensen, K. K. Nielsen, A. Camacho-Guardian, T. Pohl, G. M. Bruun, and J. J. Arlt, Nature Physics **17**, 731 (2021).

[85] H. T. Quan, Z. Song, X. F. Liu, P. Zanardi, and C. P. Sun, Phys. Rev. Lett. **96**, 140604 (2006).

[86] J. Bylander, S. Gustavsson, F. Yan, F. Yoshihara, K. Harrabi, G. Fitch, D. G. Cory, Y. Nakamura, J.-S. Tsai, and W. D. Oliver, Nature Physics **7**, 565 (2011).

[87] Y. Sung, F. Beaudoin, L. M. Norris, F. Yan, D. K. Kim, J. Y. Qiu, U. von Lüpke, J. L. Yoder, T. P. Orlando, S. Gustavsson, L. Viola, and W. D. Oliver, Nature Commun. **10**, 3715 (2019).

[88] M. T. Mitchison, T. Fogarty, G. Guarnieri, S. Campbell, T. Busch, and J. Goold, Phys. Rev. Lett. **125**, 080402 (2020).

[89] D. Adam, Q. Bouton, J. Nettersheim, S. Burgardt, and A. Widera, Phys. Rev. Lett. **129**, 120404 (2022).

[90] M. T. Mitchison, A. Purkayastha, M. Brenes, A. Silva, and J. Goold, Phys. Rev. A **105**, L030201 (2022).

[91] H. Spohn, Journal of Mathematical Physics **19**, 1227 (1978).

[92] M. Popovic, M. T. Mitchison, and J. Goold, Proc. R. Soc. A **479**, 20230040 (2023).

[93] K. Funo and H. T. Quan, Phys. Rev. Lett. **121**, 040602 (2018).

[94] R. M. de Araújo, T. Häffner, R. Bernardi, D. S. Tasca, M. P. J. Lavery, M. J. Padgett, A. Kanaan, L. C. Céleri, and P. H. S. Ribeiro, Journal of Physics Communications **2**, 035012 (2018).

[95] C. N. Murphy and P. R. Eastham, Commun. Phys. **2**, 120 (2019).

[96] R. Dann, A. Tobalina, and R. Kosloff, Phys. Rev. Lett. **122**, 250402 (2019).

[97] N. Pancotti, M. Scandi, M. T. Mitchison, and M. Perarnau-Llobet, Phys. Rev. X **10**, 031015 (2020).

[98] P. Pietzonka and U. Seifert, Phys. Rev. Lett. **120**, 190602 (2018).

[99] J. Goold, M. Paternostro, and K. Modi, Phys. Rev. Lett. **114**, 060602 (2015).

[100] T. Sagawa and M. Ueda, Phys. Rev. Lett. **100**, 080403 (2008).

[101] A. C. Barato and U. Seifert, Phys. Rev. Lett. **114**, 158101 (2015).

[102] T. R. Gingrich, J. M. Horowitz, N. Perunov, and J. L. England, Phys. Rev. Lett. **116**, 120601 (2016).

[103] G. Guarnieri, G. T. Landi, S. R. Clark, and J. Goold, Phys. Rev. Research **1**, 033021 (2019).

[104] A. M. Timpanaro, G. Guarnieri, J. Goold, and G. T. Landi, Phys. Rev. Lett. **123**, 090604 (2019).

[105] Y. Hasegawa and T. Van Vu, Phys. Rev. Lett. **123**, 110602 (2019).

[106] M. Brunelli, L. Fusco, R. Landig, W. Wieczorek, J. Hoelscher-Obermaier, G. Landi, F. L. Semião, A. Ferraro, N. Kiesel, T. Donner, G. De Chiara, and M. Paternostro, Phys. Rev. Lett. **121**, 160604 (2018).

[107] K. Micadei, J. P. S. Peterson, A. M. Souza, R. S. Sarthour, I. S. Oliveira, G. T. Landi, T. B. Batalhão, R. M. Serra, and E. Lutz, Nat. Commun. **10**, 2456 (2019).

[108] P. M. Harrington, D. Tan, M. Naghiloo, and K. W. Murch, Phys. Rev. Lett. **123**, 020502 (2019).

[109] E. Aurell, Phys. Rev. E **97**, 062117 (2018).

[110] E. Aurell, R. Kawai, and K. Goyal, J. Phys. A: Math. Theor. **53**, 275303 (2020).

[111] M. Kilgour, B. K. Agarwalla, and D. Segal, J. Chem. Phys. **150**, 084111 (2019).

[112] D. Gribben, A. Strathearn, J. Iles-Smith, D. Kilda, A. Nazir, B. W. Lovett, and P. Kirton, Phys. Rev. Research **2**, 013265 (2020).

[113] G. E. Fux, E. P. Butler, P. R. Eastham, B. W. Lovett, and J. Keeling, Phys. Rev. Lett. **126**, 200401 (2021).

[114] M. Popovic, M. T. Mitchison, A. Strathearn, B. W. Lovett, J. Goold, and P. R. Eastham, (2021), https://doi.org/10.5281/zenodo.4884728.

[115] A. Nazir, Phys. Rev. Lett. **103**, 146404 (2009).

[116] A. Recati, P. O. Fedichev, W. Zwerger, J. von Delft, and P. Zoller, Phys. Rev. Lett. **94**, 040404 (2005).

[117] L. Magazzù, P. Forn-Díaz, R. Belyansky, J.-L. Orgiazzi, M. A. Yurtalan, M. R. Otto, A. Lupascu, C. M. Wilson, and M. Grifoni, Nat. Commun. **9**, 1403 (2018).

[118] A. Silva, Phys. Rev. Lett. **101**, 120603 (2008).

[119] P. Smacchia and A. Silva, Phys. Rev. Lett. **109**, 037202 (2012).

[120] A. Sindona, J. Goold, N. L. Gullo, and F. Plastina, New J. Phys. **16**, 045013 (2014).

[121] J. Prior, A. W. Chin, S. F. Huelga, and M. B. Plenio, Phys. Rev. Lett. **105**, 050404 (2010).

[122] A. D. Somoza, O. Marty, J. Lim, S. F. Huelga, and M. B. Plenio, Phys. Rev. Lett. **123**, 100502 (2019).

[123] R. Alicki, J. Phys. A: Math. Gen. **12**, L103 (1979).

[124] C. Gerry and P. Knight, *Introductory Quantum Optics* (Cambridge University Press, 2004).

[125] R. Bulla, N.-H. Tong, and M. Vojta, Phys. Rev. Lett. **91**, 170601 (2003).

[126] R. Bulla, H.-J. Lee, N.-H. Tong, and M. Vojta, Phys. Rev. B **71**, 045122 (2005).

[127] R. Silbey and R. A. Harris, J. Chem. Phys. **80**, 2615 (1984).

[128] D. P. S. McCutcheon, N. S. Dattani, E. M. Gauger, B. W. Lovett, and A. Nazir, Phys. Rev. B **84**, 081305 (2011).

[129] A. W. Chin, J. Prior, S. F. Huelga, and M. B. Plenio, Phys. Rev. Lett. **107**, 160601 (2011).

[130] A. Nazir, D. P. S. McCutcheon, and A. W. Chin, Phys. Rev. B **85**, 224301 (2012).

[131] M. Schlosshauer, Physics Reports **831**, 1 (2019).

[132] T. Sagawa, in *Kinki University Series on Quantum Computing* (World Scientific, 2012) pp. 125–190.

[133] G. Francica, J. Goold, and F. Plastina, Phys. Rev. E **99**, 042105 (2019).

[134] J. P. Santos, L. C. Céleri, G. T. Landi, and M. Paternostro, npj Quantum Information **5**, 23 (2019).

[135] G. Francica, F. C. Binder, G. Guarnieri, M. T. Mitchison, J. Goold, and F. Plastina, Phys. Rev. Lett. **125**, 180603 (2020).

[136] A. A. Clerk, M. H. Devoret, S. M. Girvin, F. Marquardt, and R. J. Schoelkopf, Rev. Mod. Phys. **82**, 1155 (2010).

[137] G. A. Álvarez and D. Suter, Phys. Rev. Lett. **107**, 230501 (2011).

[138] L. M. Norris, G. A. Paz-Silva, and L. Viola, Phys. Rev. Lett. **116**, 150503 (2016).

[139] L. J. LeBlanc and J. H. Thywissen, Phys. Rev. A **75**, 053612 (2007).

[140] C. Chin, R. Grimm, P. Julienne, and E. Tiesinga, Rev. Mod. Phys. **82**, 1225 (2010).

[141] J. Goold, T. Fogarty, N. Lo Gullo, M. Paternostro, and T. Busch, Phys. Rev. A **84**, 063632 (2011).

[142] M. Knap, A. Shashi, Y. Nishida, A. Imambekov, D. A. Abanin, and E. Demler, Phys. Rev. X **2**, 041020 (2012).

[143] I. Klich, in *Quantum Noise in Mesoscopic Physics* (Springer Netherlands, 2003) pp. 397–402.

[144] D. A. Abanin and L. S. Levitov, Phys. Rev. Lett. **94**, 186803 (2005).

[145] R. Schmidt, M. Knap, D. A. Ivanov, J.-S. You, M. Cetina, and E. Demler, Rep. Prog. Phys. **81**, 024401 (2018).

[146] G. D. Mahan, Phys. Rev. **163**, 612 (1967).

[147] P. Nozières and C. T. De Dominicis, Phys. Rev. **178**, 1097 (1969).

[148] P. W. Anderson, Phys. Rev. Lett. **18**, 1049 (1967).

[149] Y. Morikuni and H. Tasaki, Journal of Statistical Physics **143**, 1 (2011).

[150] D. Gelbwaser-Klimovsky and A. Aspuru-Guzik, J. Phys. Chem. Lett. **6**, 3477 (2015).

[151] G. Katz and R. Kosloff, Entropy **18**, 186 (2016).

[152] P. Strasberg, G. Schaller, N. Lambert, and T. Brandes, New J. Phys. **18**, 073007 (2016).

[153] D. Newman, F. Mintert, and A. Nazir, Phys. Rev. E **95**, 032139 (2017).

[154] M. Perarnau-Llobet, H. Wilming, A. Riera, R. Gallego, and J. Eisert, Phys. Rev. Lett. **120**, 120602 (2018).

[155] D. Newman, F. Mintert, and A. Nazir, Phys. Rev. E **101**, 052129 (2020).

[156] V. Cimini, S. Gherardini, M. Barbieri, I. Gianani, M. Sbroscia, L. Buffoni, M. Paternostro, and F. Caruso, npj Quantum Information **6**, 96 (2020).

[157] H. J. D. Miller, G. Guarnieri, M. T. Mitchison, and J. Goold, Phys. Rev. Lett. **125**, 160602 (2020).

[158] R. Dann and R. Kosloff, New J. Phys. **22**, 013055 (2020).

[159] J. Iles-Smith, A. Nazir, and D. P. S. McCutcheon, Nat. Commun. **10**, 3034 (2019).

[160] D. Gribben, D. M. Rouse, J. Iles-Smith, A. Strathearn, H. Maguire, P. Kirton, A. Nazir, E. M. Gauger, and B. W. Lovett, PRX Quantum **3**, 010321 (2022).

[161] Y.-X. Wang and A. A. Clerk, Nat. Commun. **12**, 6528 (2021).